FLUXES OF NITRIC OXIDE FROM A SUGARCANE FIELD

A THESIS SUBMITTED TO THE GRADUATE DIVISION OF THE UNIVERSITY OF HAWAII IN PARTIAL FULFILLMENT OF THE REQUIREMENTS FOR THE DEGREE OF

MASTER OF SCIENCE

IN

AGRONOMY AND SOIL SCIENCE

DECEMBER 1994

By

Rodolfo Martinez

Thesis Committee:

Elizabeth Graser, Chairperson
James A. Silva
Nguyen V. Hue

We certify that we have read this thesis and that, in our opinion, it is satisfactory in scope and quality as a thesis for the degree of Master of Science in Agronomy and Soil Science.

THESIS COMMITTEE

Elizabeth A Graves
Chairperson

James A. Silva

ACKNOWLEDGEMENTS

This research was accomplished with the help of several scientists, friends, and colleagues: I profoundly appreciate the help and advise of my committee chair, Dr. Elizabeth A. Graser. I greatly appreciate my other committee members, Drs. James Silva and N. V. Hue for their wise corrections on the manuscript.

I also would like to thank Drs. Eric Davidson and Pamela Matson for their advise to start off this project. Many thanks to John Zachariassen for sharing his knowledge and practical experience.

I am very grateful for all my friends that helped me out in the many difficult moments of my program: Makoto Tajima, Kevin Grace, David Anderson, Karl Iwasaki, Darrell Herbert and my girlfriend Miki.

This research was funded in part by Grant No. NAG 2-758 from NASA/Ames.

ABSTRACT

Improved values for NO_x fluxes from tropical agriculture are needed for global climate models. Fluxes of NO were measured in a drip-irrigated, fertilized tropical sugarcane field in Hawaii. The chamber approach was used to measure surface NO fluxes, and a flux-gradient approach, to measure above-canopy NO_x fluxes. Soil water, NH_4^+, and NO_3^- content, weather data, leaf area, etc. were measured to interpret the NO fluxes. Daily surface NO fluxes tended to increase and decrease concurrently with soil water content. Peak fluxes were large (typically 120 ng NO-N m^{-2} s^{-1}) for the drip line, but much smaller between the rows (10 ng NO-N m^{-2} s^{-1}). In-air chemical reactions of the $NO-O_3-NO_2$ triad caused divergence of NO_x fluxes from inert values; the actual fluxes were calculated with the reactive eddy diffusivity model formulated by Vila-Guerau de Arellano and Duynkerke (NO fluxes were 0.5% larger). O_3 interference with the chemiluminescent analyzer introduced large errors into some fluxes. Decreasing ratios of above-canopy NO_x to surface NO fluxes late in the study are associated with increasing canopy cover. The NO_x flux was comprised more of NO early in the study and NO_2, later. The 198-d average NO flux was 9 ng N m^{-2} s^{-1} which is comparable with other studies in fertilized and irrigated systems.

TABLE OF CONTENTS

LIST OF TABLES

LIST OF FIGURES

1. INTRODUCTION

Nitrogen oxides such as NO and NO_2 (NO_x) are important trace gases in the cycling of nitrogen between the biosphere and the atmosphere. In the troposphere (Fig. 1.1) NO and NO_2 participate in photochemical reactions that regulate the production or consumption of tropospheric ozone (O_3) and hydroxyl radicals (OH), which are the primary oxidants for other tropospheric trace gases such as CH_4. Increases in NO_x could lead to increases in ozone affecting air quality. NO_2 is also a precursor in the production of nitric acid (HNO_3), which is a major component in acid rain and acid deposition (National Academy of Sciences, 1977; Anderson and Levine, 1987; Penner et al., 1991; Hutchinson and Davidson, 1993; Robertson, 1993).

In the stratosphere ozone shields the earth from harmful ultraviolet radiation; however, high ozone concentrations in the troposphere damages plants and human beings and interferes with growth (Bruce, 1990). The vertical distribution of ozone is changing due to man-made pollutants (Fig. 1.1). The ozone concentration is increasing in the troposphere but decreasing in the stratosphere. The decrease in stratospheric ozone is thought to be a cause of climate change (Bruce, 1990). It is crucial to understand the relationship between O_3 and its precursors (such as reactions with the nitrogen oxides) in order to identify specific sources and the potential of concentration change over time.

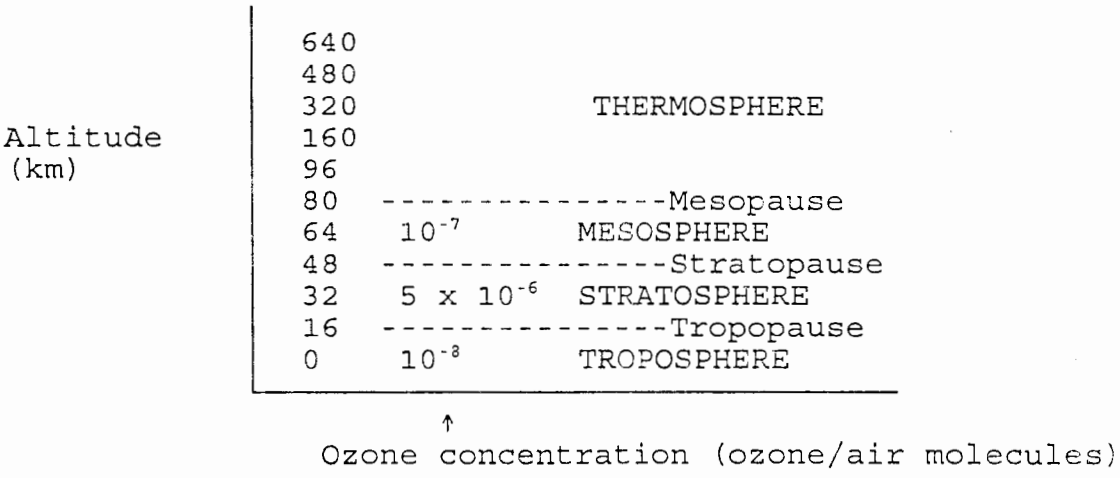

Figure 1.1. Layers in the atmosphere with typical heights and ozone concentrations (Miller et al., 1975).

The estimated global sources and sinks of atmospheric NO_x range from 25 to 99 and 24 to 64 Tg N yr^{-1}, respectively, from one study (Logan, 1983 as cited in Robertson, 1993). Other studies of atmospheric NO fluxes include those by Baulch et al., 1982; Enhalt and Drummond, 1982; Tedman and Helter, 1983; and National Academy of Sciences, 1984 (as all cited in Anderson and Levine, 1987). The main sources of NO_x in the troposphere are fossil-fuel combustion, biomass burning, lightning, soil emissions due to microbiological activity, and transfers from the stratosphere. A number of estimates of NO_x fluxes have been made (Table 1.1); however, these estimates are still being refined as more precise measurements are collected, as the data is measured to be more representative regionally, and as the understanding of the atmospheric processes responsible for NO_x production and consumption is improved. Anthropogenic sources (fossil-fuel combustion, biomass burning, and emissions from fertilized agriculture) are considered the greatest sources of NO_x, but natural factors such as lightning and soil emissions from natural ecosystems are also important particularly in areas of low human settlement. Although the estimated amount of NO_x transferred from the stratosphere is small, it is of relatively great importance since its lifetime is longer than that of NO_x emitted from the surface (Johansson and Sanhueza, 1988).

Table 1.1 Tropospheric NO_x flux in Tg N yr^{-1} (Logan, 1983 as cited in Robertson, 1993)

Sinks/sources	NO_x-N
Sinks	
Wet deposition	12-42
Dry deposition	12-22
Sources	
Combustion	
Industrial	21
Biomass burning	12
Lightning	8
Soil (microbial activity)	20
Atmospheric NH_3 oxidation	6
Oceans	<1
Stratosphere	<1
Total	68

Davidson (1991 as cited in Robertson, 1993) estimated soil emissions of NO_x of 20 Tg-N yr^{-1} based on a review of 23 studies. Estimating NO_x fluxes from soils to the atmosphere is imprecise due to the scarcity of measurements for many regions and the difficulty of interpreting soil surface measurements due to its reactivity with several compounds emitted from soils and plants and its deposition on plant canopies by dry and wet deposition which is hard to quantify (Robertson, 1993). NO emitted from soils is converted rapidly to NO_2, which can be either photolyzed back to NO, transported to the atmosphere, converted to peroxyacetylnitrate (PAN), or deposited on plant surfaces (Robertson, 1993; Delany et al., 1986; Wesely et al., 1989). The NO emitted from the soil appears to be a major contribution to the total N gas loss from natural and agricultural systems, but its transport to the atmosphere and subsequent deposition substantially changes its distribution (Williams et al., 1992 as cited in Hutchinson and Davidson, 1993).

Since natural tropical ecosystems are being converted to intensive agricultural use, they represent a major new source of NO due to fertilization, selection of specific cropping systems, and other management practices that affect the nitrogen cycle. Little is known about the NO fluxes from these ecosystems and how it contributes to the global

NO_x budget , because most research has been in temperate ecosystems. The evaluation of NO production and consumption in the soil is important to estimate its contribution to the chemistry of the atmosphere and its influence on the earth's climate, as well as, to evaluate the impact of human activities on emissions.

The purpose of this research is to measure the magnitude of NO (and related NO_x) emissions from a tropical sugarcane field and to observe how different agricultural practices affect the emissions.

2. LITERATURE REVIEW

2.1 Chemical reactions of NO in the atmosphere

NO chemistry in the atmosphere remains an active area of research. It is complicated because of the many chemical reactions produced by hydrocarbons, nitrogen oxides, carbon monoxide, water vapor, and other trace components of air, that can be present in the atmosphere. The understanding of the relationship among nitric oxide (NO), nitrogen dioxide (NO_2), ozone (O_3), and other photochemical oxidants such as peroxyacetylnitrate (PAN), hydroxyl radicals (HO), hydroperoxyl radicals (HO_2), and hydrocarbons is crucial to understanding the role of NO in the atmosphere particularly in the production of ozone and smog.

Nitrogen dioxide, a molecule with an average lifetime of 1.4 min (at a latitude of 40°), absorbs sunlight and is photolyzed to produce ozone.

$$NO_2 + \text{light (290-430 nm)} \longrightarrow O + NO \qquad (2.1)$$

$$O + O_2 + M \longrightarrow O_3 + M \qquad (2.2)$$

where M is a molecule (nitrogen or oxygen) that absorbs the energy released and stabilizes the ozone produced (National Academy of Sciences, 1977). These very active ozone molecules react with the NO which is produced in reaction 2.1 to regenerate nitrogen dioxide.

$$O_3 + NO \longrightarrow NO_2 + O_2 \qquad (2.3)$$

Reactions 2.1 to 2.3 form a cycle in which the net result is conversion of solar energy (irradiation) into

thermal energy which is released into the environment (Fig. 2.1a). This important cycle of reactions of the $NO-O_3-NO_2$ triad is summarized by Vila-Guerau de Arellano and Duynkerke, (1992) as:

$$NO + O_3 \underset{k_2}{\overset{k_1}{\rightleftarrows}} NO_2 + O_2 + h\nu \ (\lambda \leq 420 \text{ nm}) \qquad (2.4)$$

Nitric oxide is also converted to nitrogen dioxide in small amounts (up to 25 % of total NO_x) by the oxygen in the air through thermal oxidation.

$$2NO + O_2 \longrightarrow 2NO_2 \qquad (2.5)$$

This cycle of reactions with the NO, O_3, and NO_2 (Fig 2.1a) however only produces an ozone concentration of 1 ppm or less. To reach higher ozone concentrations such as hundreds of ppm, as are commonly present in a polluted air, peroxyl radicals of hydrocarbons, and RO_2, must enter the reaction (Fig 2.1b) (National Academy of Sciences, 1977). In a irradiated smog-chamber containing propylene at 2.2 ppm and nitric oxide at 1.0 ppm, ozone started to form when the $NO:NO_2$ ratio reached 1 and continued forming until all the nitric oxide was converted to nitrogen dioxide (Fig 2.2) (National Academy of Sciences, 1977). This is a simplification of what happens on a daily basis in a smoggy area.

A series of reactions including the hydroxyl radical and carbon monoxide (CO) have been used to explain the major source of nitrogen dioxide.

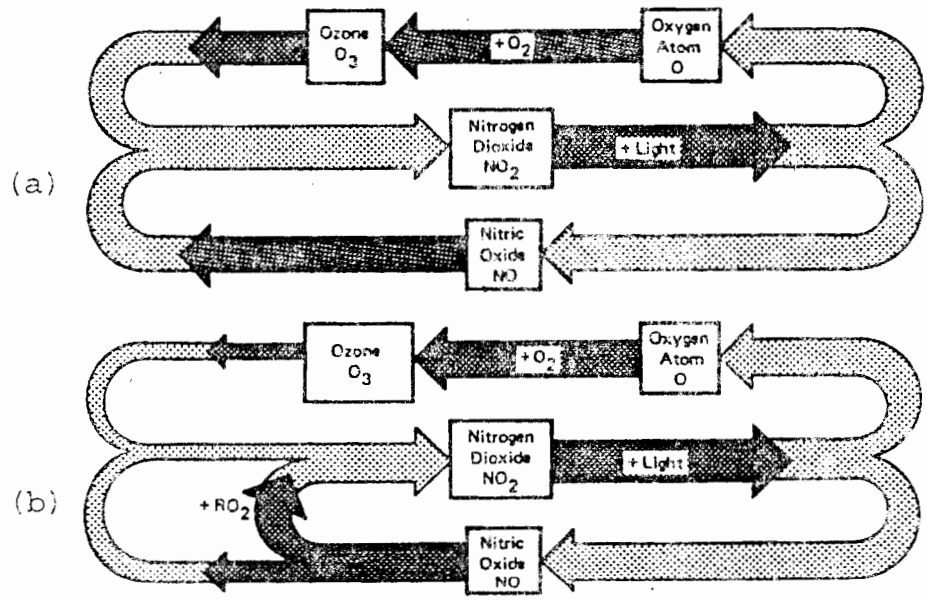

Figure 2.1. Represented above (a) is the $NO-NO_2-O_3$ cycle where nitric oxide and ozone are produced in a 1:1 ratio. Below (b), when other photochemical oxidants are present, they can form peroxy radicals which oxidize nitric oxide to nitrogen dioxide. This leads to a larger production of ozone (adapted from the National Academy of Sciences, 1977).

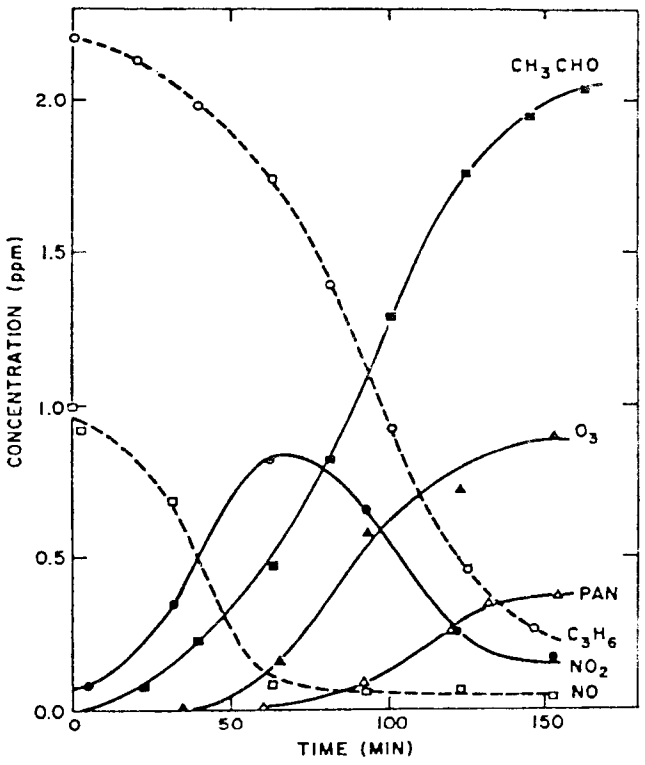

Figure 2.2. Trace-gas concentrations in a time profile for a irradiated smog chamber containing a propylene-NO mixture (Niki et al., 1972 as cited in National Academy of Sciences, 1977).

$$CO + HO \longrightarrow CO_2 + H \qquad (2.6)$$

$$H + O_2 + M \longrightarrow HO_2 + M \qquad (2.7)$$

$$HO_2 + NO \longrightarrow HO + NO_2 \qquad (2.8)$$

The hydroperoxyl radical formed in Reaction 2.7 oxidizes nitric oxide to nitrogen dioxide, and the hydroxyl radical is regenerated in Reaction 2.8 (National Academy of Sciences, 1977).

Aldehydes and hydrocarbons may contribute to production of carbon monoxide and hydroperoxyl radicals. A reaction including formaldehyde (CH_2O) the simplest example is shown:

$$HO + CH_2O \longrightarrow H_2O + HCO \qquad (2.9)$$

$$HCO + O_2 \longrightarrow HO_2 + CO \qquad (2.10)$$

$$HO_2 + NO \longrightarrow HO + NO_2 \qquad (2.11)$$

Aldehydes can also be decomposed by sunlight to form the hydroperoxyl radical (National Academy of Sciences, 1977).

$$CH_2O + \text{sunlight (3700-2900 Å)} \longrightarrow H + HCO \qquad (2.12)$$

Both the hydrogen atom and the formyl radical produced in Reaction 2.12 will react in air to form the hydroperoxyl radical:

$$H + O_2 + M \longrightarrow HO_2 + M \qquad (2.13)$$

$$HCO + O_2 \longrightarrow HO_2 + CO \qquad (2.14)$$

These oxidative cycles strongly affect the concentration of ozone (National Academy of Sciences, 1977). The products of the photolysis of nitrogen dioxide become unbalanced since most of the nitric oxide reacts with peroxyl radicals, thus the ozone concentration increases.

Also NO_2 reacts with hydroxyl to form nitric acid (HNO_3), a major component in acid rain (Penner et al, 1991).

$$HO + NO_2 + M \longrightarrow HONO_2 + M \qquad (2.15)$$

A summary of the chemical reactions of the NO-O_3-NO_2 triad, which are of most importance in this study, follows. In a clean atmosphere during the day NO reacts with O_3 to form NO_2 and O_2 and NO_2 is photolyzed back to NO and O_3 in a 1:1 ratio. During the night (without light) there is no formation of NO and O_3 from NO_2 allowing O_3 depletion and NO_2 accumulation.

2.2 Nitrogen cycling in the soil-plant-atmosphere system

All living organisms demand nitrogen in either its inorganic or organic form to accomplish their metabolic functions. Although the atmosphere consists of 78 % elemental nitrogen (N_2), this form of N is not directly available to plants (Tisdale et al., 1986; Gallon and Chaplin, 1987).

Nitrogen occurs in the environment in numerous forms in various oxidation states (Table 2.1). A reduction process, which requires an input of energy, is necessary to convert a compound from a higher oxidation state to a lower one; whereas oxidation yields energy. The more oxidized N compounds can serve as terminal electron receptors (Gallon and Chaplin, 1987).

Nitrogen is constantly cycling from the atmosphere,

Table 2.1. The different oxidation states of nitrogen when it is combined with other elements (adapted from Gallon et al., 1987).

oxidation state	compound		form
+5 (oxidized)	NO_3^-	nitrate	solid
+4	NO_2	nitrogen dioxide	gas
+3	NO_2^-	nitrite	solid
+2	NO	nitric oxide	gas
+1	N_2O	nitrous oxide	gas
0	N_2	dinitrogen *	gas
-1	NH_2OH	hydroxylamine	solid
-2	H_2NNH_2	hydrazine	liquid
-3	NH_3	ammonia	gas
-3 (reduced)	NH_4^+	ammonium	solid

* also called atmospheric, elemental, or free nitrogen

where it is in the form of N_2, to the many components of the biosphere and geosphere, where losses may occur by leaching and crop removal. Eventually nitrogen goes back to N_2 in the atmosphere (Fig 2.3).

2.2.1 Fixation of atmospheric nitrogen

Nitrogen fixation refers to the conversion of atmospheric N_2 to a non-elemental form by biological and non-biological processes. The biological process of reduction of N_2 to ammonia is carried out by Rhizobia and other symbiotic bacteria and also by free-living soil microorganisms such as diazotrops. The non-biological process refers to the fixation of N_2 into nitrogen oxides by atmospheric electrical discharges and to the fixation of N_2 into NH_3, NO_3^-, and urea (H_2NCONH_2) by the industrial manufacture of nitrogen fertilizers. Most nitrogen is fixed by microorganisms in the soil.

The following reaction represents biological fixation (Gallon and Chaplin, 1987).

$$N_2 + 3H_2O \longrightarrow 2NH_3 + 3/2O_2 \quad \Delta G^\circ = +340 \text{ kJ/mol } NH_3 \qquad (2.16)$$

On the other hand, the non-biological fixation is represented as follows:

$$CH_4 + H_2O \longrightarrow CO + 3H_2 \qquad \Delta G^\circ = +142 \text{ kJ/mol} \qquad (2.17)$$

$$N_2 + 3H_2 \longrightarrow 2NH_3 \qquad \Delta G^\circ = -33 \text{ kJ/mol} \qquad (2.18)$$

Net:

$$N_2 + CH_4 + H_2O \longrightarrow CO + 2NH_3 \quad \Delta G^\circ = +109 \text{ kJ/mol} \qquad (2.19)$$

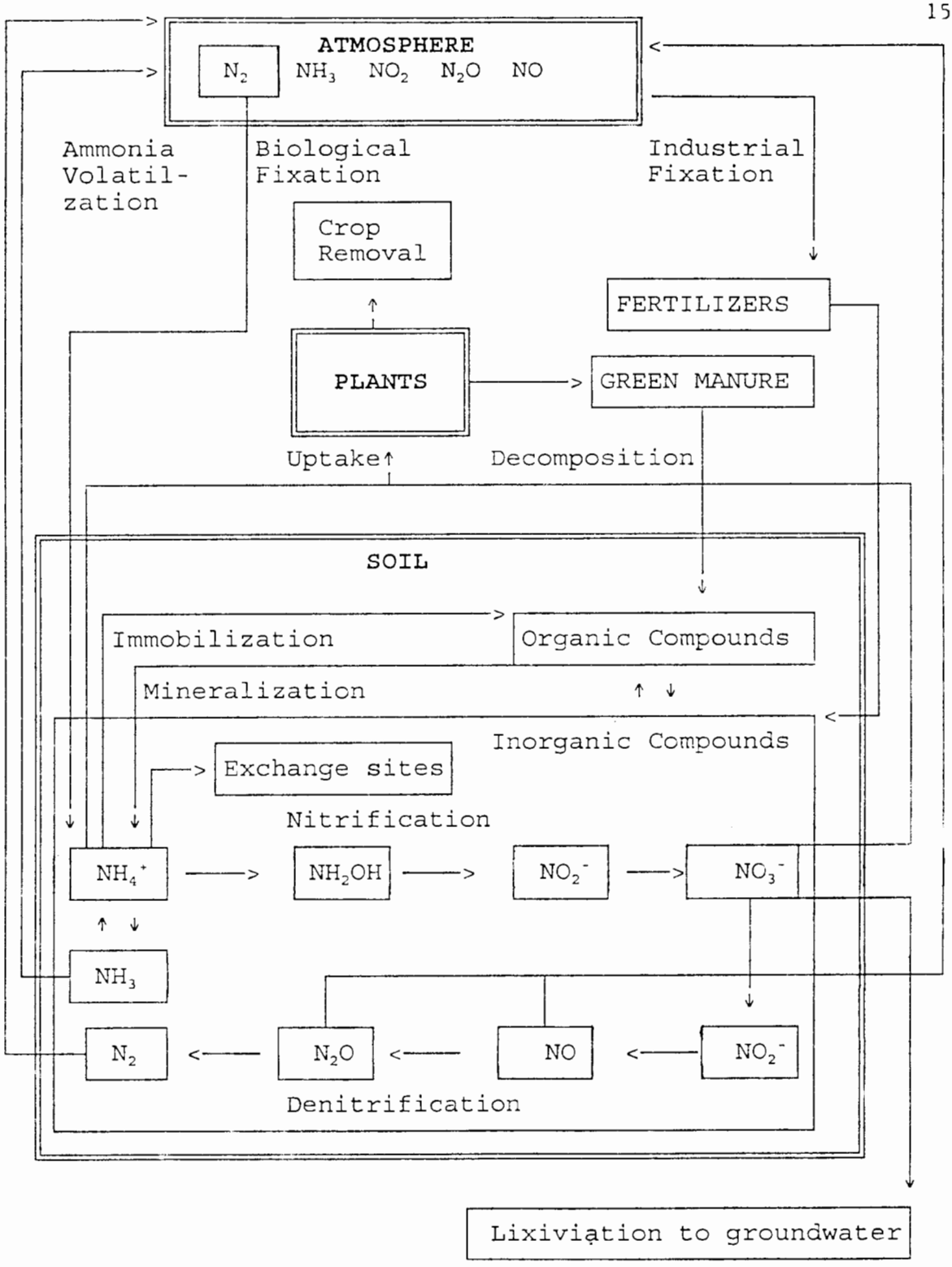

Figure 2.3. Nitrogen cycle for a cropped soil.

These reactions occur at high temperature and pressure (400-600°C and 10-20 MPa, respectively) (Gallon and Chaplin, 1987). When ΔG°, which is the standard free energy change of the reaction is positive, the reaction requires an input of energy; when it is negative, energy is released.

2.2.2 Uptake and assimilation

Inorganic compounds of nitrogen such as NH_4^+ and NO_3^- are taken up from the soil by plants to be converted into organic compounds, which animals can use. NH_4^+ is the preferred form since NO_3^- must first be reduced to be incorporated into amino acids, using energy from photosynthate; however, NH_4^+ can be held on the exchange sites and become unavailable for the plant, whereas NO_3^- can move to the roots by diffusion or by mass flow with water. NH_4^+ also depresses the absorption of other cations such as K^+, whereas NO_3^- depresses the absorption of Cl^- and SO_4^{2-} (Paul and Clark, 1989).

2.2.3 Mineralization of nitrogen compounds

Nitrogen in organic residues from dead plants and animals is converted to ammonium (NH_4^+), the mineral form, by the aerobic process of mineralization through heterotrophic microorganisms, which require organic carbon as a source of energy. Proteins are decomposed by hydrolysis to amines and amino acids, which are further used

by other heterotrophs releasing ammonium: these processes are called aminization and ammonification, as shown in Reactions 2.20 and 2.21, respectively.

$$R\text{-}NH_2 + HOH \longrightarrow NH_3 + R\text{--}OH + \text{energy} \qquad (2.20)$$

$$NH_3 + H_2O \longrightarrow NH_4^+ + OH^- \qquad (2.21)$$

where R is usually a C compound group.

Once ammonium has been formed it can have a number of fates (Paul and Clark, 1989):

1. It can be converted to nitrate by nitrification.

2. It can be absorbed by plants.

3. It can be used by soil microorganisms in further decomposing organic residues.

4. Ammonium is held on the exchange sites, where it can be replaced by cations in the soil solution.

5. NH_4^+ has a similar size compared to K^+, thus it can be fixed in the interlayers of clays.

6. If it is not adsorbed, ammonium can volatilize as ammonia (NH_3).

2.2.4 Immobilization

Nitrogen immobilization is the incorporation of ammonium into amino acids by microbial growth. It occurs when residues of low-nitrogen and high-carbon content begin to decompose. Soil microorganisms grow fast at high carbohydrate amounts, thus nitrogen is needed to form protoplasm. This leads to a reduction of available nitrogen

populations decline immobilized nutrients are released back to the soil for plant use (Paul and Clark, 1989, Tisdale et al., 1986).

2.2.5 Nitrification

Biological nitrification is the conversion of ammonium (NH_4^+) to nitrate (NO_3^-) under aerobic conditions by biological oxidation. Ammonium is first converted to hydroxylamine (NH_2OH) and nitrite (NO_2^-) mainly by Nitrosomonas, an obligate autotrophic bacteria (Tisdale et al., 1986, Gallon and Chaplin, 1987). The reaction is as follows:

$$2NH_4^+ + 3O_2 \longrightarrow 2NO_2^- + 2H_2O + 4H^+ \quad \Delta G^\circ = -65 \text{ kcal mol}^{-1} \qquad (2.22)$$

Nitrite is converted to nitrate mostly by Nitrobacter, an obligate autotrophic bacteria, but heterotrophs such as fungi, actinomycetes, and bacterial strains will also produce nitrate or nitrite, as follows:

$$2NO_2^- + O_2 \longrightarrow 2NO_3^- \qquad \Delta G_o = -18.2 \text{ kcal mol}^{-1} \qquad (2.23)$$

Once nitrate is formed in soils, it follows several paths (Fig 2.3 and 2.4): (1) it may undergo biological denitrification, (2) it may be taken up by plants and microorganisms (assimilative reduction), (3) it may used as electron acceptor and be reduced to ammonium by microorganisms under the absence of oxygen (dissimilative reduction), (4) it may be leached to the underground water,(5) it may be transported by runoff, or (6) it may accumulate in the soil (Paul and Clark, 1989).

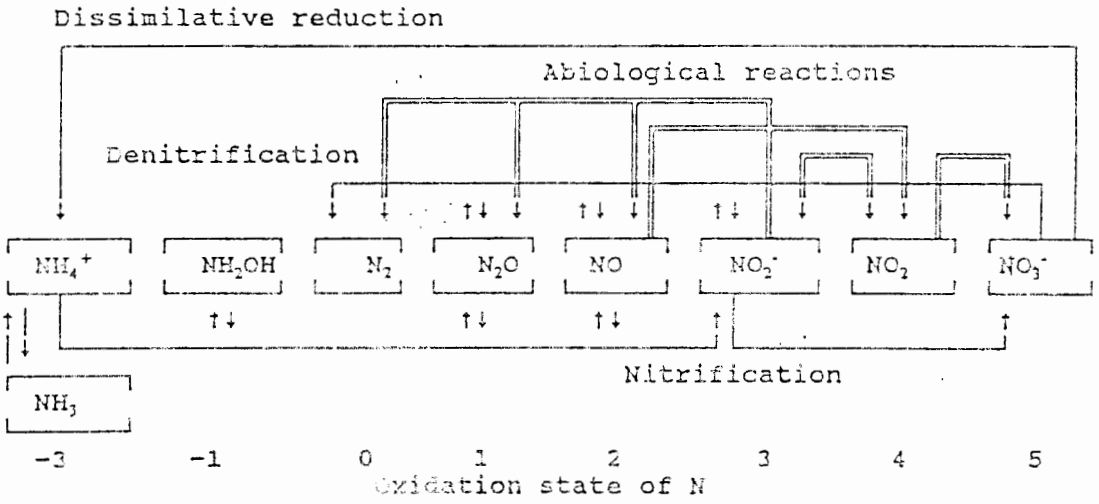

Figure 2.4 Biological and abiological production and consumption of NO and N_2O (Davidson, 1991; Fenchel et al., 1979).

A possible path of NO production by the oxidation of NH_2OH via nitrification was proposed by Firestone and Davidson, (1989) (Reaction 2.24) (Fig 2.3 and 2.4); however there is still uncertainty about how this process may occur.

$$NH_4^+ \longrightarrow NH_2OH \longrightarrow HNO \longrightarrow NO \longrightarrow NO_2^- \longrightarrow NO_3^- \quad (2.24)$$

Factors which affect nitrification rates in soils include the rate of organic-matter mineralization, the population size of nitrifying organisms, soil acidity and alkalinity, and soil physical properties such as temperature, aeration, and soil-moisture content (Fig. 2.5 shows controls on nitrification).

If conditions in soils are not favorable for mineralization and NH_3 release, no nitrification occurs due to lack of ammonium supply. The importance of NH_4^+ availability is illustrated in the conceptual model of proximal and distal factors (Fig. 2.5).

The soil water content controls the diffusion of oxygen and ammonia needed in the nitrification process under wet conditions, and controls bacterial survival under dry conditions. Aerobic bacteria require oxygen to nitrify, therefore nitrification rates generally decline as oxygen becomes unavailable (Firestone and Davidson, 1989). Autotrophic nitrification occurs over a wide range of soil moisture conditions provided that oxygen is available and the soil is not water saturated (Levine et al., 1984). The

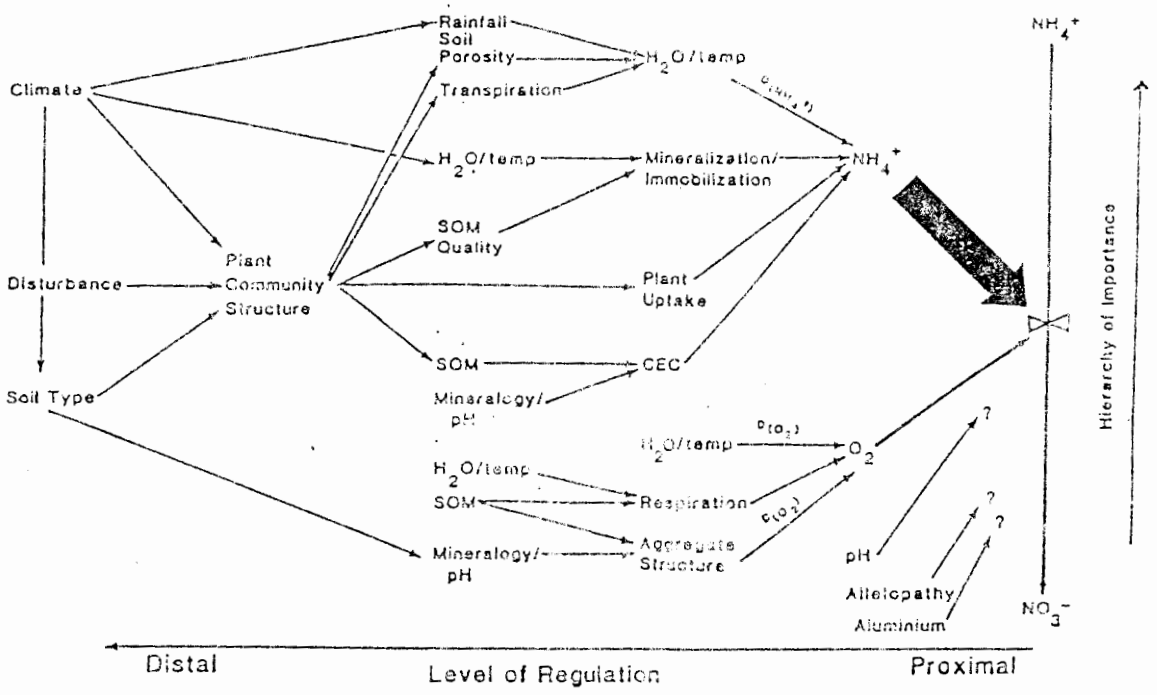

Figure 2.5 Schematic diagram showing the proximal controllers of nitrification at a cellular level, which in turn are regulated by soil and environmental factors (distal controllers) (adapted from Robertson, 1989 as given by Hutchinson and Davidson, 1993).

optimum moisture level varies with different soils, but in most, nitrification rate is highest at field capacity (soil water potential of -33 kPa), and it declines as the moisture content increases (Tisdale et al., 1986). Justice et al. (1962 as cited in Tisdale et al., 1986) found that even at a soil water potential of -1.5 MPa (wilting point) nitrification rates were near half those at 0.7 MPa.

The effect of temperature on nitrification has been studied. Below 5 and over 35 °C nitrification decreases, with a maximum rate between 30 and 35 °C (Stanford et al., 1977 as cited in Tisdale et al, 1986). Nitrification occurs in the pH range of 4.5 to about 10 and is maximal at pH 8.5 (Tisdale et al., 1986). A supply of calcium, phosphorus, iron, copper, and manganese is also needed by the nitrifying bacteria (Tisdale et al., 1986).

2.2.6. Denitrification

2.2.6.1 Biological denitrification

Biological denitrification is the conversion of nitrates to gaseous forms of nitrogen such as NO, N_2O, and N_2 by anaerobic microorganisms (Fig. 2.3 and 2.4). The ability of some microorganisms to denitrify permits electron transport in which oxides of nitrogen are used as terminal electron acceptors in place of O_2. The reactions responsible for denitrification are showed below (Tisdale et al., 1986; Gallon and Chaplin, 1987; Firestone and

Davidson, 1989):

$$2HNO_3 \xrightarrow[-2H_2O]{+4H} 2HNO_2 \xrightarrow[-2H_2O]{+2H} 2NO \xrightarrow[-H_2O]{+2H} N_2O \xrightarrow[-H_2O]{+2H} N_2 \qquad (2.25)$$

Many groups of bacteria are able to denitrify, but the Pseudomonas species has been found to be the most important group in most environments. The Alcaligenes species usually has the second most numerous population (Firestone and Davidson, 1989).

The soil factors affecting denitrification rates include the supply of oxygen and content of organic matter, nitrate, and carbon (proximal factors), which are affected by many environmental factors such as plants, soil-moisture content, soil aeration, soil pH, and soil temperature (distal factors) (Fig 2.6).

Water saturation of soils impedes O_2 diffusion by filling the pores and reducing aeration, and, hence, it creates anaerobic conditions, which enhances denitrification (Firestone and Davidson, 1989). Distal factors controlling soil moisture are rainfall, plant-water uptake, and soil texture. The soil water content is the dominant factor controlling denitrification in agricultural soils since soil nitrate levels are commonly high due to fertilization (Groffman et al., 1987).

High nitrate concentrations increase the rate of denitrification and the ratio of nitrous oxide to elemental nitrogen production (Tisdale et al., 1986). In N-fertilized

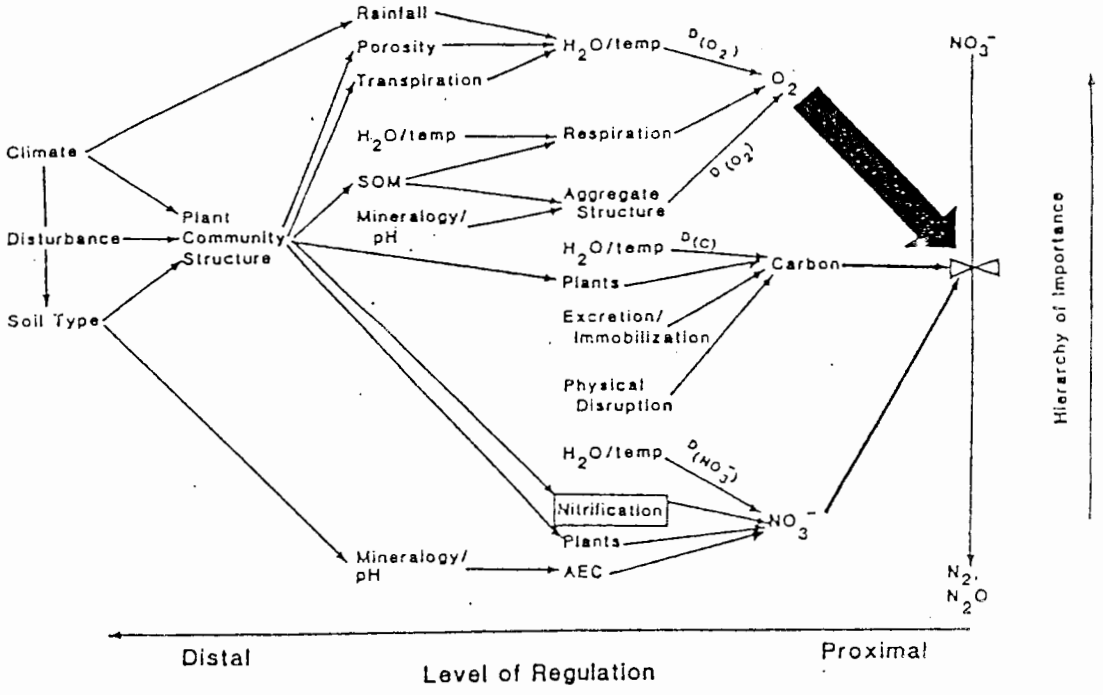

Figure 2.6 Relationships between proximal and distal factors controlling denitrification (Groffman et al., 1987 as adapted from Tiedje, 1987).

soils, nitrate is not a limiting factor; however, in unfertilized soils, mineralization is the only source of nitrate, and, thus, denitrification depends on distal factors such as soil type, soil organic matter levels, and climatic conditions (Groffman et al., 1987).

The abundance of readily decomposable organic materials will increase the soluble carbon in soil, increasing the energy source available to denitrifying bacteria (Burford and Bremmer, 1975 as cited in Tisdale et al., 1986). The following reaction illustrates this:

$$4(CH_2O) + 4NO_3^- + 4H^+ \longrightarrow 4CO_2 + 2N_2O + 6H_2O + \text{energy} \quad (2.26)$$

The rate of denitrification increases rapidly as temperature increases from 2 to 25 °C. It is slightly higher from 25 to 60 °C, and disappears at temperatures greater than 60 °C. Activity observed at about 60-65 °C is thought to be caused by Bacillus thermodenitricans (Garcia, 1974 as cited in Chalamet, 1983).

Soil acidity affects denitrification since denitrifying bacteria are sensitive to low pH. At pH values of 6 to 6.5, nitrous oxide is produced predominately. Nitric oxide is a dominant denitrification product at pHs lower than 5.0 (Fillery, 1983; Tisdale et al., 1986); however, the nitric oxide production in acidic media is not considered a biological denitrification product but to arise from chemodenitrification reactions by chemical decomposition of nitrite, which will be the next subject of discussion.

2.2.6.2 Chemodenitrification

Chemodenitrification refers to the chemical aerobic reactions that lead to nitrite (NO_2^-) decomposition by nonenzymatic pathways (Fig 2.4) (Paul and Clark, 1989; Chalk and Smith, 1983). Nitric oxide and nitrogen dioxide have been measured as nitrite decomposition products (Smith and Chalk, 1979 as cited in Chalk and Smith, 1983). The identified reactions are described below (Galbally, 1989; Firestone and Davidson, 1989; Chalk and Smith, 1983):

(1) Volatilization of HNO_2 from the soil aqueous solution.

$$HNO_2\ (g) = H^+ + NO_2^- \quad \Delta H = -7.0\ kcal/mol \qquad (2.27)$$

Since the pK_a for this equilibrium is 3.29 at 25°C (Aylward and Findlay, 1971 as cited in Chalk and Smith, 1983) in a system at pH 5, 4, and 3 the proportions of HNO_2 are 1.9, 16, and 74%, respectively. Nitrite is stable at pH ≥ 5.5.

(2) Decomposition of HNO_2 to NO and NO_3^-.

$$2H^+ + 3NO_2^- = 2NO\ (g) + NO_3^- + H_2O \qquad (2.28)$$

$$NO_2\ (g) + NO_2^- = NO_3^- + NO\ (g) \qquad (2.29)$$

$$3HNO_2 \longrightarrow H^+ + NO_3^- + H_2O + 2NO\ (g) \qquad (2.30)$$

$$2NO + O_2 \longrightarrow 2NO_2 \longrightarrow N_2O_4 + H_2O \longrightarrow HNO_2 + HNO_3 \qquad (2.31)$$

Reactions 2.28 and 2.29 show the decomposition of NO_2^- in acid soils. At equilibrium, calculated NO partial pressures of 10^{-5} to 10^{-2} bars and NO to NO_2 ratios of 10^4 to 10^8 indicate that NO will diffuse to the atmosphere (Galbally, 1989). Chemical decomposition of nitrous acid may occur spontaneously (Reaction 2.30), releasing NO which may escape

to the atmosphere or which may react with O_2 and water to form NO_3^- (Reaction 2.31) (Paul and Clark, 1989).

(3) Reaction of HNO_2 with soil organic matter.

Production of nitrogen gases by chemodenitrification of NO_2^- has been found to be increased by increased organic matter. Nitrous acid reacts with organic matter (specifically, phenolic sites according to Tisdale et al., 1986) to form CH_3ONO (methyl nitrite), which decomposes to form NO_2^- (Magalhaes et al., 1985 as cited in Galbally, 1989). Amino groups in the α position to carboxyls can also react with nitrous acid to form N_2:

$$RNH_2 + HNO_2 \longrightarrow ROH + H_2O + N_2 \qquad (2.32)$$

This reaction occurs in soil only at a pH of 5 or lower (Paul and Clark, 1989).

(4) Photolysis of NO_2^- in soil aqueous solution yielding NO.

$$NO_2^- + H_2O + h\nu \dashrightarrow NO + OH + OH^- \qquad (2.33)$$

Experiments on fertilized flooded rice found a NO flux of 5 x 10^{-6} ng N m^{-2} s^{-1} of the photolyzed NO_2^- (Galbally et al., 1987 as cited in Galbally, 1989). Apparently, this source of NO from soils is negligible.

2.3 Nitrogen balance

The atmospheric nitrogen is actively cycled to and from the surface (Table 2.2). Quantitative estimations of the nitrogen flow associated with each process of the nitrogen cycle have been made for various agricultural systems (Table

Table 2.2. Nitrogen contents and fluxes on a global basis in Tg (10^{12}g or a million metric tons) (Paul and Clark, 1989)

	Content	Annual flux
Atmospheric nitrogen (N_2)	3.9×10^9	
Soil nitrogen	105,000	
Soil N mineralized		3500
Plant uptake		1400
Symbiotic N_2 fixation		120
Associative and free living fixation		50
Fertilizer nitrogen		65
Fertilizer nitrogen utilized		26
Atmospheric inputs		25
Denitrification, volatilization		135
Runoff erosion		25
Leaching		93

2.3). The contribution of each process varies with place and time depending on environmental and other factors such as climate, type of soil, and agricultural practices. Most studies have a difficult time precisely determining the fluxes and accounting for all N. For a example, half of the studies show a difference between inputs and outputs. Small fluxes often are lost with errors. Garret (1991) found NO_2 evolution in a grassland in Ireland was 0.79% of the N cycled. Anderson and Levine (1987) in Virginia reported that 0.79 % of the added fertilizer (196.5 kg N ha^{-1} as anhydrous ammonia) was lost as NO. Johansson et al. (1988) reported that the loss of N as NO after 30 h of nitrate addition to the soil (120 kg N ha^{-1} as $NaNO_3$) was less than 0.5% of the applied N. The NO flux derived from fertilizer applications corresponded to loss rates of 0.04% for $NaNO_3$ and 3.3% for urea (Slemr and Seiler, 1984).

2.4 Nitrogen cycle processes important for NO production

In the nitrogen cycle, the NO flux is a minor flux (e.g. a NO flux of 10 ng m^{-2} s^{-1} corresponds to 3 kg ha^{-1} yr^{-1} which is small compared to many fluxes in Table 2.3). Nitrification, denitrification, and several abiological reactions including chemodenitrification have been identified as potential sources of both NO and N_2O. Generally, the nitrification process is considered the overwhelming source of NO production, while N_2O is produced

Table 2.3. Estimated nitrogen balance in kg ha^{-1} y^{-1} on agricultural systems (summarized from Frissel, 1978).

Location	U.K.	Japan	USA*	USA**	Israel	Brazil
Crop	winter wheat	paddy rice	corn grain	soy beans	grains ***	shrub tree++
Inputs:						
1. Fertilization	98	96	112	123	90	91
2. N-fixation	5	40			5	17
3. Dry and wet deposition	17	5	10	10	5	10
4. Mineralization	83		50	15	6	
5. Manure added		20				
6. Irrigation		17				
7. Plant residues					60	20
Total	203	178	172	148	166	138
Outputs:						
1. Denitrification		70	15	15		2
2. Ammonia volatilization	18					15
3. Leaching	10	20	15	10		1
4. Run-off		1	6	3		
5. Immobilization	83		10			
6. Plant uptake	95	96	126	120	166	141
Total	206	187	172	148	166	159
Inputs-outputs	-3	-9	0	0	0	-21

mainly during denitrification (Davidson, 1992; Hutchinson and Davidson, 1993).

Recent work, using chemiluminescence detectors to quantify NO and N_2O production from cultures of nitrifiers and denitrifiers, indicates that nitrifiers produced the highest concentrations of NO. The mole ratio of NO to N_2O was in most cases greater than one from nitrifiers (0.9 to 8.5) and as low as 0.01 from denitrifiers (Anderson and Levine, 1986). Chemoautotrophic nitrification has been recognized as an important source of NO and as the responsible first step of NH_4^+ oxidation to NO_2^- in cultures and more recently in soils (Hutchinson and Davidson, 1993).

Davidson (1992) reported that nitrification is a major source of NO. Measurements were made on soil incubations at, below, and above field capacity (moisture content). Acetylene was used as a nitrification inhibitor. NO production was greater below than at field capacity and it was strongly inhibited by acetylene at both moisture contents. On the other hand, N_2O production was two to five times higher when the soil was above than at field capacity, and it was not inhibited by acetylene. Both nitrification and denitrification were sources of NO and N_2O, with NO produced primarily via nitrification and N_2O produced primarily via denitrification.

Chemodenitrification is thought to be an important source of NO in acid soils by the decomposition of nitrous

acid (HNO_2). Chemodenitrification also occurs at soil microsites where NO_2^- can accumulate in thin water films and a low pH can occur (Davidson, 1992a as cited in Hutchinson and Davidson, 1993).

Chemodenitrification was responsible for most of the NO produced in cultures poisoned with saturated $HgCl_2$. Concentrations of NO in enclosed vessels peaked at about 8 and 3.8 μL NO L^{-1} for samples with and without additional nitrite, respectively (the medium initially contained 2.2 mM NO_2^- and 2.2 mM NO_2^- were added). NO emissions from nitrite supplemented samples remained high throughout the 20-h test (Anderson and Levine, 1986).

Other abiotic processes resulting in NO production in soils are the decomposition of hydroxylamine (NH_2OH) and reaction of NO_2^- with phenolic compounds in organic matter (Nelson, 1982 as cited in Hutchinson and Davidson, 1993). Abiological production of NO occurred with or without the addition of NO_2^- to sterilized samples (6.7 mg NO_2^--N L^{-1} added as KNO_2). The NO flux increased by a factor of 100 or more on samples with added nitrite (0.48 and 87.1 μg NO-N kg^{-1} non-nitrite and nitrite added respectively, during 6 h). The peak NO fluxes resulted in the loss of 6 % of the added NO_2^--N (Davidson, 1992).

Many of the numerous environmental factors that affect the nitrification and denitrification rates, as mentioned before, also affect the production ratio of NO to N_2O. NO

emissions are strongly dependant on soil temperature. Several studies have shown that NO emissions occur over a wide range of soil moisture conditions provided the soil microorganisms do not have water stress due to a deficit or saturation.

NO emission from soil is not usually considered a major denitrification product, since denitrification occurs at water contents high enough to restrict the diffusion of O_2 and other gases and, therefore, NO diffusion to the surface would be slow and the restriction might permit it to react before it reaches the surface (Hutchinson and Davidson, 1993).

Cyclic wetting and drying of the soil affect the N trace gas emissions. Changes in the O_2 diffusion produce transient periods in which both nitrification and denitrification are high, provided that there is enough N and C substrate for the microorganisms to function (Firestone and Davidson, 1989). Production of NO and N_2O was observed within one hour of wetting dry soil (Davidson, 1992) indicating that nitrifiers and denitrifiers become metabolically active rapidly after wetting.

NO and N_2O fluxes measured from an undisturbed savanna soil in Venezuela (pH 5.3, gravimetric soil water was 0.05 kg kg^{-1} dry soil, 33 ppm NH_4^+, 0.72 ppm NO_3^-) during the dry season were 7.9 and 1.2 ng N m^{-2} s^{-1} respectively (NO to N_2O ratio of 6.5) (Johansson et al., 1988).

Williams and Fehsenfeld (1991) considered the influence of temperature, soil water content and soil nitrate content on NO emissions at a grassland site in northern Colorado (pH 5.8; 1.1 and 2.8 ppm soil NO_3^- and NH_4^+, respectively; gravimetric soil water was from 0.01 to 0.13 kg kg^{-1} dry soil). Emissions nearly doubled (from 5 to 11 ng N $m^{-2}s^{-1}$) with a 10°C increase in temperature and outside a temperature range of 15 to 35 °C emissions decreased sharply. The emissions followed the soil temperature diurnal trend (the influence of light was separated from soil temperature). NO emissions from 0 to 200 ng N $m^{-2}s^{-1}$ were correlated to nitrate concentrations from 0.2 to 180 ppm.

NO emissions were higher at higher soil moisture levels in the Venezuelan savanna during the rainy season with fluxes of 16 to 117, 9 to 38, and 3 to 15 ng N $m^{-2}s^{-1}$ corresponding to gravimetric soil water levels of 0.15, 0.07, and 0.02 kg kg^{-1} dry soil, respectively (Johansson and Sanhueza, 1988). NO_2^- concentrations of 4 and 2.8 ppm corresponded to NO fluxes of 150 to 250 and 9 to 23 ng N m^{-2} s^{-1}, respectively (gravimetric soil water was 0.15 kg kg^{-1} dry soil) (Johansson and Sanhueza, 1988).

2.5 Effect of agricultural practices on NO evolution

The production and evolution of NO in the soil is dependent on various agricultural practices (Table 2.5).

Table 2.5 Management practices affecting NO emissions.

Fertilizer type
Application rate
Application technique
Timing of application
Tillage practices
Use of pesticides
Crop type
Crop structure (e.g. row spacing, crop morphology)
Irrigation type
Irrigation amount
Irrigation timing
Residual soil nitrogen and carbon

Only the general effects from fertilizer, crop, and irrigation have been studied and reported in the literature.

2.5.1 Effect of fertilizer

The effect of several fertilizer types on a hot, dry soil in Spain (pH = 7.4) showed that NO_x emissions were about 1.5, 4, 6 and 10-fold greater from plots fertilized with $NaNO_3$, NH_4NO_3, NH_4Cl, and urea, respectively compared to non-fertilized plots. The fertilizer was applied at a rate of 100 kg N ha^{-1} and 30 mm of water from irrigation and rainfall were applied for the two months of experiment (Slemr and Seiler, 1984). Slemr and Seiler (1984) in Germany observed NO_x emission peaks about 20 times bigger with fertilization than without 10 days after NH_4Cl application (pH = 7.4).

In Virginia on slightly acid soils with a gravimetric soil water ranging from 0.08 to 0.30 kg kg^{-1} dry soil,

Anderson and Levine (1987) reported NO fluxes of 1.7 ng N m^{-2} s^{-1} (0.53 kg N $ha^{-1}yr^{-1}$) from unfertilized fields, 1.9 ng N m^{-2} s^{-1} (0.61 kg N ha^{-1} yr^{-1}) from a field fertilized 3 months prior to measurements, and 6.6 ng N m^{-2} s^{-1} (2.08 kg N ha^{-1} yr^{-1}) from a moderately fertilized field (196.5 kg N ha^{-1}).

NO emissions from fertilized and unfertilized arable land in Sweden were 0.6 and 1.9 ng N m^{-2} s^{-1} (0.2 and 0.6 kg N ha^{-1} yr^{-1}), respectively (Johansson and Granat, 1984 as cited in Anderson and Levine, 1987).

In a Brazilian forest, Bakwin et al. (1990) measured NO increases of 5-fold to 150-fold 30 minutes after the nitrate and ammonium fertilizer application ($NaNO_3$ and NH_4Cl at a rate of 50 kg N ha^{-1} with water). NO emissions peaked 2 days after fertilization (10 and 87 ng NO m^{-2} s^{-1} for NH_4^+ and NO_3^- fertilization, respectively (45 and 374 x 10^9 molecules NO cm^{-2} s^{-1})).

In the same Brazilian forest as Bakwin et al. (1990), Kaplan et al. (1988) reported average NO fluxes of threefold to fourfold over NO fluxes from non-treated plots (12 $\pm$ 4 ng NO m^{-2} s^{-1} (5.23 $\pm$ 1.7 x 10^{10} molecules NO cm^{-2} s^{-1})) two weeks after a 200 kg NO_3^--N ha^{-1} fertilization.

Johansson et al. (1988) reported that the NO flux increased 100 times above the background level in a Venezuelan savanna after nitrate was added to the soil (120 kg N ha^{-1} (12 g N m^{-2}) as $NaNO_3$ dissolved in water corresponding to 3 mm of rain). The peak of 900 ng N m^{-2} s^{-1}

was observed 12 h after the fertilizer application. NO emissions were 70 times higher than N_2O emissions (810 and 12 ng N m^{-2} s^{-1}, respectively).

By providing an additional source of available nitrogen to the soil, mineral N fertilizers increase the emissions of nitrogen gases. Apparently the magnitude of N lost from applied fertilizers is small (about 1%) (Section 2.3) and the simultaneous increase in NO flux happens in a short time period (from hours to days). Contributions of nitric oxide from fresh crop residues have not been investigated.

2.5.2 Effect of irrigation

The effect of irrigation on the NO flux was studied in a savanna ecosystem during the dry season. The soil was extremely dry (gravimetric soil water of 0.005 kg kg^{-1} for the top 0.03 m of the soil). When 15 mm of water were applied only once to a plot, NO fluxes peaked (from 5 to 300 ng N m^{-2} s^{-1}) after the first 6 hours and decreased steadily to near zero over the following 4 days as the soil dried (Johansson et al., 1988). In another plot 3 mm of water was applied by sprinkler daily for 4 days. The NO emissions increased only 5 to 10 min after irrigation (from 5 to 70 ng N $m^{-2}s^{-1}$), peaked (at 140 ng N $m^{-2}s^{-1}$) one hour after the first irrigation, and thereafter decreased. The NO flux increase in response to subsequent irrigations was lower (e.g 50 ng N m^{-2} s^{-1}) compared with the increased emissions in response to

the first irrigation. Apparently large amounts of NO are emitted into the atmosphere at the beginning of the wetting period, but the emissions are slowly reduced once the soil remains wetted and the readily available N-containing compounds in the soil have been decomposed. This could be attributed partially to nitrogen mineralization rates. Further mineralization provides N-containing compounds to the microorganisms slowly but soil moisture favors mineralization. In fact, there was an increase of ammonium and nitrate concentration in the irrigated plots (Table 2.6).

Table 2.6. Changes in NH_4^+ and NO_3^- concentrations and pH after water treatments (0.1-m sampling depth) (Johansson et al., 1988).

Treatment	NH_4^+	NO_3^-	pH
	$\mu g\ N\ g^{-1}$ dry soil		
Control	33	0.72	5.3
Irrigated daily (3 mm d^{-1})	66	2.8	5.1
Irrigated once (3 mm d^{-1})	46	0.59	5.2
Irrigated once (15 mm d^{-1})	44	5.6	4.4

Anderson and Levine (1987) measured NO emissions from a wheat field in Colorado after an extended period of dry weather. The soil was unvegetated and the gravimetric soil water was 0.11. Application of 25.4 mm of water did not reach the field-capacity water content of 0.32 (the resulting gravimetric soil water content was 0.25). The NO flux was 6 and 16 ng $N\ m^{-2}s^{-1}$ a day before and a day after irrigation, respectively. The large increase in NO flux was

partially attributable to changes in the exchangeable NH_4^+ and NO_3^- concentrations from 4.6 to 17.1 and from 3.3 to 2.4 $\mu g\ g^{-1}$ soil, respectively, from one day to the other. They also measured NO and N_2O fluxes from a soybean field in Virginia following a 25.4 mm rain. The gravimetric soil water content before and after the rain was 0.18 and 0.25 (the water content of this soil at field capacity is 0.21). The site had been fertilized (exchangeable nitrate was 37 μg N g^{-1} soil). NO fluxes ranged from 8 to 48 ng N $m^{-2}s^{-1}$ before and decreased to 15 ng $m^{-2}s^{-1}$ 4 h after the rain, whereas N_2O increased sharply from 150 to 500 ng N $m^{-2}s^{-1}$ before and to 850 ng N $m^{-2}s^{-1}$ after the rain.

Slemr and Seiler (1984) observed that NO and NO_2 fluctuations from 10 to 100 ng N m^{-2} s^{-1} followed gravimetric soil water content fluctuations from 0.01 to 0.15 in Germany and Spain.

The water content in soils is an important factor controlling the activity of microorganisms and, thus, the biogenic emissions of NO from soil. NO emissions from soils respond to soil water content with initial irrigation causing the largest response. Large NO emissions are observed after wetting dry soil on a time frame of minutes to hours.

2.5.3 Effect of vegetation and crops

Vegetation affects NO and NO_2 fluxes in various ways.

The plant canopy acts as a porous source and sink to NO_x gas fluxes. NO and NO_2 can also be emitted or absorbed by plants. In a forest canopy, NO_x decreased gradually through the canopy away from the surface (Bakwin et al., 1990). Vegetation affects the emission of NO and NO_2 from soils by influencing the soil nutrient levels (ammonium, nitrate and carbon), aeration, temperature, and water content in the soil; through this influence the presence of plants has a strong impact on microbial nitrification and denitrification (Johansson, 1989). In this section, emissions and absorption by plants will be discussed.

2.5.3.1 NO_x deposition on plants

The uptake of NO_x is described in terms of the dry deposition, which depends on the surface and meteorological conditions. Deposition velocities (the flux divided by the concentration at a reference point above the surface) are the inverse of resistances to transport:

$$1/v_d = r_a + r_b + r_s \qquad [2.1]$$

where v_d is the dry deposition velocity, r_a is the aerodynamic resistance to turbulence, r_b is the boundary layer resistance to diffusion, and r_s is the surface resistance.

NO uptake constitutes a small flux compared to that of NO_2 (Galbally, 1989; Johansson, 1987 as cited in Johansson, 1989). NO can also be taken up by plants but at a much

slower rate than NO_2 due to its lower solubility (Hill, 1971 cited in Galbally and Roy, 1983); however, NO can be absorbed on soils by microbial processes such as nitrification and denitrification (Johansson and Galbally, 1984 cited in Johansson, 1989).

The leaf boundary layer resistance constitutes a small fraction of the total resistance, thus it has a negligible effect on the dry deposition velocity (Meyers, 1987 as cited in Johansson, 1989).

In the case of NO and NO_2, major emphasis will be given to the surface resistance since it consists of the resistance for plant uptake through the stomata and leaf surfaces and uptake on soil and litter (Johansson et al., 1989).

By one approach, the stomatal resistance can be derived from the following equation (Johansson, 1989):

$$r_s = r_{s,min}(1 + \beta/LA)\ D_w F_t D_g \qquad [2.2]$$

where $r_{s,min}$ is the minimum stomatal response; β is a light response factor; F_t, D_w, and D_g are functions of temperature, water vapor deficit, and gas diffusivity, respectively; and LA is the leaf area. Other important factors controlling stomatal resistance which are not in this equation are the leaf level in the canopy, absorbed photosynthetically active radiation, shading, leaf morphology, leaf age, and water stress.

A mesophyllic resistance (this involves NO_2 diffusion

and/or metabolic limitation), which seems to be independent from the stomatal resistance, has also been observed in several studies (Johansson, 1987 and Weseley et al., 1982 as cited in Johansson, 1989). It appears to be a major resistance to plant uptake. This resistance is associated with the diffusion paths of water vapor as it passes through the intercellular cavities within the leaves (Johansson, 1989; Galbally and Roy, 1983).

Grantz and Meinzer (1991) observed diurnal trends in canopy conductance for sugarcane that were parallel to those for net radiation, evapotranspiration, and photon flux density. The canopy conductance which included the stomatal, boundary layer, and aerodynamic components (which were not separated in their analysis) increased from 0.25 to 0.75 mol m^{-2} s^{-1} in the morning and decreased to about 0.1 mol m^{-2} s^{-1} in the afternoon.

NO_2 uptake on the cuticle of the leaves is only relevant at higher NO_2 concentrations (hundreds of ppbv) than those normally found in the atmosphere (Johansson, 1989).

Measurements on grassland using micrometeorological methods showed that stomata were the major sink for NO_2 with deposition velocities of 3 to 9 mm s^{-1} (Hargreaves et al., 1990 as cited in Fowler, 1992). NO_2 uptake by vegetation in rural areas of Europe and North America can be up to 6 or 8 mm s^{-1} at concentrations of 20 ppb or greater. NO_2 can also

be adsorbed within the plant cuticle (Lendzian and Kerstiens, 1988 as cited in Fowler, 1992).

Johansson, 1989 calculated a NO_2 dry deposition rate from 2 to 16 ng N m^{-2} s^{-1} based on a daytime deposition velocity of 5.6 mm s^{-1} determined by Wesely et al., (1982), and NO_2 concentrations of 0.5 to 5 ppbv in clean continental air. This dry deposition rate is similar to typical NO emission rates of 1 to 10 ng N m^{-2} s^{-1} from uncultivated soils (Johansson, 1989). Vitousek and Walker (1989) estimated a nitrogen deposition rate of 12 ng-N m^{-2} s^{-1} (3.8 kg-N ha^{-1} yr^{-1}) comprised mainly of NO_x species based on wet deposition at Kilauea, Hawaii.

2.5.3.2 NO_x release by plants

NO_x, which is taken up by plants through the stomata, absorbed onto leaf surfaces, or possibly by root uptake, may be later released making plants a source of NO_x. NO_2 fluxes can follow a diurnal trend possibly due to the diurnal trend in stomatal aperture which controls emission of NO_x and which in turn depends on radiation, leaf water potential, vapor pressure deficit, and temperature (Delany et al., 1986; Johansson, 1989).

The NO_2 absorbed by plants is rapidly converted (a matter of minutes) to other readily metabolized forms. In plants harvested and freeze-dried immediately after a 3-hr exposure to $^{15}NO_2$, 3% of the ^{15}N was found as $^{15}NO_3^-$, 35% as

soluble reduced ^{15}N (amino acids, amides, lipids, and chlorophyll), and 63% as insoluble ^{15}N compounds (proteins and nucleic acids) (Rogers et al., 1979 as cited in Galbally, 1989). Most of these N-comtaining compounds are unlikely to be quickly released as NO.

NO emissions from plants via absorption of inorganic nitrogen from the soil have not been confirmed by studies in the field.

Plants emit NO_x under special circumstances. It has been suggested that senescing plants can emit NO_x to the atmosphere (Wetselaar and Farquhar, 1980 as cited in Galbally, 1989). Herbicide treated plants can emit NO due to cell nitrite accumulation, which may be reduced to NO and NO_2 (Klepper, 1979 as cited in Johansson, 1989).

2.6 Comparison of NO fluxes

A summary of NO emissions from the soil measured by chambers in fertilized and non-fertilized land in agricultural and natural ecosystems is presented in Table 2.7. NO emissions are generally higher when fertilizer is applied simultaneously with water (from 0.1 to 250 ng N m^{-2} s^{-1}) than when water is applied alone to the soil (from 0.1 to 150 ng N m^{-2} s^{-1}). NO emissions from tropical agriculture have not been reported.

Table 2.7 Summary of NO emissions from soils as affected by agriculture from different sources (adapted from Kaplan et al., 1988; Johansson et al., 1988; Williams and Fehsenfeld, 1991)

Land use	Place	Time period	NO ($ngNm^{-2}s^{-1}$) mean flux	range	Ref
A. Fertilized					
Temperate cropland	Sweden	Apr-Sept	1.9*	0.1-62	1
Subtropical cropland	Spain	Sept-Oct		2-250	2
Temperate flooded rice	Australia	Dec		<0.2-0.95	3
Temperate cropland	USA	1 year	6.7*		4
Temperate pasture	UK	July-Aug	8	0-36	5
Grass			1.9*		6
Bermuda grass	Texas	0-9 week	44	13-186	7
Beans	Canada	0-5 month	25	0.42-162	8
Corn	Pennsylvania	1 month	94	1.6-338	9
B. Unfertilized or not recently fertilized					
Temperate cropland	Sweden	Apr-Sept	0.6*	0.3-17	1
Temperate cropland	USA	May-June	1.7*	0.003-67	4
Temperate cropland	UK	July-Aug	0.5**	-12-26	5
Bermuda grass	Texas		13	1-71	7
Beans	Canada	19 years		0.42-11.6	8
Wheat	Pennsylvania	1 year	1.2	0.21-3.8	9
C. Irrigated (wet/dry), or in rainy season					
Savanna, rainy	Venezuela	season	0.64	0.07-0.7	10
Savanna, rainy	Venezuela	season	56	2-250	11
Savanna, dry	Venezuela	season	8	3-15	12
+Chaparral, wet/dry	California		31	6-101	13
++Chaparral, wet/dry	California		13	0-35	13
Forest, upland, dry	Mexico	season	0.92		14
Forest, upland, wet	Mexico	season	2.8		14
Evergreen forest	Brazil		10.2	9.2-16	15

* weighted annual average, ** as NOx-N, + burned, ++ unburned, Ref = references, (1)Johansson and Granat, 1978, (2)Slemr and Seiler, 1984, (3)Galbally et al., 1987, (4)Anderson and Levine, 1987, (5)Colbourn et al., 1987, (6)Johansson and Galbally, 1984, (7)Hutchinson and Brams, 1992, (8)Shepherd et al., 1991, (9)Williams et al., 1988, (10)Sanhueza et al., 1990, (11)Johansson ans Sanhueza, 1988, (12)Johansson et al., 1988, (13)Anderson et al., 1988, (14)Davidson et al., 1991, (15)Kaplan et al., 1988.

2.7 NO_x conservation

2.7.1 Reactions which produce or consume NO_x

A number of reactions outside the $NO-O_3-NO_2$ triad produce or consume NO_x; however, they are not important in a short time-scale. Some examples are given. The NO_x concentration in the atmosphere can be modified by the oxidation of ammonia (NH_3) by reaction with hydroxyl radicals. The reactions are represented as follows:

$$NH_3 + OH \longrightarrow NH_2 + H_2O \quad (2.34)$$

$$NH_2 + NO \longrightarrow \text{products } (N_2, N_2O) \quad (2.35)$$

$$NH_2 + NO_2 \longrightarrow \text{products } (N_2, N_2O) \quad (2.36)$$

$$NH2 + O3 \longrightarrow \text{products (NH, HNO, NO)} \quad (2.37)$$

These reactions consume NO_x if the concentration of NO and NO_2 is greater than 0.06 ppbv or produce NO_x if the concentration of NO and NO_2 is less than 0.06 ppbv (Logan et al., 1981 as cited in Galbally and Roy, 1983). Another important reaction during night is the formation of NO_3 which reacts rapidly with NO_2 to form HNO_3 on a longer time scale (10 to 15 hours) (Johansson, 1989).

2.7.2 NO_2 emissions from the soil

NO_2 is somewhat soluble in water, but at equilibrium most NO_2 is in the gaseous and not in the aqueous phase. Further loss of NO_2 is limited by its reactions with species in water to form nitric acid, reactions which are slower than those in the air (B. Hubert to E.A. Graser, personal communication, 1994).

The importance of NO_2 emissions from the soil relative to contributions of NO to NO_x is still unresolved in the literature (Delany et al., 1986; Johansson, 1989; Wesely et al., 1989; Lee and Schartz, 1981 cited in Slemr and Seiler, 1984; Table 2.8).

Table 2.8 Surface fluxes of NO_2 from different sources (from Williams et al., 1987).

% of NO flux	Galbally and Roy (1978)	Slemr and Seiler (1984)	Johansson and Granat (1984)	Williams et al. (1987)	Williams et al. (1988)
NO_2 flux	< 4 %	125 %	5.9 %	10 %	6 %

Delany (personal communication to E.A. Graser, 1994) explains that NO_2 is harder than NO for the soil microorganisms to make. Johansson and Granat (1984 as cited in Delany et al., 1986), using a chamber system that removed O_3, found that the NO_2 flux was less than 10 % of the NO flux. Williams et al. (1987) found that the NO_2 flux was substantially reduced by wet soil and vegetation. NO_2 emissions were less than 2 % of the NO flux after precipitation. After precipitation NO_2 fluxes were strongly attenuated apparently by dampened vegetation, soil, and chamber walls. NO_2 was not detected during early morning measurements when the soil and vegetation were wet from condensation. They reported that the NO_2 flux was 9.7 % of the NO flux for the whole period. They expected that NO_2 would not contribute significantly to the NO_x emissions from

soils except in dry and bare areas. Williams et al. (1988) reported that the NO_2 emissions increased by a factor of 8 and 56 on two occasions after the vegetation in the chamber site was removed. Overall, they reported that the NO_2 emissions were about 6 % of the NO emissions. Slemr and Seiler (1984) reported large NO_2 fluxes from the surface and explained that NO_2 is mainly produced in the uppermost layer of the soil, and that it can be produced by biological and non-biological processes in the soil. Others have suggested that this NO_2 could have been formed in the measurement system which could indicate these measurements were artifacts of the measurement method (Williams et al., 1992 as cited in Hutchinson and Davidson, 1993). Slemr and Seiler (1984) observed that the NO_2 flux was positively correlated with solar radiation and soil moisture. They observed negative NO_2 fluxes on plant-covered soils, whereas emissions rates up to 417 ng N m^{-2} s^{-1} (1500 μg N m^{-2} h^{-1}) were measured on bare soils. The NO_2 flux was reduced by vegetation either by shading or by actual plant uptake at the leaf surface. Any NO_2 produced deeper in the soil has its transport to the surface limited because it is slightly soluble in water, reactive with organic matter, and easily absorbed by the soil (Lee and Schartz, 1981 as cited in Slemr and Seiler, 1984).

2.7.3 NO_x deposition on plants

(see Section 2.5.3.1)

2.7.4 NOx release by plants

(see Section 2.5.3.2)

2.8 Techniques for measuring trace gas fluxes

2.8.1 Chamber methods

Two kinds of chamber systems are commonly used to measure gas exchanges from the soil to the atmosphere in field conditions: transient systems where gas is allowed to accumulate, and steady-state systems where a steady concentration resembling that in ambient air is maintained in the chamber by circulating air with an appropriate concentration. A transient system is simpler because it does not require control of the air stream concentration to maintain the inside concentration at a constant level. The control required for a steady-state system requires real time monitoring of the chamber concentration, air flow control, and concentration control. Transient systems do not require air-flow and concentration control but reactive gases do require real-time monitoring.

Unfortunately the type of chamber affects the measured fluxes. The intent is to measure fluxes which would exist if no chamber were present, but any chamber has some effect on the flux. A major way chambers affect the flux by

changing the microclimate in the enclosed space (Section 2.8.1.1). A transient chamber also changes the atmospheric gas concentration and the soil to atmosphere gradient which drives the flux; a steady-state chamber minimize this modification (Section 2.8.1.1.3). To minimize these problems chambers are not left in place longer than necessary. Systematic differences in measured fluxes have been found depending on how long a transient chamber is left on the ground and on the flow rate for a steady-state chamber (Denmead 1979 as cited in Jchansson 1989).

Transient chambers tend to be closed chambers, but sometimes they are vented to avoid pressure differences from outside conditions (Section 2.8.1.1.2). Steady-state chambers may be open if outside air is used to maintain the steady inside concentration, but they also can be closed if the concentration of the inside air is kept steady by a scrubber or gas source (Denmead and Raupach, 1993).

The flux coming in or out of the soil into transient chambers is calculated based on the rate of concentration change over time in the chamber:

$$F_g = (V/A)\ d\rho_g/dt \qquad [2.3]$$

where F_g is the gas flux density, V is the volume enclosed in the chamber, A is the enclosed surface area, ρ_g is the density of the gas inside the chamber, and t is the time.

In steady-state systems, the flux is calculated as follows:

$$F_g = \nu\ (\rho_g - \rho_b)/A \qquad [2.4]$$

where ν is the gas flow rate, ρ_b is the background concentration of the gas, ρ_g is the concentration of the gas drawn from the chamber, and A is the cross-sectional area of the withdrawal port.

Although chamber methods have been criticized because of the non-representative microclimate that is formed inside the enclosure and the small surface area enclosed, they are used extensively in studies where replication in space and time is needed, because of their potentially low cost and portability. In the following sections, several of the physical and biological disturbances of the soil and the air above it caused by chambers and various other errors associated with chamber usage and data analysis will be discussed in more detail.

2.8.1.1 Physical and biological disturbances

2.8.1.1.1 Temperature effects. The biological production of trace gases such as NO, N_2O, CO_2, and CH_4 in the soil strongly depends on temperature, so the temperature inside chambers should be maintained like that outside; however, it is difficult to keep the same temperature inside and outside the chamber, because the energy balance at the soil surface is modified. The magnitude of this disturbation can be minimized by sampling for short-time periods (minutes) and by using a chamber which has been

designed to reduce solar heating (for example by using a insulative material and external reflective cover). Matthias et al. (1980 as cited in Hutchinson and Livingston 1993) found that chambers made of insulated metal caused the least temperature perturbation on both air and soil temperature compared to other materials such as plexiglas or metal alone.

2.8.1.1.2 Pressure effects. Atmospheric pressure differences between inside and outside of the chamber can be either mean pressure differences or differences in the pressure fluctuations. The mean air pressure is caused by the modification of the energy balance inside the chamber if the chamber interior is not connected (such as by a vent) to the atmosphere. Fluctuations in air movement over the soil surface causes pressure fluctuations which cause air to "pump" into and out of the soil (Hutchinson and Livingston, 1993; Denmead, 1979a as cited in Denmead and Raupach, 1993). If the pumping action induced by the pressure fluctuations are eliminated by the chamber, then the gas exchange reduces, and the flux rate is mainly determined by a concentration buildup that represents the net gas production in the soil (Kimball, 1983 as cited in Hutchinson and Livingston, 1993). Differences between instantaneous air pressure inside and outside of the chamber can be made negligible if a closed chamber is vented with a hole of

proper size and shape, but this solution also allows exchange of air between inside and outside of the enclosure. Hutchinson and Mosier (1981 as cited in Hutchinson and Livingston, 1993) suggested using a vent tube with a sufficient volume to hold exhausted air and return it back to the chamber when ambient pressure decreases and increases, respectively. This would allow losses of the trace gas only by diffusion down the tube.

2.8.1.1.3 Concentrations effects. The exchange rate of a trace gas is decreased immediately by the reduction of the concentration gradient due to a concentration buildup in either a closed or an open chamber. The concentration buildup is most severe in a closed chamber and continues throughout the whole sampling period. Equation [2.4] assumes a constant flux over time and can underestimate fluxes if they change over time. Gas sampling over-short time periods reduces the non-linearity (Anthony and Hutchinson, 1990 as cited in Hutchinson and Livingston, 1993).

2.8.1.1.4 Site disturbances. Soil compaction caused by the installment of chamber collars and by frequent walking around the chamber site during sample collection can affect soil properties important to microbial activity and can modify gas path ways as soil pores are blocked. The

collar insertion can also modify the nutrient cycling between plants and microorganisms by destroying plant roots.

2.8.1.2 Measurement and flux estimation bias

2.8.1.2.1 Analysis bias and sample handling. Trace gas exchange measurement bias can be introduced by the sample transport and/or storage procedure and the analytical procedure. Photochemical reactions between the NO-NO_2-O_3 triad continue to occur while the air sample is transported from the chamber to the analyzer, and gas uptake (or production) by the chamber walls and tubing can lead to NO flux underestimation (Johansson, 1989; Hutchinson and Livingston, 1993). The chemical reaction bias is not a problem in closed chambers when the NO_x flux is measured.

2.8.1.2.2 Flux calculation bias. Procedures to calculate trace gas fluxes from concentration measurements need to account for the effect of chambers on the measured process or estimation errors will occur. For the transient chamber approach, exchange rates are best predicted by linear regression from concentration changes measured just after the chamber is installed on the ground, because at that time a linear trend is followed and disturbance of the soil environment is still minimal. A non-linear model is needed for longer sampling periods to account for the decreases in the rate of exchange over time that result from

concentration buildup in the chamber (Hutchinson and Livingston, 1993).

2.8.1.3 Sampling design and data analysis errors

Trace gas exchange measurements based on chambers without extensive sampling are criticized because they do not represent the extent of spatial and temporal variability existing in a field. Trace gas production in soil can be highly variable over a distance of less than one meter and over time of less than one hour (Morrissey and Livingston, 1992 and Williams and Fehsenfeld, 1991 as cited in Hutchinson and Livingston, 1993). The environmental factors which affect the trace gas exchange rate, the variability in the field, and the anticipated statistical analysis should be considered in order to determine the number and location of chamber-measurement sites (Hutchinson and Livingston, 1993).

2.8.2 Micrometeorological methods

Micrometeorological techniques are used for measuring trace gas exchange because they provide an average flux over large areas thereby accounting for the spatial variability, they do not disturb the biological and physical processes responsible of gas production in the soil, and they allow monitoring of environmental factors effects by rapid and continuous measurements. The practical considerations limit

the application of these methods: a large, level, and homogeneous site is needed, so the gas concentration profile is adjusted to the local rate of exchange, horizontal concentration gradients are negligible, and the vertical flux is constant with height; accurate instruments with a rapid response are required to measure the small gas concentration differences (Denmead, 1983; Denmead and Raupach, 1993). Such fields are not always available and such instruments are not available for all gases.

Above-canopy placement of the instruments is limited by field characteristics. The air stream is affected by surface characteristics. When the air passes over a new surface, at the "leading edge", air begins to adjust to it forming what is called the "internal boundary layer" (Fig. 2.7). Only 10 % of the internal boundary layer is "fully adjusted", or in complete equilibrium with the new surface conditions (Rosenberg, 1983). The thickness of the fully adjusted layer (FAL) above the zero plane displacement (d) can be calculated as:

$$FAL = 0.1\ x^{4/5}\ z_0^{1/5} \qquad [2.5]$$

where x is the distance downwind from the leading edge and z_0 is the roughness parameter for the new surface. d and z_0 are approximately 64% and 13% the height of the crop (Campbell, 1986). This layer is important since it provides the limit below which sensors must be placed to represent the surface conditions. Equation [2.5] yields a height-to-

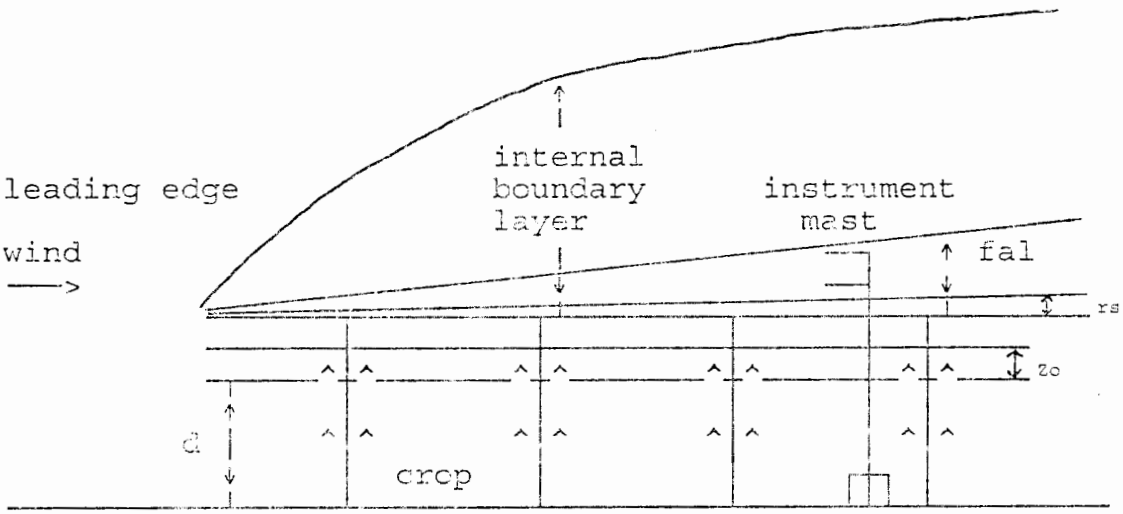

fal = fully adjusted layer
rs = roughness sublayer

Figure 2.7 Layers formed as air flows from a smooth to a rougher crop surface.

fetch ratio of about 1:50 for crops; however, it is good practice to use the more conservative ratio of 1:100 (Rosenberg et al., 1983). Oke (1987) suggests 100-200:1.

Within the turbulent surface layer, also called the "constant flux" layer, which reaches from immediately above the surface to 100 m above the surface in the daytime and to 10 m at night (Lenschow and Delany, 1987; Vila-Guerau de Arellano and Duynkerke, 1992; Oke, 1987, p.40), fluxes are constant with height and horizontally homogeneous with an adequate averaging period of 20 minutes to 1 hour (Rosenberg et al., 1983). For crops, the internal boundary layer remains within the constant flux layer.

2.8.2.1 Gradient techniques

Flux-gradient methods are based on the principle that the vertical transport of trace gases in the lower atmosphere occurs by turbulent diffusion along a gradient of mean concentration. The relationship can be written as follows:

$$F_g = -\overline{\rho_a} \, K_g \, \overline{\partial s/\partial z} \qquad [2.6]$$

where ρ_a is the density of dry air, K_g is the eddy diffusivity of the gas, $s (=\rho_g/\rho_a)$ is the mixing ratio of the gas with respect to dry air, z is the height, and the overbar denotes a time average. This equation is for mean conditions which can usually be represented by a 20 to 30 minute average. Unlike molecular diffusion which is the

movement of individual molecules, eddy diffusion is the movement of groups of molecules. Therefore the eddy diffusivity is much greater than the molecular diffusivity. The eddy diffusivity depends on wind speed, height above the surface, aerodynamic roughness of the surface, and atmospheric stability (Denmead and Raupach, 1993).

The energy balance Bowen-ratio method is a flux gradient approach to determining K_s. This method is based on the principle that the energy that is gained by natural systems is balanced by losses of energy to the atmosphere and soil and changes in the energy storage in the system. For cropping systems, the relationship is represented as follows:

$$Rn + H + LE + GO + M + St = 0 \qquad [2.7]$$

where Rn is the net radiation (the difference between downward and upward radiation fluxes), LE is the latent energy flux density, H is the sensible heat flux density, GO is the flux of heat into the soil or water, M is the heat stored by photosynthesis and by other miscellaneous processes, and St is the storage of heat in the air and plants by changes in system temperature and humidity. M and St are usually so small as to be negligible. The eddy diffusivities for the transport of heat (K_h), water vapor (K_v), and trace gases (K_g) are assumed to be equal, so, consequently, the eddy diffusivity for heat or water vapor are measured to give the eddy diffusivity for the trace gas.

Sensible heat flux (H) is the energy moved through the air by convection along the temperature gradient (heat transfer occurs from warm to cool areas). During the day this energy typically comes from surfaces heated by solar radiation such as the soil, plants, etc. The sensible heat flux density can be expressed in terms of gradients (for example, for the Bowen-ratio-energy-balance method):

$$H = \rho\ c_p\ K_H\ \Delta T/\Delta z \qquad [2.8]$$

where ρ is the density of air (0.0012×10^3 kg m^{-3}),

c_p is the specific heat of air at a constant pressure (1.01×10^3 J kg^{-1} K^{-1}),

K_H is the eddy diffusivity for heat,

ΔT is the temperature gradient, and

Δz is the vertical height interval (m).

Latent heat flux (LE) is the energy transfer carried by the water vapor coming from the evapotranspiration process (evaporation and transpiration). The water vapor flux density, E, can be expressed by the following gradient formula:

$$E = K_v\ \Delta\rho_v/\Delta z\ [m^2\ s^{-1} * kg\ m^{-3} * m^{-1} = kg\ m^{-2}\ s^{-1}] \qquad [2.9]$$

where ρ_v is the vapor density, and K_v is the eddy diffusivity for water vapor. Adding the latent heat of vaporization (L) we can convert water vapor flux density into latent heat flux density.

$$LE = L\ K_v\ \Delta\rho_v/\Delta z \qquad [2.10]$$

Equation [2.9] can be simplified and rearranged as follows:

$$Rn + GO + LE + H = 0 \quad [2.11]$$

$$Rn + GO = - (LE + H) \quad [2.12]$$

$$Rn + GO = - K (L (\Delta\rho_v/\Delta z) + \rho_a Cp (\Delta T/\Delta z)) \quad [2.13]$$

Thus K can be expressed as follows:

$$K = - (Rn + GO)/(L \Delta\rho_v/\Delta z) + \rho_a Cp (\Delta T/\Delta z)) \quad [2.14]$$

The Bowen ratio method is less accurate at night when net radiation, water vapor, and heat fluxes are near zero, so errors in the eddy diffusivity are greatest.

Webb et al. (1980) suggested that corrections for density effects on gas transfer should be made due to gas density variations in the air due to sensible heat and water vapor fluxes; however, when the gas concentration is measured relative to dry air and at a common temperature this correction is not needed. Often gradient techniques can be designed to remove water vapor and unify temperatures.

2.8.2.2 Eddy correlation

The mean flux density of a gas is the product of the instantaneous vertical wind speed (w) and the instantaneous gas density (ρ_g), and it is represented as follows:

$$F_g = \overline{w\rho_g} \quad [2.15]$$

Both w and ρ_g can be expressed as sums of means and fluctuations from those means (the mean is represented by an overbar and the fluctuation is denoted by a prime) where $w = \overline{w} + w'$ and $\rho_g = \overline{\rho_g} + \rho_g'$. Thus

$$F_g = \overline{w}\,\overline{\rho_g} + \overline{w'\rho_g'} \qquad [2.16]$$

Because there is not flow of air into the ground, w = 0, so this equation can be simplified to just the average of the product of the fluctuations. For many trace gases, an analyzer to measure ρ_g or ρ_g' is not yet available.

2.9 Micrometeorological principles applied to reactive trace gas fluxes

The flux of inert species is constant with height in the surface layer with adequate fetch, and it can be determined from the gradient and the eddy diffusion coefficient or eddy diffusivity (K) which is equivalent for sensible heat, water vapor, and trace gases.

The measurement of fluxes of chemically reactive gases above the canopy such as the NO-O_3-NO_2 triad can be difficult because reactions begin happening even before the species reach the measurement height and continue in the measurement layer causing a flux divergence which violates the assumptions of the flux gradient approach. This happens because the reaction time scale for the NO-O_3-NO_2 triad is of the same order of magnitude as the turbulent time scale. Lenschow and Delany (1987) reported a reaction time scale of 30 to 70 s in the boundary layer. The turbulent diffusion time scale at a measurement height z is determined by $z/\kappa u_*$ (Lenschow and Delany, 1987) where $\kappa = 0.4$ is the Von Karman constant and u_* is the friction velocity, or $\tau_t = z\kappa/u_*$.

(Fitzgerald and Lenschow, 1985), or $\tau_t = \kappa\ (z + z_0)/Au.$, where A is $w^2/u.^2$ or 1.56 (Panofsky and Dutton, 1984 as cited in Vila-Guerau de Arellano and Duynkerke, 1992), or $\tau_t = z/u.$ (Stull, 1980). A diffusion time scale of 100 to 200 s at 8 m above the ground was reported by Delany et al. (1986).

The NO and NO_2 fluxes determined by inert K approaches (Section 2.8.2.1) based on NO or NO_2 concentration gradients can be and usually are erroneous because of the chemical reactions between NO, O_3, and NO_2. The inert K approach can be applied to a conserved entity such as NO_x (NO + NO_2). The inert eddy diffusivity needs to be modified for reactive species.

Several theoretical studies have already been done on the effect that chemical reactions have on estimation of the flux of reactive species. Using a numerical model that included the chemical reactions, Fitzjarrald and Lenschow (1983) reported that the calculated fluxes for NO/NO_x ratios less than 0.1 were 10 to 20 % different from the non-reactive fluxes; Lenschow and Delany (1987) reported that the flux at a height of about 1 m already deviates from its surface value by 23%. When they assume ozone is constant with height and the photostationary state is reached at large heights, they find the ratio of the flux of NO to NO_2 is equal to the ratio of their concentrations. Vila-Guerau de Arellano and Duynkerke (1992) developed a reactive K-

theory model and compared it to the inert K-theory model. They found that the maximum difference between the reactive and inert K is 30 % for NO, 5 % for NO_2 and 3 % for O_2. The Vila-Guerau de Arellano and Duynkerke approach will be developed further and two other approaches discussed.

The effect of chemical reactions on turbulent transport is frequently analyzed under conditions of neutral atmospheric stability because then the shape of the wind profile can be expressed in a simple logarithmic form. Changes in the shape of the wind profile due to thermal stability are accounted for by ϕ_m the empirically determined Monin-Obukhov function as follows (Rosenberg et al., 1983; Oke, 1987):

$$\frac{\partial U}{\partial z} = \frac{u_*}{\kappa z} \phi_m \qquad [2.17]$$

where $\partial U/\partial z$ is the vertical gradient of mean wind speed, u^* is the friction velocity, κ is the Von Karman's constant, and z is height. For neutral conditions ϕ_m equals to 1 and Equation [2.6] converts into a logarithmic wind profile equation written as:

$$U(z) = \frac{u_*}{\kappa} \ln \frac{z}{z_0} \qquad [2.18]$$

The chemical cycling of the NO-O_3-NO_2 triad is represented as follows:

$$NO + O_3 \underset{k_1 \longrightarrow}{\overset{\longleftarrow k_2}{}} NO_2 + O_2 + h\nu \ (\lambda \leq 420 \text{ nm}) \qquad (2.4)$$

where k_1 and k_2 are the reaction rates of the second and first order reactions, respectively (sometimes they are called k and j, Lenschow and Delany, 1987). The flux equation for the $NO-O_3-NO_2$ triad that includes the turbulence in the neutral boundary layer and also the chemical reactions can be written as follows:

$$\underset{(a)}{\frac{\partial \overline{wc_i}}{\partial t}} + \underset{(b)}{\overline{w^2}\left(\frac{\partial \overline{C_i}}{\partial z}\right)} + \underset{(c)}{\frac{1}{\rho}\overline{\left(c_i \frac{\partial p}{\partial z}\right)}} + \underset{(d)}{\frac{\partial \overline{w^2 c_i}}{\partial z}} \qquad [2.19]$$

$$= v_i \Big(\underset{m,n}{\overset{2}{\Sigma}} (1 - \delta_{mn}) k_1 \overline{C_m} \overline{wc_n} - k_2 \overline{wc_3} \Big)$$

$$\underset{(e)}{\qquad\qquad} \underset{(f)}{\qquad\qquad}$$

where the values $i = 1$, 2 and 3 represent NO, O_3, and NO_2, respectively; $\overline{(C_i)}$ and (c_i) are the time-averaged and fluctuating terms of the decomposed (split) concentrations (c_i), respectively; w is the vertical velocity; p is the pressure; ρ is the density; Kronecker's delta (δ_{mn}) is equal to 1 if $m = n$ and equal to 0 if $m \neq n$; and the vector v_i is equal to (-1, -1, 1). The overbars represent averaging over time. The terms represent (a), the flux change over time; (b), the flux along the concentration gradient; (c), the flux due to a pressure gradient; (d), the flux due to the vertical velocity; and (e) and (f), the fluxes produced/destroyed by the second-order and first-order chemical reactions, respectively. Terms (a) and (d) are small compared to the others (Wyngaard, 1982 as cited in

Vila-Guerau de Arellano and Duynkerke, 1992). Term (c) can be parameterized as a function of the turbulent time scale (Wyngaard and Cote, 1971 as cited in Vila-Guerau de Arellano and Duynkerke, 1992) and is written as:

$$\frac{1}{\rho}\overline{\left(c_i \frac{\partial p}{\partial z}\right)} = \frac{\overline{wc_i}}{\tau_t} \qquad [2.20]$$

The flux equation is summarized as follows:

$$\overline{wc_i} = K_{ij}\left(\frac{\partial \overline{C_j}}{\partial z}\right) \qquad [2.21a]$$

where the units of $\overline{wc_i}$ are ppb m s^{-1}, or

$$\overline{wc_i} = K_{ij} * \frac{\partial \overline{c_j}}{\partial z} * \frac{mw_j\ P}{R\ T} \qquad [2.21b]$$

where the units of $\overline{wc_i}$ are ng m^{-2} s^{-1} (Section 5.2.2.2) and where K_{ij} is the effective reactive turbulent exchange coefficient that can be expressed as follows in the form of a matrix:

$$K_{ij} = \frac{\kappa u_*(z + z_0)}{1 + r_1 + r_2 + r_3}\begin{pmatrix} 1 + r_1 + r_3 & -r_1 & r_3 \\ -r_2 & 1 + r_2 + r_3 & r_3 \\ r_2 & r_1 & 1 + r_1 + r_2 \end{pmatrix} \qquad [2.22]$$

where r_1, r_2, and r_3 are the ratios between the turbulent and chemical reaction time scales and are defined as:

$$r_1 = \frac{\kappa(z + z_0)k_1\overline{NO}}{Au_*} \qquad [2.23]$$

$$r_2 = \frac{\kappa(z + z_0)k_1\overline{O_3}}{Au_*} \qquad [2.24]$$

$$r_3 = \frac{\kappa(z + z_0)k_2}{Au_*} \qquad [2.25]$$

This model requires six boundary conditions (the concentrations and fluxes of NO, O_3, and NO_2) in order to solve the three differential equations (Vila-Guerau de Arellano and Duynkerke, 1992). The flux of NO_x is obtained by adding equations 1 and 3 in the matrix (Eq. [2.23]).

If this model is applied to fluxes of slowly reactive or inert species near the ground (where chemical reactions are not influenced by turbulence and the chemical transformations time scale is much larger than the turbulence time scale so if r_1, r_2, and $r_3 \ll 1$), K11 = K22 = K33 = $\kappa u_*(z + z_0)$, that is,

$$K_{ij} = -\kappa u_*(z + z_0) \begin{pmatrix} 1 & 0 & 0 \\ 0 & 1 & 0 \\ 0 & 0 & 1 \end{pmatrix} \qquad [2.26]$$

In this case the eddy diffusivity has its inert value.

The application of this model to moderately reactive species (the time scale for chemical transformations and turbulence is the same and therefore r_2 and r_3 are close to 1 and r_1 is much less than 1) such as with the NO-O_3-NO_2 triad at the top of the surface layer ($z \approx 100$ m) where the O_3 concentration is assumed to be several times higher than the NO concentration (O_3/NO ≈ 50) results in the following

expression for K (Vila-Guerau de Arellano and Duynkerke, 1992):

$$K_{ij} = \frac{-\kappa u_*(z + z_0)}{1 + r_2 + r_3} \begin{pmatrix} 1 + r_3 & 0 & r_3 \\ -r_2 & 1 + r_2 + r_3 & r_3 \\ r_2 & 0 & 1 + r_2 \end{pmatrix} \quad [2.27]$$

The effect of turbulence on chemical reactions can be seen when the time scale of chemical transformations is smaller than the turbulence time scale. This usually happens above the top of the surface layer ($z \geqslant 100$ m). If the O_3 concentration is assumed to be much higher than the NO concentration (Vila-Guerau de Arellano and Duynkerke, 1992), r_2, $r_3 \gg r_1 \gg 1$ and K can be expressed as:

$$K_{ij} = \frac{-\kappa u_*(z + z_0)}{r_2 + r_3} \begin{pmatrix} r_3 & 0 & r_3 \\ -r_2 & r_2 + r_3 & r_3 \\ r_2 & 0 & r_2 \end{pmatrix} \quad [2.28]$$

Two other approaches for correction of inert K for reactive species have been reported in the literature: Fitzjarrald and Lenschow (1983) and Lenschow and Delany (1987). The first gives three second-order differential equations modeling the steady-state vertical profiles of O_3, NO, and NO_2 concentration in the atmospheric surface layer. A disadvantage of this approach is that they showed that the fluxes and concentrations increased exponentially for large z; however, as fluxes are considered away from the surface they should approach the photostationary state (i.e. the concentrations should depend only on the chemical reactivity, and not on their surface fluxes). A problem

with using this approach is that the authors did not give a working version of their approach. The latter approach provided an analytical solution for tne flux and concentration profiles of NO and NO_2, with the disadvantage of assuming that the ozone concentration is constant with height. Another problem with using their approach is that their equation is full of constants with unknown values.

The photostationary state (that is, chemical equilibrium, $Q_s = 0$ meaning there are no internal sources and sinks) for the NO-O_3-NO_2 triad generally will not happen in the surface layer because vertical turbulent diffusion continues to bring NO from the surface (Fitzjarrald and Lenschow, 1983). When the air is at the photostationary state the following holds:

$$\frac{k_1 NO(z_t) O_3(z_t)}{k_2 NO_2(z_t)} = 1 \qquad [2.29]$$

3. HYPOTHESES

1. Nitric-oxide emissions are greater when the soil water content is less than field capacity than when it is greater than field capacity. Changes in the soil moisture content also affect the NO emissions.

2. Simultaneous applications of nitrogen fertilizers and water increase the NO emissions more than if water is applied alone.

3. Production of NO is greater during the daytime than during nighttime.

4. NO fluxes are larger at the beginning of the experiment with bare soil and gradually decrease as the sugarcane grows.

4. OBJECTIVES

The objectives of this study are

1. To quantify nitric-oxide (NO) fluxes from a tropical sugarcane field to the atmosphere.

   a) To measure NO emissions from the soil.

   b) To determine the influence of agricultural practices such as fertilization and irrigation on NO emissions.

   c) To measure NO_x fluxes above the sugarcane canopy through canopy closure and to compare them to the soil emissions in order to evaluate the sources and sinks of NO_x.

   d) To monitor environmental factors (such as air temperature, soil temperature, solar radiation, rainfall, and pH) to evaluate their effect on NO_x fluxes and speciation of NO and NO_2 from the soil and above the canopy.

2. To compare NO production from a tropical sugarcane field with published data for natural and agricultural systems in other regions, in order to determine the significance of tropical agriculture as a NO source.

5. METHODS

5.1 Site description

The experiment was conducted on a sugarcane field (Block 5 of Helemano 12) at the Waialua Sugarcane Co., Inc., Oahu, Hawaii. The soil is in the Wahiawa series which is a Tropeptic Eutrustox, clayey, kaolinitic, isohyperthermic which developed on a olivine-basalt parent material. The site is a low, slightly sloping upland with an elevation of between 150 to 350 m. The field was well drained with a moderate to moderately rapid permeability. The volumetric water contents at wilting point (1.5 MPa), field capacity (0.01 MPa) and saturation (0.001 MPa) are 0.24, 0.36, and 0.57, respectively. The average annual rainfall is from 1000 to 1500 mm and most of it occurs between November and April. The mean annual soil temperature is 22 °C (Soil Conservation Service, 1976).

The sugarcane (Saccharum species hybrid) cultivar 74-4527 was planted in a 26.2-ha field (Fig. 5.1) which was surrounded by sugarcane fields planted within several weeks of the experiment field. These other fields were irrigated and fertilized on slightly different schedules. The row spacing was 2.74 m (Fig. 5.2). "Seed" cane was planted on 6 to 8 September 1993 (day of the year, DOY, 249 to 251). Drip irrigation was applied continuously for several weeks after planting, usually on a weekly schedule for the first 4 months, and almost every day for the rest of the season.

Fertilizer applications were made about every month through the irrigation lines (Table 5.1). Herbicide was applied about 2 days, 4 weeks, and 2 months after planting.

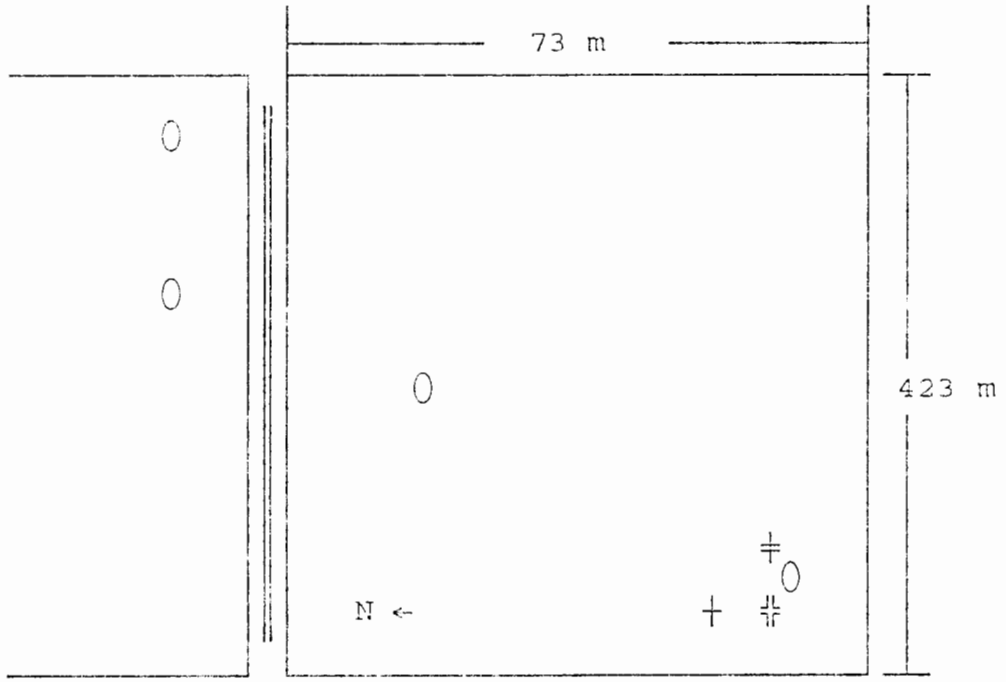

⫫ Bowen-ratio and NO_x system, ⫞ Weather station, ⫩ Sonic anemometers, ○ Chamber sites, ═══ Narrow field road.

Figure 5.1 A generalized map of the area in the field where data was collected.

5.2 Measurement of nitric-oxide fluxes

The experiment consisted primarily of 1) measurements of NO fluxes from the soil by a chamber method, and 2) measurements of NO, NO_2, and NO_x fluxes above the sugarcane canopy by the flux-gradient method.

5.2.1 NO fluxes from the soil by the chamber approach

The NO flux from the soil was measured by covering the

Table 5.1. Fertilization schedule and amount of N applied.

DOY	TYPE	kg-N ha^{-1}
259	11-37*	34
292	urea**	21
309	11-37	20
315	urea	39
11	urea	22
25 (376)	urea	29
40 (405)	urea	32
55 (420)	urea	24
73 (438)	urea	55
74 (439)	urea	11
101 (466)	urea	25
103 (468)	urea	22
104 (469)	urea	22

* 11 % nitrogen, ** 46 % nitrogen

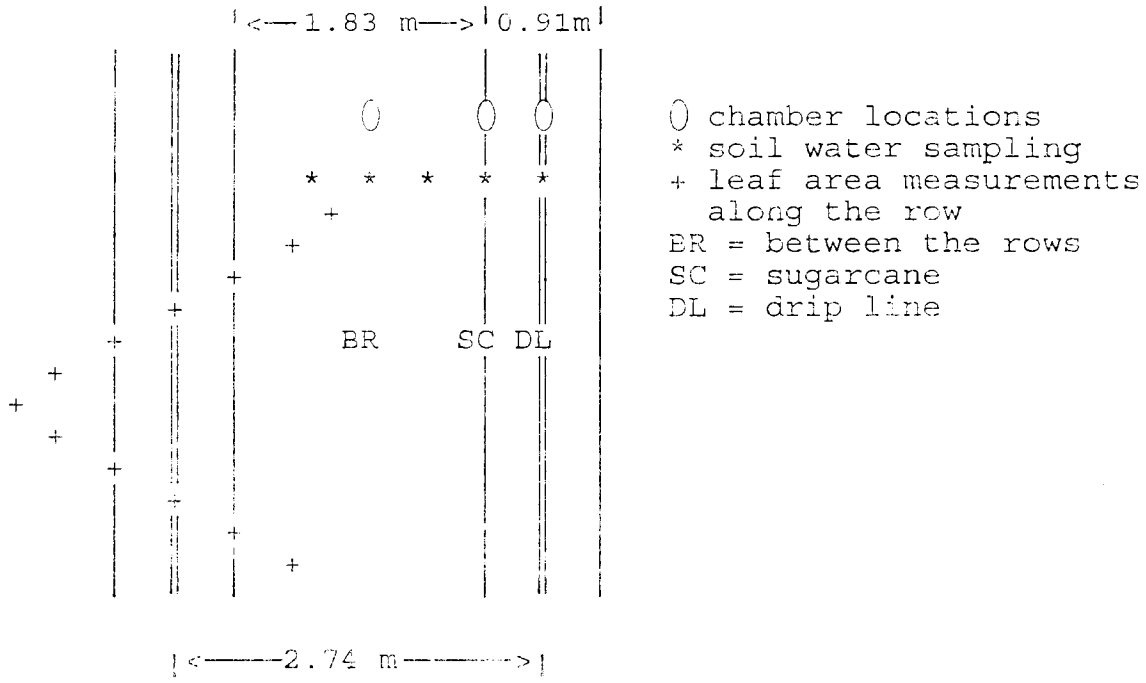

Figure 5.2 Spacing of sugarcane rows (—) and drip-irrigation lines (═) in the sugarcane at Waialua, Oahu.

soil with a vented closed chamber and determining changes in the chamber NO concentration over time. Because the placement of a chamber can disturb the natural soil environment, data was collected immediately after the chamber was put in place, but the initial data was not reliable because the analyzer was adjusting to the new condition and the NO_2 was depositing on the chamber walls. It was assumed that both NO_2 and O_3 rapidly deposited within the soil chamber so that only NO should increase with time within the chamber (Johansson et al., 1988 as cited in Davidson et al., 1991), that the rate of air withdrawal for sampling did not disturb the concentration in the chamber, and that NO build up during the measurement period (3-4 min) was not enough to reduce the flux. Air exchange through the hole is assumed to occur in a representative way, that is, the air in the chamber is assumed to be well mixed and the concentration in the chamber from NO emissions from the soil is assumed not to be depleted by the withdrawal and replenishment (Davidson et al., 1991).

A cylindrical frame ring (0.25-m diameter by 0.1-m height) made of polyvinylchloride (PVC) was inserted into the soil to a depth of about 0.02 m, several minutes before air sampling. The removable top of the chamber (0.13 m height), which was made of white acrylonitrile-butadiene-styrene, was not installed until the measurements begin to let natural conditions prevail. The chamber rings were

removed and the spot flagged after each measurement to avoid much disturbance to the soil. A small inlet (0.003-m diameter hole) on the top of the chamber allowed replenishing of the removed air and equilibration of the chamber air pressure with ambient pressure. The temperature was measured in the chamber with a mercury-in-glass thermometer which was laid on the soil in the chamber during data collection. The height was measured on 4 sides of the chamber and the average taken.

Air was pumped from the chamber with the internal analyzer pump at a rate of 1.5 L min^{-1}. Two flow meters (Size 1 and 2, glass float, Gilmont Instruments, Inc.) controlled the air flow from the chamber at a rate of 0.2 L min^{-1} (FR_{ch}), and the NO_x-free dilution air flow at a rate of 1.3 L min^{-1} (FR_{dil}). The flow rates were recorded. The dilution air passed through a NO_x scrubber (crystalline ferrous sulfate; its use was recommended by John Drummond, Unisearch Associates, Inc., 1993) to remove NO_x. The air sample was mixed in a T connector and passed along the teflon tubing (FEP tubing Cole-Parmer Instrument Co., Niles, Illinois) before it passed through the converter where NO was converted to NO_2 (Model LNC-3, Scintrex). The NO_2 concentration was measured by a chemiluminescence detector (Model LMA-3, Scintrex Ltd., Concord, Ontario, Canada) (Fig. 5.3). The NO concentration was recorded every 10 s for 3 min (every 30 s for 5 min at the beginning of the study).

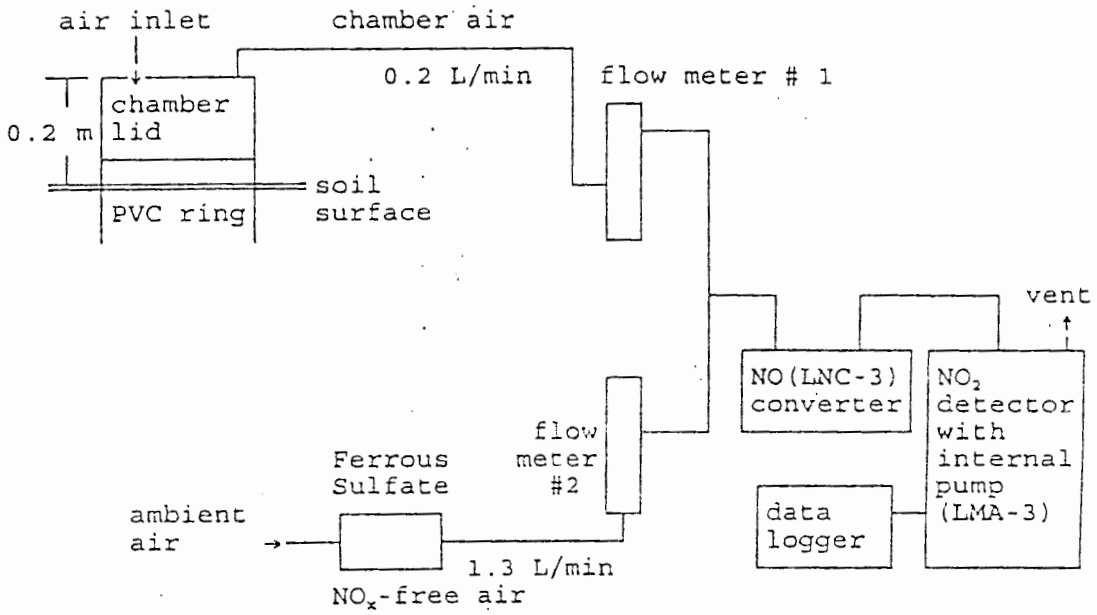

Figure 5.3 Diagram of the apparatus for NO-flux measurements from chambers.

The zero was deducted from the concentration at each time interval, the calibration equation applied (Section 5.2.3), the data graphed, and the steepest portion of the curve selected (Hutchinson and Livingston, 1993). If the curve was not smooth, a representative or average slope was selected.

The NO flux is calculated from the following equation:

$$F_{NO} = ((FR_{ch} + FR_{dil})/FR_{ch}) * \Delta X/\Delta t * h * mw_{NO}P/RT \quad [5.1]$$

where F_{NO} is the NO flux rate (ng NO-N m^{-2} s^{-1}); FR_{ch} and FR_{dil} are the flow rates of the chamber air and NO_x-free dilution air in mL min^{-1}, respectively; $\Delta X/\Delta t$ is the rate of NO increase (after calibration) in ppb; h is the height of the chamber from the surface (chamber volume per surface area); mw_{NO} is the molecular weight of NO which is 30 g $mole^{-1}$; P is the atmospheric pressure; R is the ideal gas constant (0.0083143 m^3 kPa $mole^{-1}$ K^{-1}); and T is the chamber air temperature (K) (Davidson, 1991). Based on the Ideal Gas Law and Amagat's Law of Partial Volumes (Barrow, 1979);

$$ppb_{vol} = \frac{V_{NO}}{V_{air}} = \frac{n_{NO}\ RT/P_{atm}}{V_{air}}$$

$$= \frac{m_{NO}\ RT}{mw_{NO}\ P_{atm}\ V_{air}} = \rho_{NO}\ \frac{RT}{mw_{NO}\ P_{atm}}$$

and

$$\rho_{NO} = ppb_{vol}\ \frac{mw_{NO}\ P_{atm}}{RT} \quad [5.2]$$

The unit analysis is represented as follows:

$$\frac{ng\text{-}N}{m^2\ s} = \frac{mL\ min^{-1}}{\underset{in\ chamber}{mL\ min^{-1}}} * \frac{\frac{10^{-9}m^3\ NO}{m^3_{air\ in\ analyzer}}}{s} * \frac{\frac{m\ g\ kPa}{mole}}{\frac{m^3\ kPa}{mole\ K} * K} * \frac{10^9 ng}{g}$$

Because NO, NO_2, and NO_x fluxes are being compared with each other and the literature, the flux is reported as a flux of N, for example, NO-N, and the mw used in Equation 5.1 is mw_N rather than mw_{NO}.

Measurements with the chambers were made at two or three different row positions at four sites upwind of the site at which above-canopy fluxes were measured (total of 8 to 12 chambers) (Fig. 5.2). The row positions were: 1) at the drip line (wet and fertilized area), 2) at the sugarcane row, and 3) in the space between the double rows of sugarcane (often drier area). The sites were immediately upwind of the flux-gradient instrumentation and at three other positions further upwind (Fig. 5.1). The system is portable battery operated and was moved by hand cart.

The chamber measurements were coordinated with the flux measurements above the canopy (Section 5.2.2) since only one NO_2 analyzer was available. Chamber measurements and calibrations (Section 5.2.3) were usually done between noontime and about 1500 h. Measurements were made on days when above-canopy data was collected and were also made on days after each fertilization with decreasing frequency about a week after the fertilization.

5.2.2 Measurement of NO fluxes above canopy by the flux-gradient method

5.2.2.1 Field measurements

The NO fluxes above the sugarcane canopy were determined by measuring the NO gradient and the eddy diffusivity. Three methods to measure the eddy diffusivity were used because of unsolved problems (leaks which affected the water vapor measurements) with the first: the Bowen-ratio-energy-balance method, a sensible heat flux and temperature gradient method, and a prediction method. The Bowen-ratio method provides the turbulent exchange coefficient or eddy diffusivity for NO (K) as follows:

$$K = - (Rn + GO)/(L\ \Delta\rho_v/\Delta z) + \rho_a Cp\ (\Delta T/\Delta z)) \qquad [2.14]$$

and the combination method was used to determine the soil heat flux (GO).

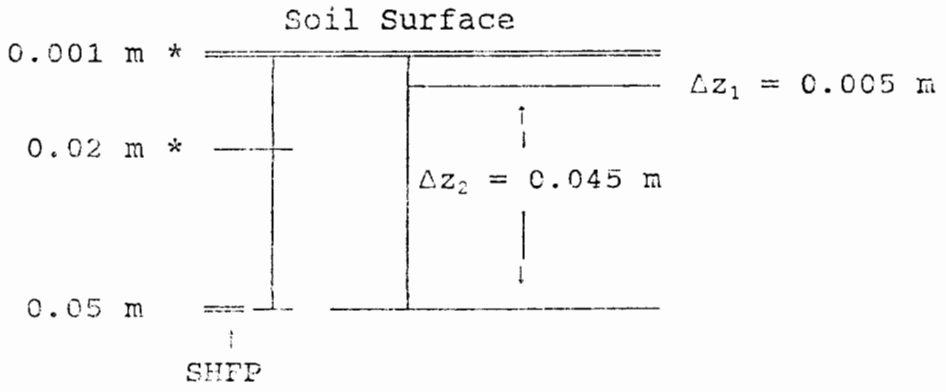

Figure 5.4 Placement of thermocouples (*) and soil heat flux plate (SHFP).

The combination method to determine GO can be described in equation form by:

$$GO = G_5 - C_2\,\Delta z_2(T_2(t+\Delta t) - T_2(t))/\Delta t - C_1\,\Delta z_1(T_1(t+\Delta t) - T_1(t))/\Delta t \quad [5.3]$$

where G_5 is the soil heat flux at a 0.05-m depth; T_1 and T_2 are the soil temperatures at depths of 0.001 and 0.02 m; Δz_2 and Δz_1 are the thicknesses of the layers in which the soil temperature is measured, where Δz_1 is 0.005 m and Δz_2 is 0.045 m; t is the starting time of each averaging period; Δt is the time interval in seconds over which the data are averaged; C_1 and C_2 are the heat capacities of the soil layers about 0.001 and 0.02 m in J m^{-3} $°C^{-1}$, and are calculated as follows:

$$C = Xm\,Cm + Xw\,Cw + Xo\,Co + Xa\,Ca \quad [5.4]$$

where Xm, Xw, Xo, and Xa are the volume fractions of the mineral, water, organic matter, and air and Cm, Cw, Co, and Ca are the heat capacities of each. Estimated values of these heat capacities are 1.925 x 10^6, 4.184 x 10^6, 2.510 x 10^6, and 0.0012 x 10^6 J m^{-3} $°C^{-1}$, respectively (Oke, 1988; Monteith and Unsworth, 1990). Xm equals the bulk density over the particle density, Xo is the organic-matter content by volume (0.0284) (Soil Conservation Service, 1976), Xw is commonly called the volumetric water content (θv) and is obtained by multiplying the soil bulk density by the gravimetric water content and dividing by the density of water.

The second method provides the eddy diffusivity (K) as follows:

$$K = H/\rho_a c_p dT/dz \qquad [5.5]$$

where H is the sensible heat flux density (J m^{-2} s^{-1}), ρ_a is the air density (1200 g m^{-3}), c_p is the specific heat of air (1.01 J g^{-1} $°C^{-1}$), and dT/dz is the temperature gradient (°C/m).

The instruments were located in a downwind area selected to maximize fetch with prevailing wind directions (that is, trade winds) (Fig. 5.1). An upwind fetch of about 500 m or more was achieved when wind angles were from 10 to 80 degrees from north.

Measurement heights of 4 and 5 m were chosen (1) to keep measurements (1a) above the influence of the roughness sublayer (Graser, et al., 1985; Cellier, 1985; Fig. 2.7) associated with the initial surface pattern and the eventual crop height and (1b) below the top of the fully adjusted layer, and (2) to ensure an adequate separation of the arms to allow a measurable, but approximately linear, gradient. Two arms of the Bowen ratio system (Campbell Scientific, Inc., Logan, Utah) were positioned at 4 and 5 m on a tripod for air sampling and air temperature measurement. The air intakes for the NO_x sample were located 0.3 m behind the intake for the water-vapor sample.

Net radiation was measured using a Fritschen type net radiometer (Q-6, Radiation and energy balance systems, Inc., Seattle, WA). Although it has been demonstrated that

simple net radiometers including some Fritschen net radiometers are not always accurate in measuring net radiation, mainly due to design and calibration errors, such net radiometers are still commonly used by agricultural meteorologists. Errors of -10 to +10 % were expected depending on the environmental conditions (Halldin and Lindroth, 1991).

Surface soil-heat flux was measured at 5 row positions (see Fig. 5.2) to get a field average from the soil heat flux at each row position using the combination method with a soil heat flux plate (SHFP) (Model HFT-1, Campbell Scientific, Inc) at a 0.05-m depth and measured soil temperatures (0.0001 m copper-constantan thermocouples, Omega gauge) at 0.001 and 0.02-m depths above the plate to calculate heat storage (Fig. 5.4).

The temperature gradient was measured with fine thermocouples of the Bowen-ratio-energy-balance system (pairs of 0.0005 inch and later 0.003 inch thermocouples, Campbell Scientific, Inc., Logan, Utah).

The sensible-heat flux density was measured at a 4.5-m height with two sonic anemometers (Model CA27, Campbell Scientific, Inc.) positioned over the sugarcane and the area between the sugarcane to provide a good average and/or to ensure the height was adequate for horizontal homogeneity. The sonics were in close agreement (for example, less than 10 W m^{-2} difference) most of the time. The sonics were located near the Bowen-ratio system (Fig. 5.1).

The volumetric water content was measured at the 5 row positions and at two depths: 0 to 0.005 m and 0.005 to 0.050 m. The soil samples were taken nearly every time the NO measurements above and below the canopy were done.

The NO gradient was measured with the a chemiluminescence analyzer (NO_2 analyzer, Model LMA-3, Scintrex Ltd.) with a converter-scrubber-switch instrument (Model LNC-3, Scintrex Ltd.) to convert NO to NO_2 and to allow automated switching between two heights under datalogger control (modified for us by J. Drummond at Unisearch Associates Ltd.). The switch instrument had 6 modes (NO_x, NO_2, and zero reading for upper and lower air intakes) which were sequentially set every 4 min. Continuous air flow was drawn at both heights. 40 s on each mode allowed 20 s for stabilization and 20 s for averaging.

One datalogger (Model 21X, Campbell Scientific, Inc) was used to control the Bowen ratio system; a second datalogger, to collect the soil heat flux data; a third, to control the LNC-3 and log the LMA-3; a fourth, to log data from the two sonic anemometers; and a fifth, to log weather data (Section 5.4.1). All 5 dataloggers were programmed for a 20-min output interval. Local time was set in all 5 dataloggers. The Bowen-ratio and sonic anemometer programs were the commercial ones. The NO_x program was an elaborate modification of the Bowen-ratio program. The system as described runs off battery power.

The NO flux was calculated as follows:

$$F_{NO} = K * dC_{NO}/dz * mw_{NO}P/RT \qquad [5.6]$$

where F_{NO} is the NO flux, K is the eddy diffusivity, dC_{NO}/dz is the gradient of mixing ratio by volume (ppb) over a height interval, z. Hourly atmospheric pressure was obtained from the Honolulu International airport from the National Weather Service. The unit analysis is shown below:

$$\frac{\text{ng NO}}{\text{m}^2\ \text{s}} = \frac{\text{m}^2}{\text{s}} * \frac{\frac{10^{-9}\ \text{m}^3\ \text{NO}}{\text{m}^3\text{air}}}{\text{m}} * \frac{\frac{\text{g}}{\text{mole}} * \text{kPa}}{\frac{\text{m}^3\ \text{kPa}}{\text{mole}\quad \text{K}} * \text{K}} * \frac{10^{9}\ \text{ng}}{\text{g}}$$

Fluxes will be described as being towards or away from the surface to avoid confusion with the typical opposite sign convention for chambers.

A correction for sensible heat and latent heat flux density effects on the NO concentration was not needed, because the air is brought to a common temperature and water vapor content in the analyzer by the Nafion drier tubes in the converter-scrubber, and because the analyzer determines concentration in mixing ratio by volume relative to ambient air (Webb et al., 1980).

Measurements started one month after planting due to technical problems with the NO_2 analyzer (excessive zero drift) which required returning it to the factory and using another instrument for several months. Data was collected

on the vast majority of dry and some wet days with suitable wind direction from the north east (45°) or trade winds (60-70°). The NO_2 analyzer was usually available for measurements above the canopy during the morning and afternoon.

20-minute outputs were eliminated when there was a lack of zero stability of the NO_2 analyzer (zero variations of greater than 6 ppt or greater than the gradients of NO and NO_2), when the wind direction was outside the field fetch (less than 10° or greater than 80°), when atmospheric conditions were transitional resulting in the temperature gradient having the opposite sign as the sensible heat flux (an apparent negative K) or a small air temperature gradient (within the 0.001 to 0.009 °C range) such as when conditions changed between stable and unstable or when the sonic anemometers did not agree in sign, and/or when one of the instruments was not in operation such as when chamber data was collected or rains prevented collection of sonic anemometer data.

5.2.2.2 Regression equation for prediction of K

Because of leak problems with the Bowen-ratio-energy-balance system, the eddy diffusivity (K) from DOY 286 to 342 was predicted based on the relationship between the measured eddy diffusivity and relevant environmental and plant characteristics from DOY 350 to DOY 117 using a regression

equation. The environmental and plant factors considered for the regression equation were global solar radiation, net radiation, air temperature, soil surface temperature, volumetric soil water content at the drip line and between the rows, wind speed, wind speed squared, wind direction, standard deviation of wind direction, the product of wind speed and the standard deviation of wind direction, plant height, and leaf area index (the collection of much of this data is described in Sections 5.3 and 5.4). Scatter plots of these factors against K were inspected to detect the type of relationship. Highly significant variables at a 5% probability were determined by stepwise regression. Variables for the model were selected by comparison of the model adjusted r^2 and PRESS values (predicted residual sum square) as well as consideration of the physical significance of the factor in the system. The selected model (r^2 = 0.3327, PRESS = 226.6) is shown below:

$$K = 0.2756 + (-0.0187 * TS) \quad (0.008793) + (0.0494 * WS^2) \quad (0.008517) + (0.0086 + WSxSD) \quad (0.001578) \qquad [5.7]$$

where TS is the temperature of the soil surface (0.001 m) (see Fig. 5.3) between the row, WS^2 is the squared wind speed, and WSxSD is the wind speed times the standard deviation of the wind direction. The standard error is in parenthesis to the right of each term.

5.2.3 Instrument calibration

The NO_2 analyzer and converter system was calibrated in the field nearly every day with 10 concentrations of NO from 0 to 13.3 ppb with 4 points from 0 to 1.11 ppb. A 0.111 ppm NO-in-N_2 standard gas (Scott-Marrin, Inc., Riverside, CA) was diluted to a range of concentrations with NO_x-free air. The concentration of NO in the calibration air stream was varied by adjusting the flow rates of the NO standard (FR1) and NO_x-free dilution air (FR2) using a mass flow controller system (Model UFC-1100A with controller, Unit Instruments Inc, Yorba Linda, California). A portable generator was operated during calibration to provide power for the mass flow controllers. The excess of mixed air was vented at a T with a 0.2-m tube open to the atmosphere (Fig. 5.5). The actual NO concentration in ppb was calculated as:

$$[NO] = FR1/(FR1 + FR2) * 111 \qquad [5.8]$$

The analyzer span and the zero reading were set initially with at least five iterations between the highest concentration and the zero air. The span and zero were not changed from day to day. A third or fifth order polynomial equation, as needed to get good fit of the curve through the calibrated data as verified by graphing, was fit to the calibration data to serve as the calibration equation. The calibration equation was not used for extrapolation.

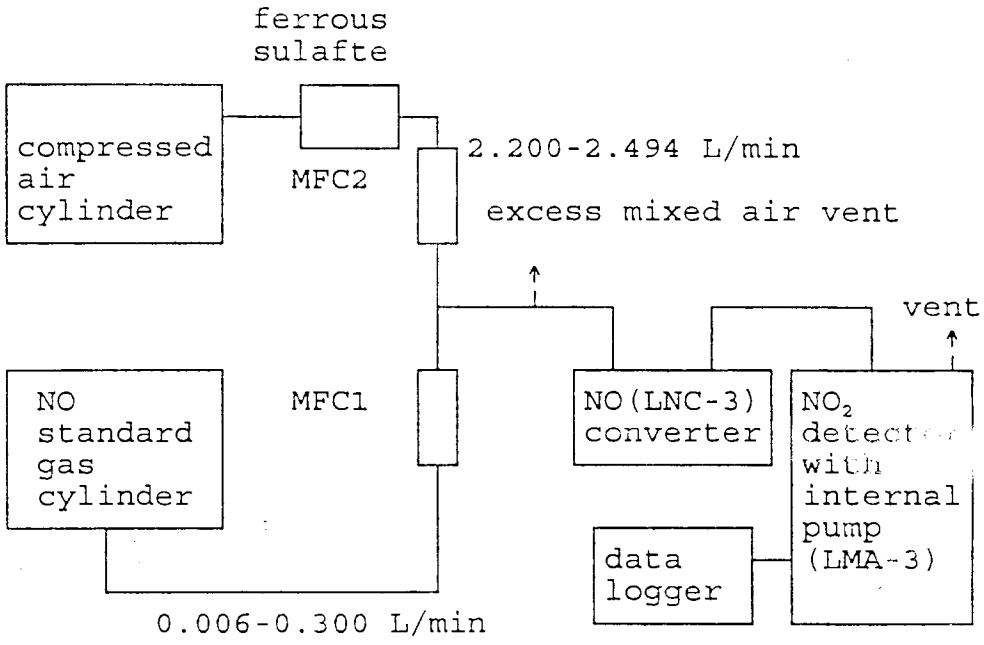

MFC = mass flow controller

Figure 5.5 Diagram of the apparatus for LNC-3 and LMA-3 calibration with NO standard gas.

5.3 Supplemental plant measurements

5.3.1 Leaf area and plant height

Leaf area was measured with an Area Meter (LI-3100, Li-cor Inc, Lincoln, Nebraska) until the sugarcane canopy became close enough (3 months after planting) for the effective use of the Plant Canopy Analyzer (Model LAI-2000, Li-cor Inc, Lincoln, Nebraska). Measurements were made about every 3 weeks. Three randomly-selected but representative areas were sampled outside the upwind area, to avoid creating non-uniformity. Along 5 m of row the total number of plants was counted and 10 representative plants were cut for leaf-area measurement. The leaf area index (LAI) was calculated as follows:

$$LAI\ (m^2/m^2) = LA * TNP/GA \qquad [5.9]$$

where LA is the leaf area (m^2/10 plants), TNP is the total number of plants along 5 m of row, and GA is the ground area (5m * 1.5m; the width is more precisely 1.37 m so the leaf area was underestimated slightly).

When the Plant Canopy Analyzer was used, ten sites in the upwind area were selected randomly for the measurements. Three readings below and one reading above the canopy were taken for each of the four replicates along the sugarcane double row at each site (Fig. 5.2). The 12 readings are the three readings and 4 replicates.

The plant height was measured at the same time as the leaf area measurements.

5.3.2 Stomatal resistance

Stomatal resistance is associated with the closure of the stomata in response to environmental conditions and plant water status, and it is the inverse of stomatal conductance. The stomatal resistance was measured with a steady-state diffusion porometer (Model 1600, Li-cor, Inc). About 10 representative plants were selected in the vicinity of the micrometeorological instrumentation. A diurnal curve (from about 1000 to 1600 h) was measured for two days (DOY 288 and 309). The stomatal resistance was measured for the lower leaf surfaces. The most recently fully expanded sunlit leaf on the plant was monitored. An area near the mid-vein, but not across it, of the selected leaf was selected.

5.4 Supplemental environmental measurements

5.4.1 Weather station

A weather station was installed to measure various environmental factors continuously throughout the field study. Wind speed and direction were measured using a cup anemometer (Model 2012, Campbell Scientific Inc, Logan, Utah) and a wind vane (micro response wind vane, Model 2020, Qualimeters Inc., Sacramento, California). Precipitation was measured with a tipping bucket rain gauge (Model TE525, Campbell Scientific Inc., Logan, Utah). Global solar radiation was measured using a pyranometer (Model LI-200SZ,

Licor Inc., Lincoln, Nebraska). All sensors were installed at a 4-m height. A datalogger (Model 21X, Campbell Scientific, Inc., Logan, Utah) was programmed for a 20-min output interval.

5.4.2 Soil exchangeable nitrate and ammonium

Soil samples to a depth of 0.10 m were usually taken around each chamber location right after and a week after fertilization to determine soil exchangeable nitrate and ammonium, and pH. 24 soil samples across the whole field were taken before the first fertilization to characterize the field variability. Ammonium and nitrate were analyzed using a technicon autoanalyzer by the Agricultural Diagnostic Service Center, University of Hawaii.

5.4.3 Net mineralization and nitrification rates, and nitrification potential

NO emissions from the soil are associated with microbial mineralization, nitrification rates, and nitrification potential. Measurements of these rates were made on DOY 288 and DOY 34. Soil was sampled to a depth of 0.10 m and taken to the Agricultural Diagnostic Service Center, University of Hawaii within hours of sampling with it kept cool in the interim. The procedure followed is explained in Appendices 1 and 2.

5.4.4 Ozone concentration

Ozone concentrations were measured at 5 m from DOY 115 to 117 (Model 1003-AH, Dasibi Environmental Corp., Glendale, CA). Because the analyzer did not permit automation, ozone gradients were determined by repeated manual sampling of air from the two heights throughout each 20-min time interval. The samples were drawn through a teflon tubing attached to the Bowen ratio arms. The ozone analyzer required power from a generator, so the generator was located 50 m downwind of the instrument stand and the wind direction was observed carefully during its operation. The instrument was calibrated with an ozone-analyzer of the same type kept by Jeff Castillo at the Department of Health in Honolulu, Hawaii for calibration purposes.

5.4.5 Methane, carbon dioxide, and nitrous oxide fluxes

Methane (CH_4), carbon dioxide (CO_2), and nitrous oxide (N_2O) flux densities were measured from DOY 115 to 117. A closed chamber was placed on the ground DL and BR. 8-ml air samples were drawn from the chamber at 0, 10, 20, and 30 min using 10-ml syringes. Samples were analyzed within 24 hours by gas chromatography (Model GC-mini2, Shimadzu Chromatograph Company) by John Zachariassen. Half of each sample was used to determine N_2O (electron capture detector) and the other half was used to determine CH_4 and CO_2 (flame detector). Two standard concentrations were analyzed for

each gas just before the analysis of air samples. A calibration equation was obtained by linear regression. Fluxes were calculated using the following equation:

$$F = \Delta X/\Delta t * h * mw_{gas}P/RT \qquad [5.10]$$

6. RESULTS AND DISCUSSION

6.1 NO fluxes from a sugarcane field

Nitric-oxide fluxes from the soil surface were determined regularly between 13 October 1993 (day of the year, DOY 286) and 27 April 1994 (DOY 117, or equivalently, 482), while the crop grew from a height of 0.40 to 2.5 m and a leaf area index of 0.12 to 6.5 (Fig. 6.1). Net mineralization (NM), net nitrification (NN), and nitrification potential (NP) were determined early and late in the study (DOY 288 and DOY 34 (399)) (Table 6.1). Flux densities of carbon dioxide (CO_2) and methane (CH_4) measured on DOY 115 to 117 of 1994 are shown in Table 6.2. The soil pH was 5.0.

Table 6.1 Net mineralization, net nitrification, and nitrification potential at DL, SC, and BR.

DOY	NAME	VALUES			STANDARD ERROR		
		DL	SC	BR	DL	SC	BR
288	NM	0.68	-0.16	-0.31	0.5	0.05	0.17
	NN	2.4	0.14	0.04	1.2	0.03	0.06
	NP	1.2	0.78	0.54	0.8	0.10	0.07
34	NM	-0.86		0.18	1.6		0.06
	NN	-0.83		0.15	1.6		0.05
	NP	13.8		1.33	4.7		0.66

NM and NN are in μg-N g^{-1} soil, NP is in μg-N g^{-1} h^{-1}, DL = drip line, SC = sugarcane, BR = between the row.

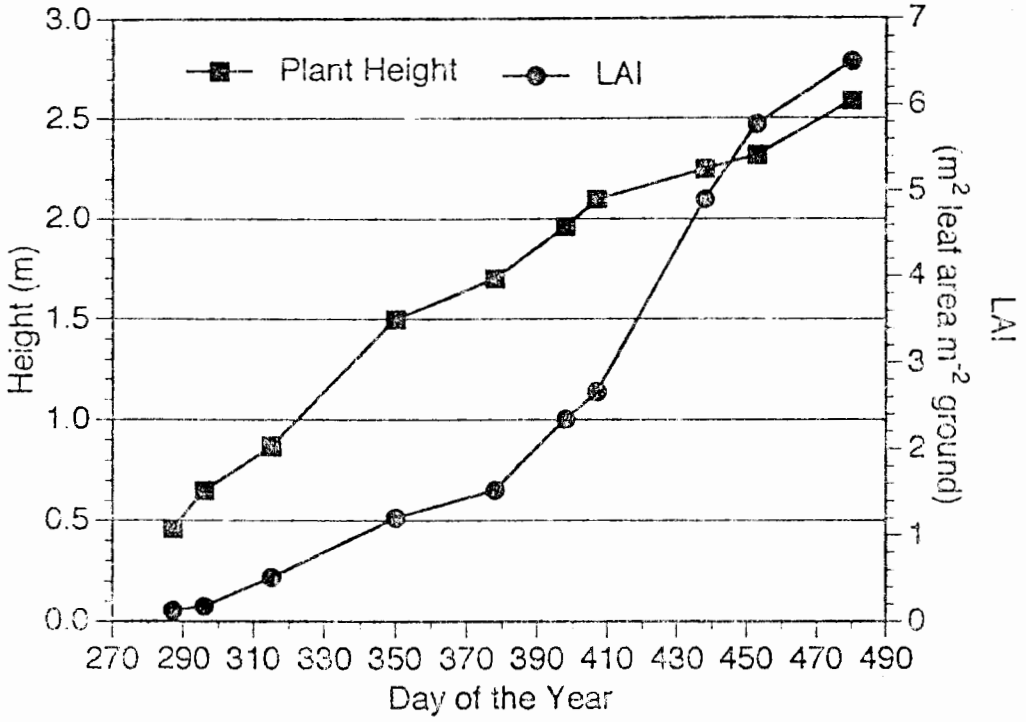

Figure 6.1 Crop height and leaf area index (LAI) for the experimental period from DOY 286 in 1993 to DOY 118 in 1994. In the year 1994, 365 d was added to the day of the year.

Table 6.2 Flux densities of CO_2 and CH_4 at DL and BR

DOY	POSITION	FLUX DENSITY ($ng\ m^{-2}\ s^{-1}$) CO_2	CH_4
115	DL	120	-18
	BR	97	-28
116	DL	150	-18
	BR	115	-23
117	DL	173	-10
	BR	123	-17

6.1.1 Surface emissions

Nitric oxide (NO) emissions from the soil were highly variable over time and at the different locations throughout the field. The sources of this variability will be examined and explained.

6.1.1.1 Row positions

Large fluxes of NO were observed at the drip line (DL) (from 10 to 130 ng NO $m^{-2}\ s^{-1}$), whereas fluxes one-tenth as large were observed between the sugarcane rows (BR) (from 1 to 15 ng NO $m^{-2}\ s^{-1}$), except for a peak on DOY 300 and 302 where BR fluxes exceeded DL (70 versus 34 ng NO $m^{-2}\ s^{-1}$). At the beginning of the experiment NO fluxes were measured in the sugarcane row (SC); they were slightly larger than BR emissions (2 to 20 ng NO $m^{-2}\ s^{-1}$) (Fig. 6.2).

Significant differences were found between NO fluxes at DL and BR ($P < 0.0001$) (Table 6.2). Both means were significantly different from one another (59 and 9 ng NO-N $m^{-2}\ s^{-1}$ for DL and BR, respectively) by the least significant

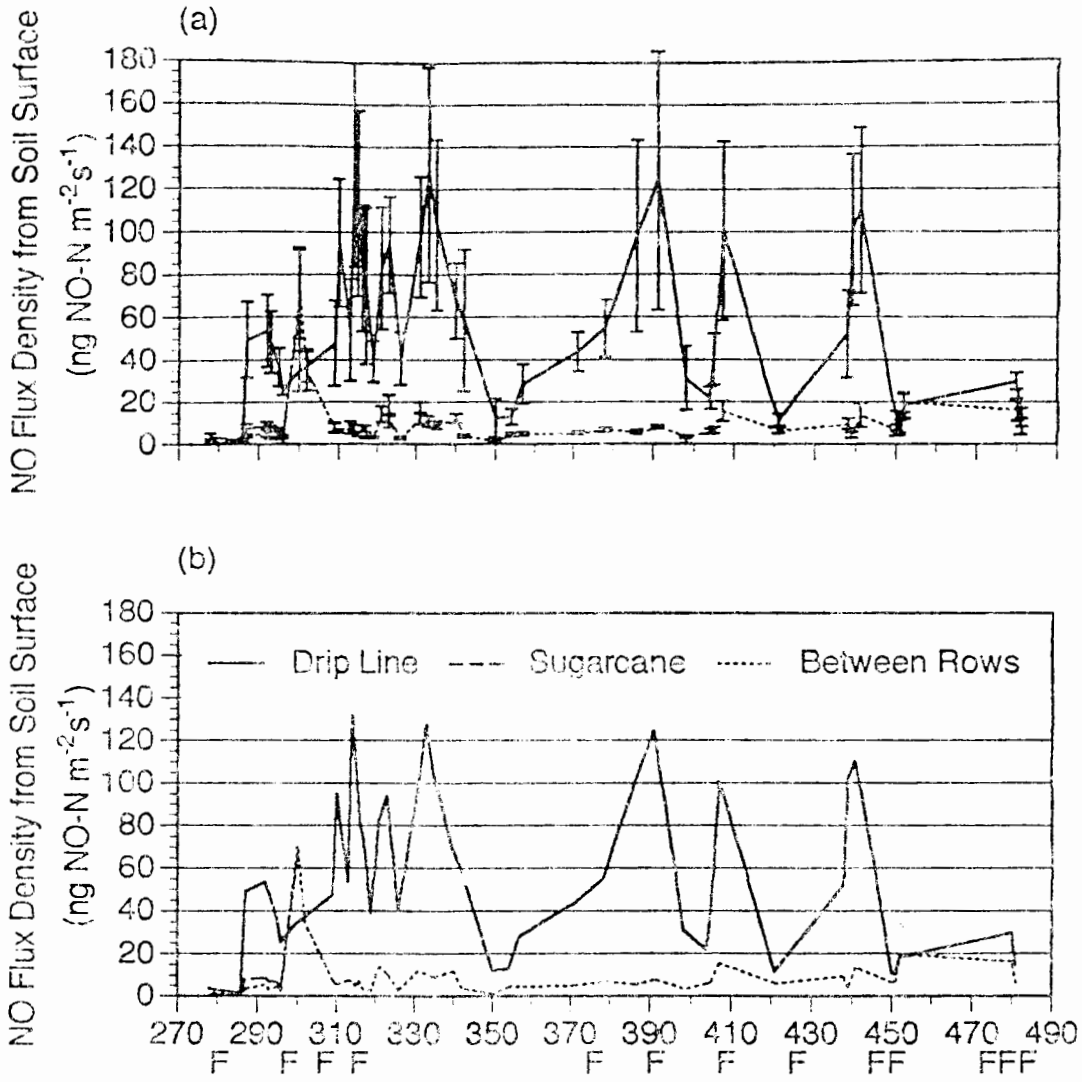

Figure 6.2 Upward directed NO flux densities from the soil surface measured by chambers at three row positions for the experimental period from DOY 286 in 1993 to DCY 118 in 1994. In the year 1994, 365 d was added to the day of the year. (a) The standard error is shown by a bar; (b) the figure is shown without error bars for visual clarity. Each fertilization is represented by an F along the X axis.

difference (LSD) pairwise comparison of means. Much of the variability in fluxes is due to row position, which is completely predictable. The causes of the row pattern variability will be discussed in detail in Section 6.1.1.3.

Table 6.3 Analysis of variance to test positions and sites using a nested design.

SOURCE	DF	SS	MS		F	P
Site	3	58940	19646	†	0.286	0.8340
Pos/site	4	274700	68673	†	38.5	0.0000
Day/pos/site	328	584600	1782	‡		

Pos = Row position, that is, DL and BR.
† Error term for site, ‡ error term for pos/site.

6.1.1.2 Field-scale variability

A great deal of variability was found among the four chamber sites distributed along the center line of the field. For example, the site located in the lower part of the field near the above-canopy measurement site was always very wet and commonly had lower NO emissions compared to the other sites. A pattern of high or low fluxes was characteristic of each site, but the data at the sites did not vary with distance from the field edge (i.e. sites 1, 2, and 3 which were progressively further from the micrometeorological station, had lower fluxes of 30, 31 and 20 ng NO m^{-2} s^{-1} on average, than site 4, which was further away, with a flux of 56 ng NO m^{-2} s^{-1} on average). The variability in the field appeared during field measurements to be related to the influence of microtopography on soil

water content (e.g. site 2 was better drained than site 1). Although the volumetric water content was monitored at five row positions at a central location, the data from this location is not representative of all four separate chamber sites and it gave only field patterns and we did not consistently record our impressions of which sites were wetter or drier than others. Because the measurements were sometimes made while the irrigation was progressing, this might have caused additional differences in volumetric water content between the sites.

In spite of the observed variation among sites in the field, there was no statistically significant difference in NO fluxes between them according to the F test in the ANOVA ($F = 0.29$) ($P > 0.0001$) and to the pairwise comparison of means by the least significant difference (Table 6.2).

6.1.1.3. Field scale trends and causative factors

6.1.1.3.1 Fertilization and volumetric water content. The rapid fluctuations in volumetric water content (Fig. 6.5) especially through DOY 410 when LAI began a rapid increase (Fig. 6.1) are due to irrigations and rain frequently wetting the soil and evaporation drying the soil rapidly particularly for the 0.000 to 0.005-m layer.

The volumetric water content from the top soil layer (0.000 to 0.005 m) experienced similar fluctuations compared to the NO fluxes from the soil, whereas the volumetric water

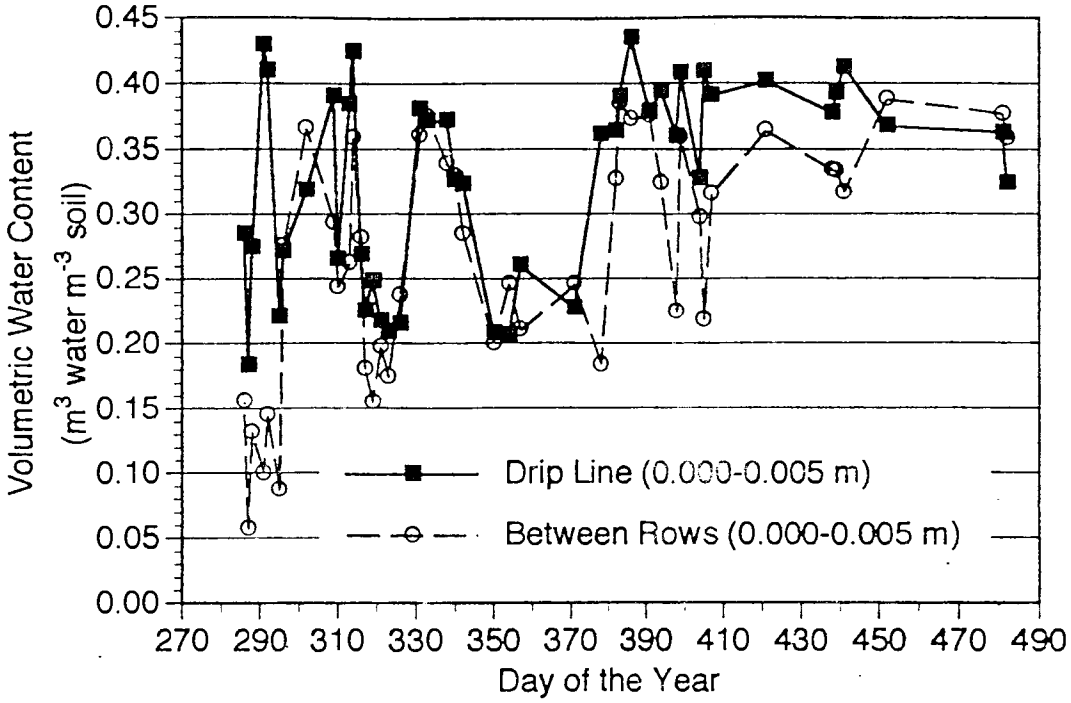

Figure 6.3 The soil surface volumetric water content at 2 row positions for the experimental period from DOY 280 in 1993 to DOY 118 in 1994. In the year 1994, 365 d was added to the day of the year.

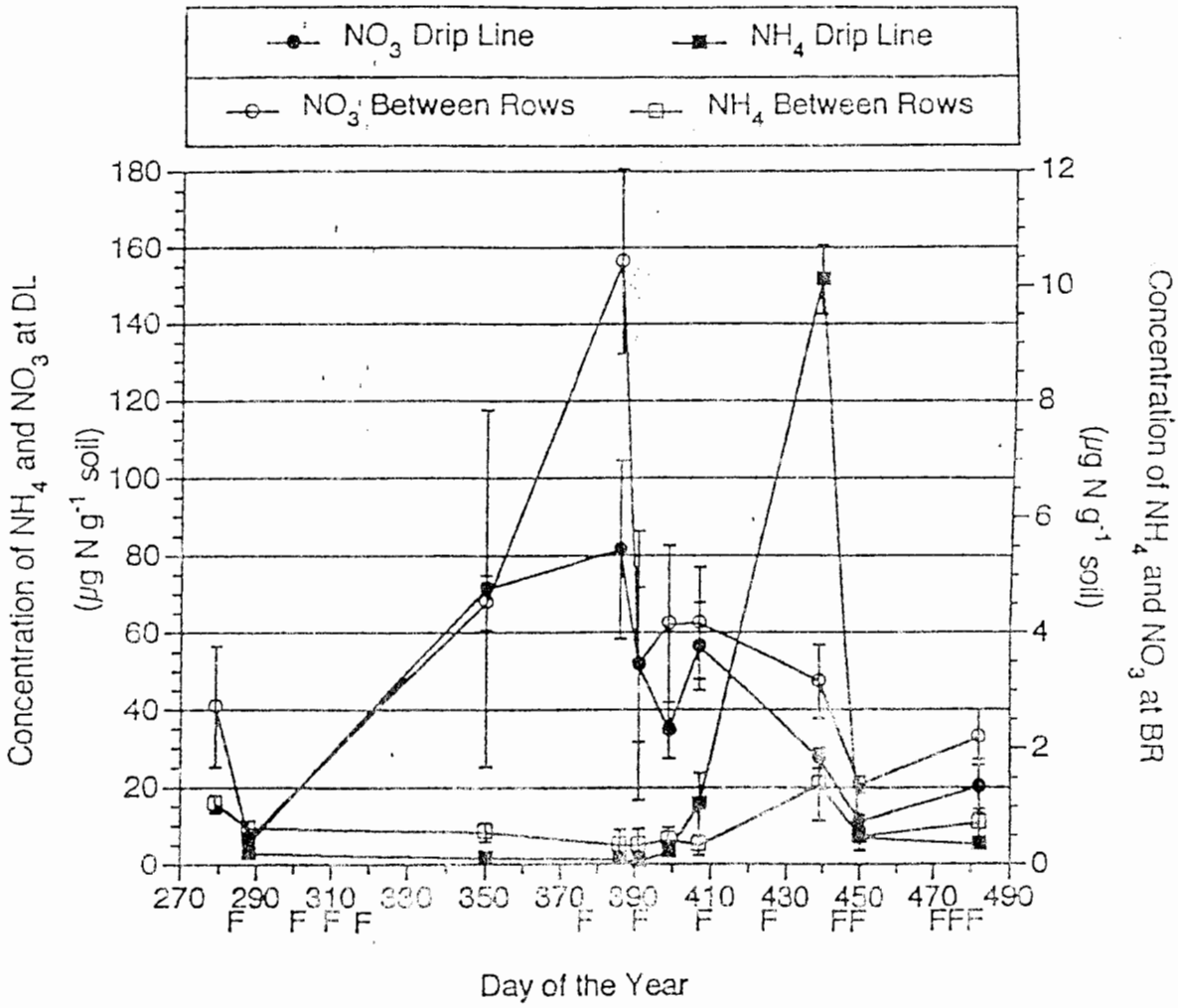

Figure 6.4 Soil NH_4^+ and NO_3^- content at two row positions for the experimental period from DOY 286 in 1993 to DOY 118 in 1994. In the year 1994, 365 d was added to the day of the year. The standard error is shown by a bar. Each fertilization is represented by an F along the X axis.

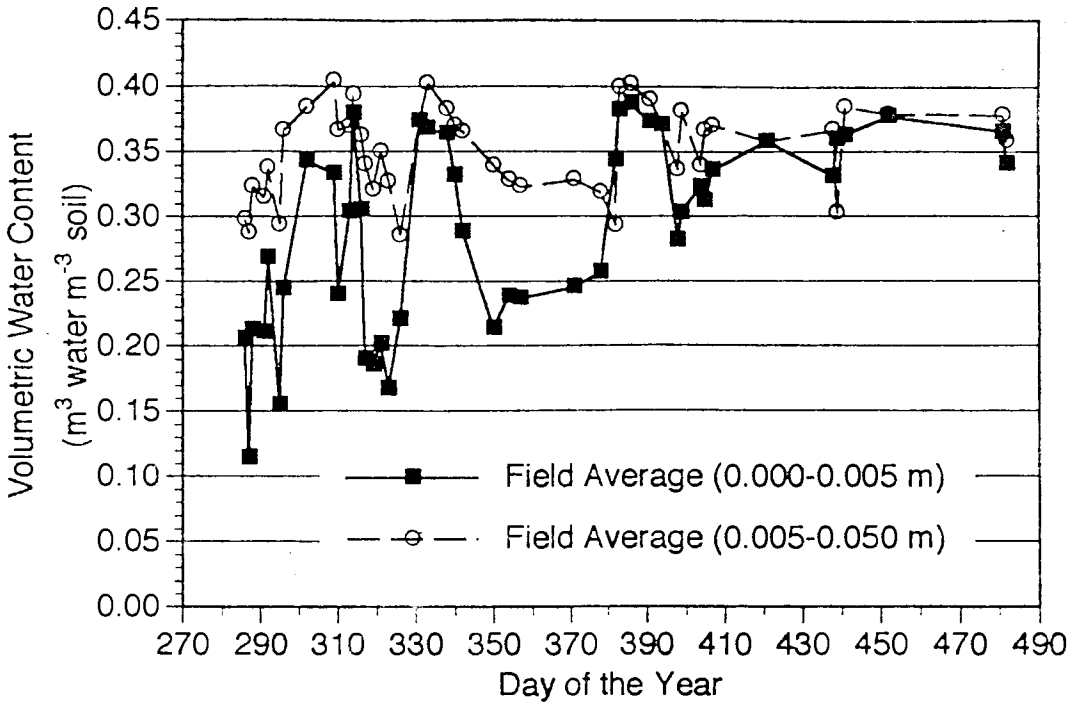

Figure 6.5 The field-average volumetric water content for the soil surface and subsurface for the experimental period from DOY 286 in 1993 to DOY 118 in 1994. In the year 1994, 365 d was added to the day of the year.

content for the deeper soil layer (0.005 to 0.050 m) was more constant (Fig. 6.5). After planting, the soil between the row remained relatively dry due to direct exposure to solar radiation. Later shading caused the water content to be more uniform across the row.

The nutrient substrate (NH_4^+, NO_3^-) through the season probably remained nearly constant because fertilization was frequent. Urea converts to NH_4^+ in 2 to 3 days after application to the soil and to NO_3^- 7 to 14 days after application (Tisdale et al., 1986). For this reason it is assumed that there should be DL NH_4^+ and NO_3^- so DL chamber fluxes would be limited by water and not nutrient substrate (NH_4^+, NO_3^-). BR fluxes are much smaller even with similar water content suggesting that the substrate is limiting. The NO_3^- measurements suggest plant uptake became important around DOY 390. The NH_4^+ data appears unreliable and too low based on the fertilization data (N. Hue and J. Silva, personal communication, 1994). The soil samples were kept frozen and taken to the lab the next business day after sampling, and the lab was contacted several times about the data, but the reason for the apparent error is unknown.

NO emissions (Fig. 6.2) were highly dependent on fertilizer application (Table 5.1, Fig. 6.4) and volumetric water content (Fig. 6.3). Fluxes changed rapidly over time because the water content changed rapidly over time and they could switch from high to low fluxes within a few days. The

effect of irrigation and fertilization on NO emissions will be discussed together because the fertilizer was applied through the drip line.

Fluctuations of NO fluxes were similar to the volumetric water content fluctuations at DL (Fig. 6.2 and 6.3). A time lag of about two days between soil water content and the NO flux peak was observed from a cross-correlation analysis (correlation coefficient for time lags of -1, 0, 1, 2, 3, and 4 days were 0.28, 0.34, 0.36, 0.35, 0.29, and 0.20, respectively). Since data were not collected daily for the whole experiment, a linear interpolation between the data points was made in order to make a cross correlation. NO fluxes at BR did not follow the fluctuations in volumetric water content and remained practically constant throughout the experiment; however, a better correlation was obtained for BR (0.46 for time lag 0 d) compared to DL, but since the fluxes were stable over time the cross-correlation peak would be broader for BR than for DL. NO fluxes are not expected to be perfectly correlated in magnitude with soil water content since, for example, soil mineralization rates are reduced in subsequent irrigations (Johansson et al., 1988; see Section 2.5.2). Although we only measured the water content at one point, the increase should occur at the same time at all points in the field because irrigation and rainfall occur simultaneously spatially. Even if the volumetric water

content field average is a little different from that at the chamber sites, the time relationship between peaks of NO flux and volumetric water content is the same.

The NO flux cycles with volumetric water content. The cycles will be considered in the next few pages. Some examples are given which highlight this correlation. The NO flux increases tend to correspond with volumetric water content increases. From DOY 287 to 292 DL fluxes increased from 49 to 53 ng NO m^{-2} s^{-2} while the volumetric water content increased from 0.18 to 0.40; and the NO flux remained fairly low at BR while the volumetric water content was low (0.05 to 0.10) (Fig. 6.2 and 6.3). Nitrogen fertilization was applied on DOY 292 (21 kg N ha^{-1}) (Table 5.1, Fig. 6.4). A rapid burst of NO evolution from 4 to 71 ng NO m^{-2} s^{-1} was observed at BR on DOY 300 following a volumetric water content increase from 0.08 to 0.36, compared to a modest NO emission increase from 25 to 34 ng NO m^{-2} s^{-1} at DL following a volumetric water content increase from 0.27 to 0.31. The whole field was uniformly wet because a 150-mm-rain fell on DOY 299. The highest NO emission of 132 ng NO m^{-2} s^{-1} at DL corresponded to the highest volumetric water content of 0.42 on DOY 314. Although this peak NO flux could be attributed to the nitrogen fertilization on DOY 309, it is not possible to confirm from our data whether this NO emission was the actual peak because the volumetric water content was never constant.

The NO flux decreases tend to correspond with volumetric water content decreases. Some examples are given. The NO emission rate at DL (DOY 293, 295, 296) decreased drastically from 48 to 25 ng NO m^{-2} s^{-1} following a volumetric water content decrease from 0.40 to 0.27. NO emissions at BR were reduced to 35 and 8 ng NO m^{-2} s^{-1} for DOY 302 and 309, respectively, which corresponded to a volumetric water content decrease to 0.24 (Fig 6.2 and 6.3). A NO emission decrease from 132 to 75 ng NO m^{-2} s^{-1} at DL from DOY 314 to 317 could be strongly attributed to a volumetric water content decrease from 0.42 to 0.22. Although the fertilizer was applied (39 kg N ha^{-1}) on DOY 315, the flux follows the water content and so with the soil drying the emissions were decreased by half (Fig. 6.2, 6.3, and 6.4).

The NO flux increases and decreases tend to occur with volumetric water content increases and decreases. An interesting relationship of NO emissions to wetting and drying cycles at DL can be seen from DOY 326 to 335. NO emissions increased from 40 to 127 and decreased back to 103 ng NO m^{-2} s^{-1} from DOY 326 to 333 and 335, respectively. The volumetric water content increased from0.21 to 0.37 from DOY 326 to 333 and remained constant at 0.37 up until DOY 338. Although the amount of soil substrate during this time period was not measured, there apparently is still

sufficient substrate from the last fertilization, for the soil microorganisms to reach the highest peak in NO production. The NO emissions dropped for the following two days even when the volumetric water content remained relatively stable. This is in agreement with the findings of Johansson et al. (1988; Section 2.5.2).

The correspondence of flux and volumetric water content increases and decreases indicates that the NO-producing bacteria respond rapidly to increases and decreases in water content and inorganic nitrogen in the soil. NO production in the soil can be strongly inhibited at low water content, and large amounts of NO can be emitted rapidly as soon as the soil is wetted. This rapid response to wetting by the microorganisms which produce NO in soil agrees with NO measurements on a dry savanna ecosystem (Johansson et al., 1988) and laboratory studies (Davidson, 1992).

There are situations where the surface NO flux does not correspond with the surface volumetric content. Often these situations are for BR fluxes and are caused by low NH_4^+ and NO_3^- levels. On DOY 314 the volumetric water content had increased back to 0.35 whereas the NO emitted remained low at BR (6 to 7 ng NO m^{-2} s^{-1}) (Fig. 6.2 and 6.3). The large amount of NO produced following the wetting of dry soil on DOY 300 and 302 was not duplicated when the soil was rewet. This tendency suggests that NO emissions from soils depend strongly on the availability of readily decomposable

nitrogen compounds; as well as the microorganisms response to abrupt wetting. The concentration of ammonium and nitrate (0.6 and 0.4 ppm, respectively) measured on DOY 288 at BR was relatively low (Fig. 6.4).

NO emissions at DL increased from 48 to 95 ng NO m^{-2} s^{-1} and dropped back to 54 ng NO m^{-2} s^{-1} while the volumetric water content decreased from 0.39 to 0.26 and increased back to 0.38 for DOY 309, 310 and 313, respectively (Fig. 6.2 and 6.3). Evidently NO emissions do not strictly increase with increases in the volumetric water content, but a negative correlation can be present. The increase in NO emission associated with a decrease of the volumetric water content from DOY 309 to 310 may be due to the increase of soil inorganic substrate by the application of 21 kg N ha^{-1} on DOY 309 (Table 5.1).

Irregular patterns on NO emissions fluctuating from 3 to 7 ng m^{-2} s^{-1} at BR did not follow the trend in volumetric water content change from 0.18 to 0.35 from DOY 309 to 317 (Fig. 6.2 and 6.3). Apparently the small amount of substrate, which was carried from DL to BR by mass flow through water movement (Stanley et al., 1990) when fertilization occurred on DOY 292, was mostly depleted on DOY 300 and 302 when high NO emissions occurred.

An increase in NO emissions at DL from 39 to 94 ng NO m^{-2} s^{-1} from DOY 319 to 323 corresponded to a small decrease in volumetric water content (from 0.24 to 0.20) (Fig. 6.2

and 6.3). Such a small decrease in soil water content probably did not affect the microbial activity in the soil; the urea application on DOY 315 provided a substrate for nitrifiers and had a stronger influence on NO production than the volumetric water content.

Small NO fluctuations following volumetric water content fluctuations were observed at BR from DOY 319 to 342. NO emissions and the volumetric water content ranged from 3 to 14 ng NO m^{-2} s^{-1} and 0.15 to 0.37, respectively. Apparently only a small portion of the substrate added to the soil from fertilization on DOY 309 and 315 was able to reach this row position limiting the magnitude of the flux response to the increase in soil moisture.

Factors other than soil water content and fertilization can also come into play. A drastic drop in NO emissions (from 103 to 12 ng NO m^{-2} s^{-1}) concurred with a volumetric water content drop (from 0.37 to 0.20) from DOY 338 to 354 (Fig 6.2 and 6.3). Although this NO decrease can be attributed to the decrease in the volumetric water content, it seems that there is another unknown factor affecting the NO emissions: a much higher NO flux was observed on DOY 323 (94 ng NO m^{-2} s^{-1}) although the volumetric water content was similarly low (0.20).

A NO flux increase from 13 to 124 and decrease to 22 ng NO m^{-2} s^{-1} corresponded to a volumetric water content increase from 0.20 to 0.43 and decrease to 0.32 at DL (DOY

354 to 26 (391) to 39 (404)) (Fig. 6.2 and 6.3). Fertilizer was applied on DOY 25 (376) (Table 5.1). After fertilization on DOY 40 (405), the NO fluxes at DL increased from 40 to 100 ng NO m^{-2} s^{-1} (from DOY 40 to 42 (407)) while the volumetric water content remained fairly stable (0.40) (Fig. 6.2 and 6.3). From DOY 56 (421) to 74 (439), the NO fluxes increased from 11 to 101 ng NO m^{-2} s^{-1} while the volumetric water content remained high (0.37 to 0.40). Fertilization occurred on DOY 55 (420), 73 (438), and 74 (439). By DOY 86 (451), the NO flux decreased to 7 ng NO m^{-2} s^{-1} following a small drop in the volumetric water content to 0.36 (Fig 6.2 and 6.3).

6.1.1.3.2. Implications of soil fluxes for nitrification and denitrification. Biological nitrification is thought to have been an important source of NO surface emissions throughout the whole study. The volumetric water content generally ranged from 0.20 to 0.38 (Fig. 6.3), which is considered to be in and near the optimum volumetric water content range for nitrifiers to remain active, provided that the amount of NH_4^+ in the soil is sufficient for this process to occur. If the NH_4^+ content in the soil is too low, nitrification will not occur regardless of the water content.

A transient high NO flux was observed immediately following a large increase in water content at BR (DOY 300)

(Fig. 6.2), which indicates that both nitrifiers and denitrifiers became metabolically active after wetting (Firestone and Davidson, 1989; Davidson, 1992). The reduction in NO flux on DOY 310 is most likely due to a decline in the activity of the denitrifiers. This activity continued until the local substrate in the vicinity of the individual microorganisms became depleted of NO_3 or the content of O_2 became too high for further denitrification.

The data on NH_4^+ and NO_3^- content in the soil is limited and the NH_4^+ data is suspect but a good supply of NO_3^- at DL throughout the season and probably NH_4^+ as well due to frequent fertilizations suggest a substrate for nitrification and denitrification was present. The denitrification at BR on DOY 300 despite low NO_3^- levels suggests substrate levels did not prevent denitrification at this time.

Nitrous oxide (N_2O) fluxes which exceed NO fluxes at DL on DOY 480 to 482 by about three times give further evidence that denitrification is important (Fig. 6.6). N_2O fluxes remained fairly stable, while NO fluxes dropped by about half following a volumetric water decrease from 0.36 to 0.32. This may indicate that even though the soil did not reach saturation, denitrification at the microsite level could have been a major source of N_2O at DL and BR. Because the soil was wet, NH_4^+ and NO_3^- diffuse to the microsites through the soil water films at DL, but at BR where both NO

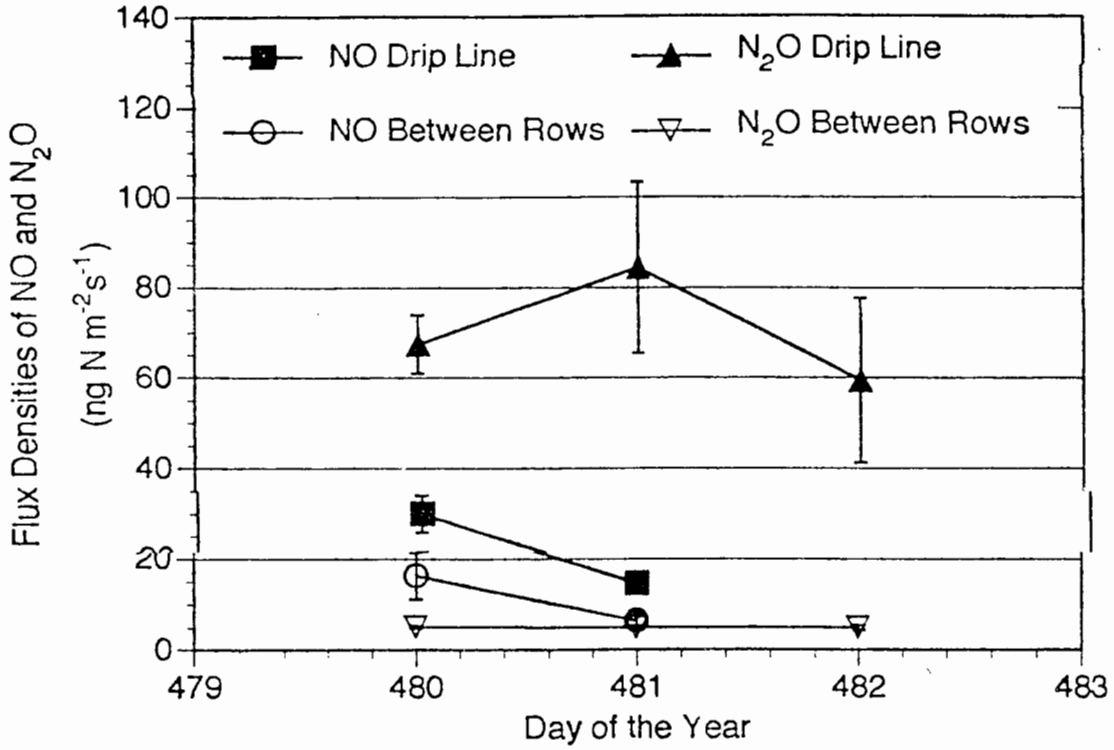

Figure 6.6 The upward-directed soil-surface flux densities of NO for DOY 115 to 116 in 1994 and N_2O for DOY 115 to 117 in 1994 measured by chambers. In the year 1994, 365 d was added to the day of the year. The standard error is shown by a bar.

and N_2O fluxes were about 1/7 as large as that at DL apparently the lack of substrate (NH_4^+ and NO_3^-) was a very limiting factor for denitrification to occur. At BR the NO flux was twice the N_2O flux on DOY 480 and of about the same magnitude the following day (DOY 481) while the volumetric water content was fairly stable (it dropped from 0.37 to 0.35). The modest NO flux at BR and its decrease following a water content decrease could indicate that nitrification was responsible for NO production.

The N_2O to NO ratio gives further evidence of the role of denitrification in soil NO emissions. At higher pHs only N_2O is released by denitrification, but at pH of 5.0 (such as in this soil) or lower, nitric oxide has been found to be a dominant gaseous denitrification product (Fillery, 1979 as cited in Fillery, 1983). Generally, nitric oxide production in acid soils (where nitrite is accumulated) is attributed to chemodenitrification reactions by nitrite decomposition (Chalk and Smith, 1983; Fillery, 1983).

6.1.2 NO_x conservation

In this section we will consider whether NO_x can be considered conserved and so the NO_x flux constant with height and under what conditions sources and sinks of NO_x may exist in the surface layer. NO_x is not reactive with

species in the air for the short-time frame important for determining surface fluxes unlike NO and NO_2 which react and interconvert.

NO_2 emissions from the soil are thought to be low based on the literature (Section 2.8.2) and the frequent wet-surface conditions at the experimental site. We did not have plants in our chambers which can reduce NO_2 fluxes below soil surface values.

NO_2 uptake by plants is most likely when stomata are open (the stomatal conductance measured on DOY 288 and 309 ranged from 0.2 to 0.4 mol m^{-2} s^{-1} and did not have a clear diurnal pattern) and when leaf surfaces are wet. NO release by plants would occur when stomata are open but further controlling factors are not well understood.

Deposition rate of 12 ng N m^{-2} s^{-1} measured on the Island of Hawaii by Vitousek and Walker (1985) appears too large because it is similar in magnitude, but opposite in sign, to our typical chamber fluxes which would yield a net flux of zero, whereas our above-canopy fluxes are much bigger. In a clean marine environment, usually minimal deposition is expected.

We will consider the NO_x flux constant with height, so NO fluxes from the soil equal NO_x fluxes at 4.5 m, unless the data suggest a role for plants or deposition.

6.1.3 Above-canopy fluxes

6.1.3.1 Experimental errors

6.1.3.1.1 Corrections for analyzer interference.

According to the LMA-3 manual section on the luminol solution, "below 5 ppbv [NO_2], the O_3 interference is less than 1% expressed as an equivalent mixing ratio of NO_2." Prior to measuring NO_2 and O_3 this statement had little meaning and suggested ozone interference was small. Actually it means that 1% of the atmospheric ozone concentration will be indicated to be NO_2 by the LMA-3 NO_2 analyzer (John Drummond, Unisearch, personal communication to Graser, 1994). With an O_3 concentration of 30 ppb the analyzer will indicate 300 ppt NO_2 before considering the NO_2 concentration in the air. With an actual NO_2 concentration of about 300 ppt, the LMA-3 will indicate an NO_2 concentration of 600 ppt. In addition John Drummond indicates that new luminol preparations may have an interference of 0.3% or less. This would mean the LMA-3 reading is closer to 25% from O_3 (100 ppt from O_3 + 300 ppt from NO_2) rather than 50% from O_3, but even with O_3 data since the interference isn't known quantitatively it can't be removed by calculation.

The O_3 interference has an effect on the calibration as well. Our mass flow controllers operated most accurately with both the standard and dilution gases coming from compressed gas cylinders, rather than the standard being under pressure and the dilution gas under vacuum.

Consequently, compressed air was used with probably a zero O_3 concentration because O_3 is destroyed and it sticks on walls (Roger Atkinson, University of California, Riverside, personal communication to Graser, 1994; their measurements of ozone in a compressed air cylinder showed no ozone). Because the ozone-free calibration dilution gas does not match the variable atmospheric concentration of ozone and because the calibration curve is non-linear, the O_3 interference can put the LMA-3 output on the wrong part of the calibration curve with the wrong curvature. NO_x and NO_2 concentrations with the new luminol are clearly in error by 25% with O_3-free calibration dilution.Since NO is determined by difference (that is, $(NO_2 + NO + iO_3) - (NO_2 + iO_3)$) and the O_3 interference (iO_3) is identical for the corresponding NO_x and NO_2 measurements, the NO concentration is nearly accurate except for the NO_x and NO_2 concentrations that will be on the wrong part and curvature of the calibration curve. Since measurements will be too high due to ozone interference, a flatter part of the calibration curve will be used than should be and the gradients will be smaller than they should be.

The effect of O_3 interference on the NO_x gradient determinations can be considered for several cases (Table 6.4). When the O_3 gradient is large, the NO_x and similarly the NO_2 gradient can look small, zero, or negative.

Table 6.4 Magnitudes of error in gradient caused by O_3 interference.

CASE	ACTUAL CONCENTRATION $[O_3]$	iO_3	$[NO_x]$	LMA-3 OUTPUT $[NO_x]$
1 (typical concentrations)				
High level	31 ppb	310 ppt	300 ppb	610 ppb
Low level	30 ppb	300 ppt	330 ppb	630 ppb
Gradient	1 ppb		30 ppt	20 ppt
Note: the O_3 gradient reduces the measured ΔNO_x				
2 (ΔO_3 = 0, ΔNO_x = big)				
High level	30 ppb	300 ppt	300 ppt	600 ppt
Low level	30 ppb	300 ppt	350 ppt	650 ppt
Gradient	0 ppb		50 ppt	50 ppt
Note: if there is no O_3 gradient, the O_3 interference cancels out in the absence of a calibration problem				
3 (ΔO_3 = big, ΔNO_x = small)				
High level	32 ppb	320 ppt	300 ppt	620 ppt
Low level	30 ppb	300 ppt	320 ppt	620 ppt
Gradient	2 ppb		20 ppt	0 ppt
Note: if the O_3 gradient is large it can make the ΔNO_x look small, zero, or negative.				

6.1.3.1.2 **Predicted eddy diffusivity.** Before DOY 350, K was calculated based on a statistical regression model. The model has the disadvantage of being applied to extrapolate data: the missing data occurred in a different season of the year when the crop was shorter. During model development, the anemometer and wind vane were about 2.0 to 3.0 m above the crop, while during model usage for prediction, the anemometer and wind vane were up to 3.0 to 4.0 m above plant height. With equal regional wind speeds, wind speeds at 4.5 m are thought to be higher during the K-model prediction period than the K-model development period by more than the increase in mixing, possibly leading to

inflated estimates of K. Regardless, the NO fluxes based on predicted Ks (DOY 286 to 340) are not as reliable as the NO fluxes based on measured Ks (DOY 350 to 481).

6.1.3.1.3 Fluxes determined with the effective reactive K. The NO and NO_2 fluxes determined by inert K approaches based on NO and NO_2 concentration gradients can be and usually are in error because NO and NO_2 can react creating a flux divergence (fluxes are no longer constant with height). The inert K approach can be applied to a conserved entity such as NO_x (NO + NO_2). In order to determine our NO fluxes above the canopy, a consideration of the rapid in-air chemical reactions experienced by the NO-O_3-NO_2 system during the day and night is made. Our calculations are based on the complete reactive K model based on the ratio of turbulence and chemical transformation time scales formulated by Vila-Guerau de Arellano and Duynkerke (1992).

The flux equation was summarized as follows:

$$\overline{wc_i} = K_{ij}\left(\frac{\partial \overline{C_j}}{\partial z}\right) \qquad [6.1a]$$

where the units of $\overline{wc_i}$ are ppb m s^{-1}, or

$$\overline{wc_i} = K_{ij} * \frac{\partial \overline{c_j}}{\partial z} * \frac{mw_j\ P}{R\ T} \qquad [6.1b]$$

where the units of $\overline{wc_i}$ are ng m^{-2} s^{-1}, mw_j is the molecular

weight of species j, P is the atmospheric pressure, R is the ideal gas constant, T is the absolute temperature, and where K_{ij} is the effective reactive turbulent exchange coefficient that can be expressed as follows in the form of a matrix:

$$K_{ij} = \frac{\kappa u_* (z + z_0)}{1 + r_1 + r_2 + r_3} \begin{pmatrix} 1 + r_1 + r_3 & -r_1 & r_3 \\ -r_2 & 1 + r_2 + r_3 & r_3 \\ r_2 & r_1 & 1 + r_1 + r_2 \end{pmatrix} \quad [6.2]$$

where r_1, r_2, and r_3 are the ratios between the turbulent and chemical reaction time scales and are defined as:

$$r_1 = \frac{\kappa (z + z_0) k_1 \overline{NO}}{u_*} \quad [6.3]$$

$$r_2 = \frac{\kappa (z + z_0) k_1 \overline{C_3}}{u_*} \quad [6.4]$$

$$r_3 = \frac{\kappa (z + z_0) k_2}{u_*} \quad [6.5]$$

O_3 gradients were only measured briefly on DOY 115. NO, O_3, and NO_2 fluxes are calculated with our experimental data using the effective reactive K approach (the general matrix eq. [6.2]) from Vila-Guerau de Arellano and Duynkerke (1992) and two sets of values for the chemical reaction rates (Table 6.5). Although the approach is for neutral conditions where $K = \kappa u_* z$, we are using measured K which is correct for each stability.

Table 6.5. Comparison of fluxes calculated using the inert K and the effective reactive K for three time intervals on DOY 115.

Time [h]	Species	Concentration [ppb]	Fluxes determined with — Inert-K	Reactive-K* [ng N m^{-2} s^{-1}]	Reactive-K**
1620					
	NO	0.351	-0.00776	-0.00744	-0.00748
	NO_2	0.170	0.00287	0.00255	0.0026
	NO_x	0.521	-0.00488	-0.00488	-0.00488
	O_3	27.13	0.24495	0.24604	0.24589
1640					
	NO	0.310	-0.0051	-0.00461	-0.0047
	NO_2	0.144	0.00668	0.00619	0.00628
	NO_x	0.454	0.00158	0.00158	0.00158
	O_3	27.27	-1.0649	-1.0632	-1.0635
2120					
	NO	0.205	-0.0002	2.4×10^{-5}	1.59×10^{-5}
	NO_2	0.664	0.00025	2.8×10^{-5}	3.74×10^{-5}
	NO_x	0.869	5.33×10^{-5}	5.3×10^{-5}	5.33×10^{-5}
	O_3	21.75	-0.09376	-0.0929	-0.09301

u_* = 0.34, 0.33 and 0.011 for 20-min time intervals ending at 1620, 1640 and 2120 h, respectively as calculated from $u_* = K/\kappa z$; $z + z_0 = 4.5$ m;
* $k_1 = 0.000416$ $ppbv^{-1}$ s^{-1}, $k_2 = 0.008$ s^{-1} (Vila-Guerau de Arellano and Duynkerke, 1992);
** $k_1 = 0.0004$ $ppbv^{-1}$ s^{-1}, $k_2 = 0.004$ s^{-1} (Fitzjarrald and Lenschow, 1983).

For this small data set, the fluxes calculated using the reactive-K approach were on average 10 % smaller for NO_2, 8 and 0.5% larger for NO and O_3, respectively, compared to the fluxes calculated using the inert-K approach. Vila-Guerau de Arellano and Duynkerke (1992) reported differences between the reactive and inert exchange coefficient of 30, 5, and 3% for NO, NO_2, and O_3, respectively. Fitzjarrald and Lenschow (1983) reported that when the NO/NO_x concentration ratio does not exceed 0.1, the NO_x reactive fluxes may differ from the non-reactive fluxes from 10 to

20%. Their reactive O_3 fluxes were equal to the O_3 non-reactive fluxes.

The use of the effective reactive Ks had a relatively small effect on the fluxes, apparently because the 1 m spread between the arms of the instruments did not permit much time for the reaction to take place while the gas was mixing across this distance. Examination of the 2 days of O_3 concentration data for this site and 6 months of Department of Health O_3 concentration data for elsewhere on Oahu (Sand Island) suggests the small effect of the reaction on our fluxes is typical of our entire study. In fact, earlier in the season when the arms were further above the crop, mixing was greater allowing less reaction to occur.

6.1.3.2 Diurnal patterns in concentration

It was expected from the literature (Delany et al., 1986; Wesely et al., 1989) that at night in the absence of photochemistry, that NO_2 would no longer dissociate to form O_3, O_3 would be depleted by surface deposition and reaction with NO, and, after the O_3 was depleted, the NO concentration would increase. Nighttime data was collected from DOY 87 to 88 and 115 to 118, but O_3 data was only collected from DOY 115 to 117 (Fig. 6.7 and 6.8). Our data does not show O_3 decreasing nor NO increasing during the night. O_3 has peaks during the night similar in magnitude to those during the day (28 to 30 ppb).

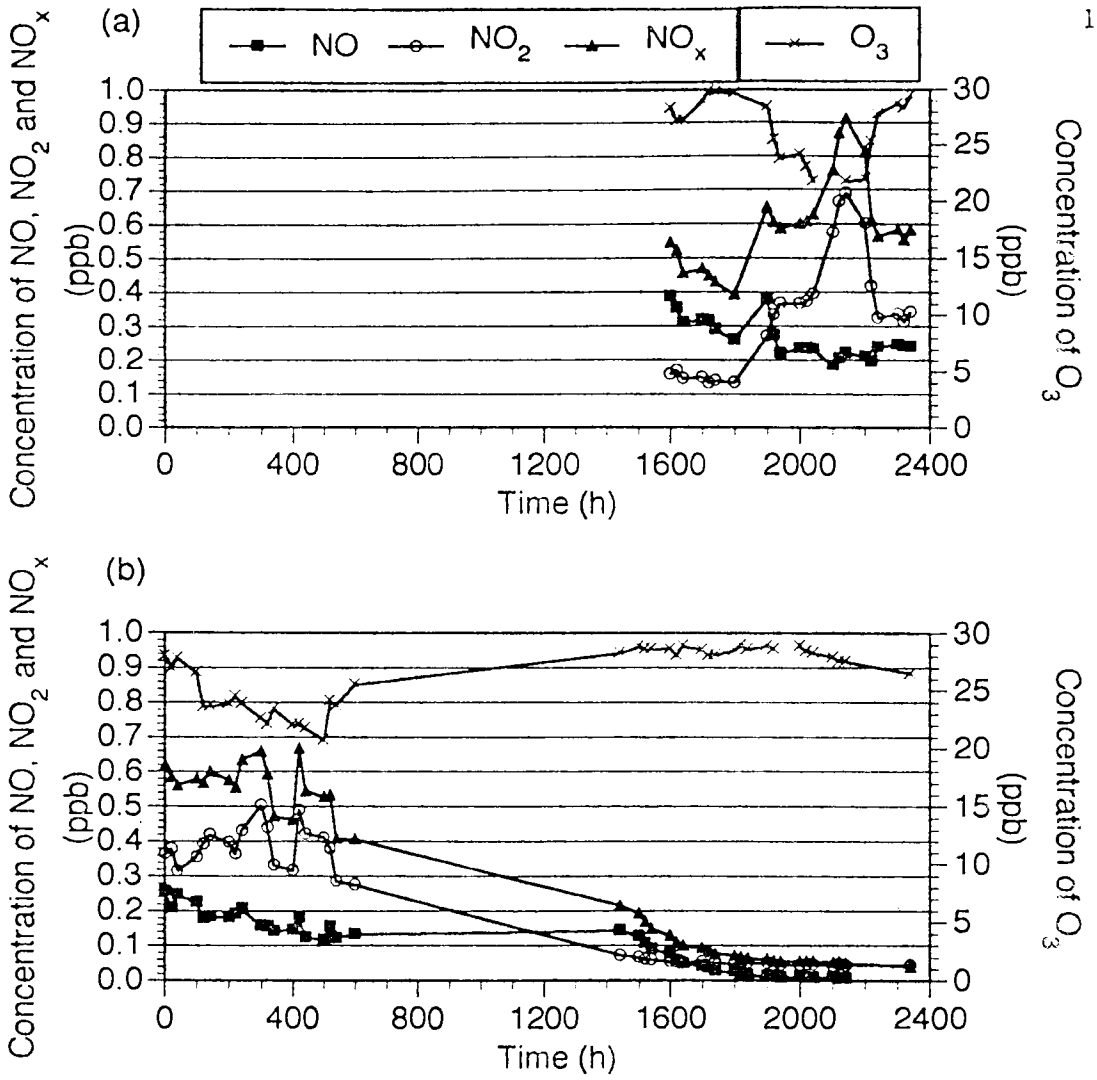

Figure 6.7 The concentration of NO, NO_2, NO_x, and O_3 as a function of time for (a) DOY 115 in 1994 and (b) DOY 116 in 1994.

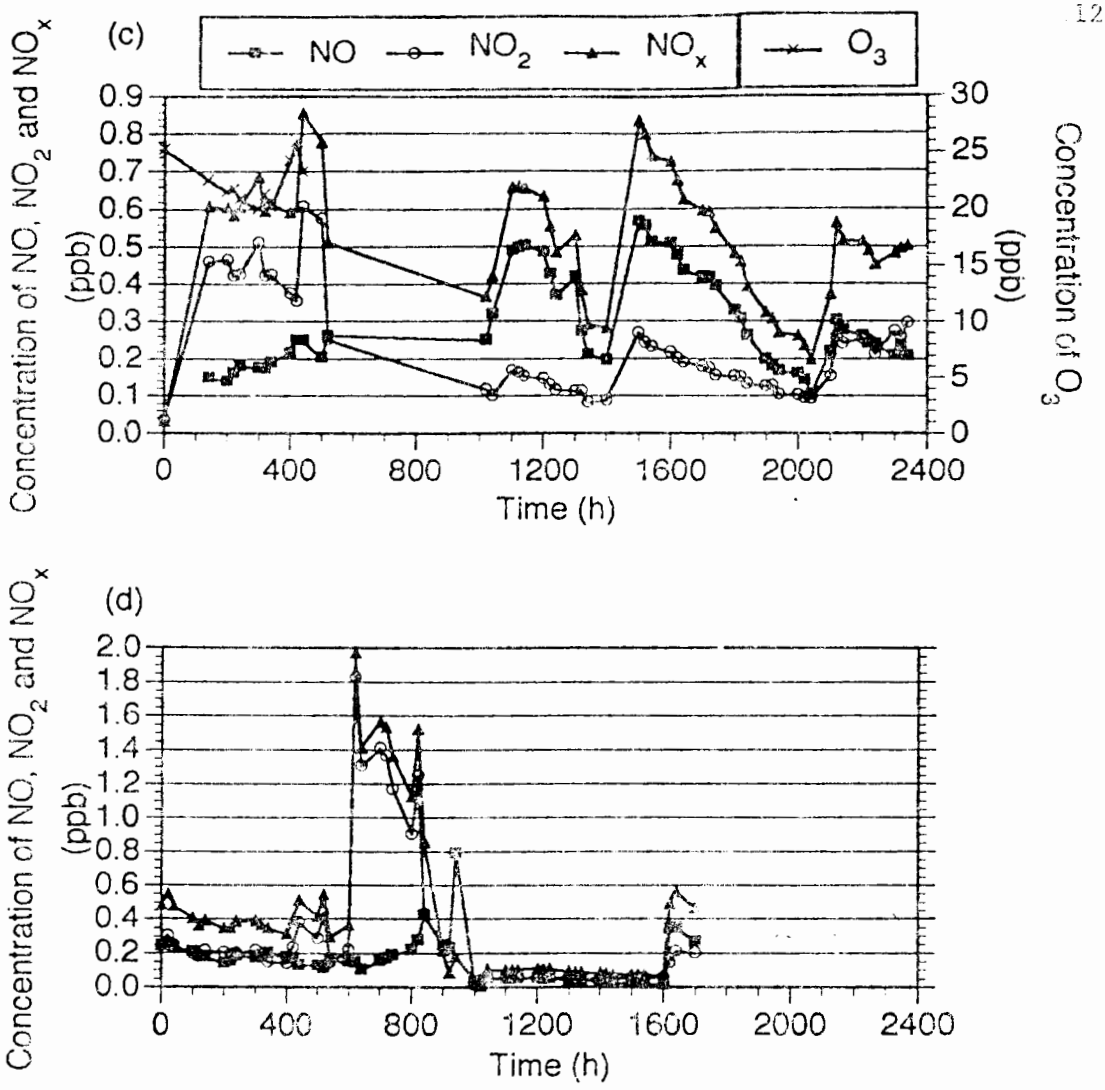

Figure 6.7 (continued) (c) DOY 117 in 1994 and (d) DOY 118 in 1994.

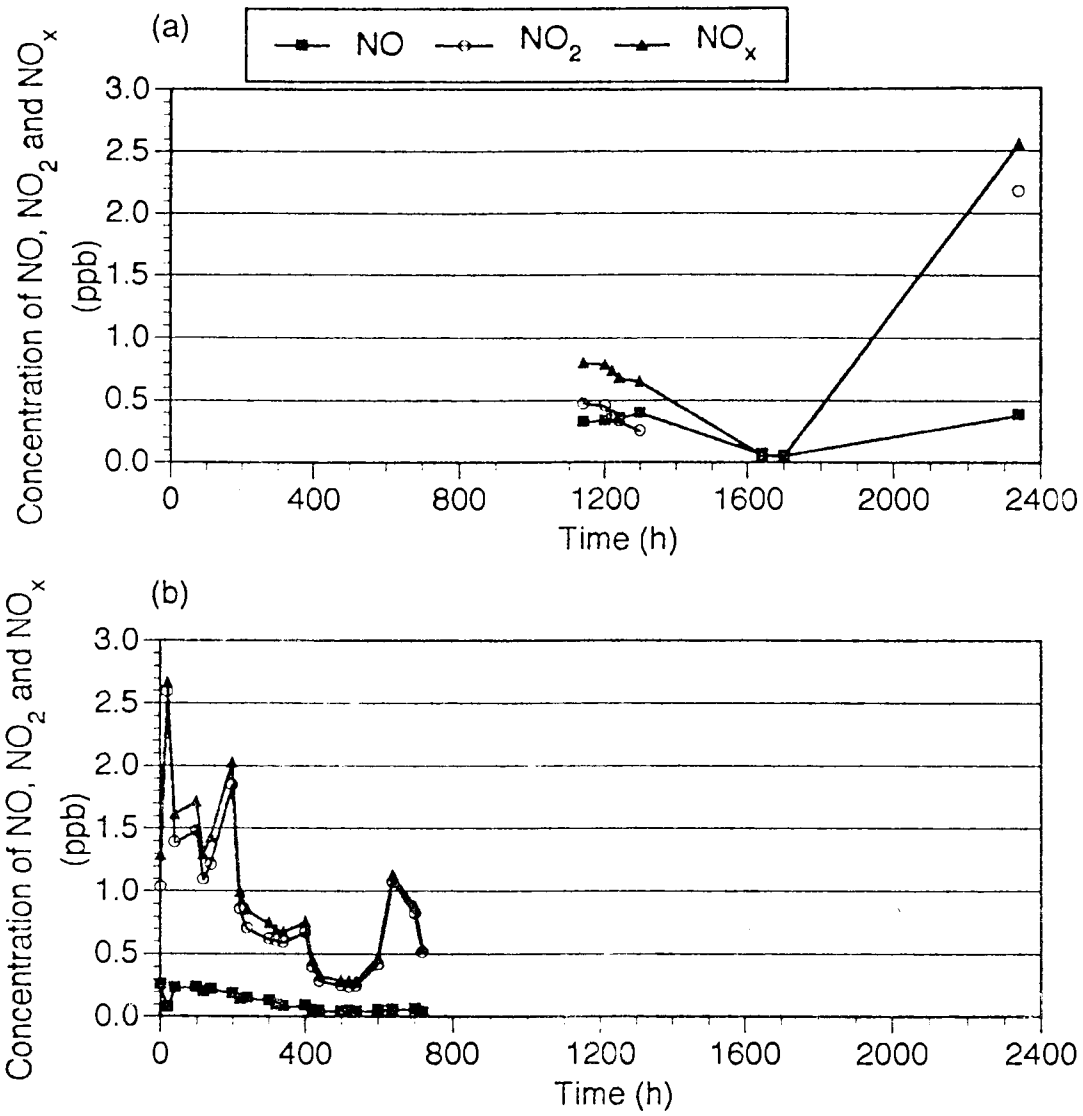

Figure 6.8 The concentration of NO, NO_2, and NO_x as a function of time for (a) DOY 87 in 1994 and (b) DOY 88 in 1994.

Decreases in NO_x and NO_2 concentration corresponded to increases in O_3 concentration and vice verse, whereas the NO concentration remained lower and showed a weak relationship with NO_x and O_3 (Fig. 6.7). This same pattern was observed for both day and night. A gradual decrease in the NO_x concentration from 0.9 to near 0 ppb was observed from DOY 115 to midnight of DOY 116, followed by a drastic increase of NO_x back to 0.9 ppb by the morning of DOY 116. Apparently a source of O_3 and a sink for NO_x existed at this height. The source may be mixing from the upper surface layer during the night or NO production and consumption by the nitrate radical NO_3 (Wesely et al., 1989). A dense cloud cover at midnight on DOY 116 could have carried a source of NO_x from other areas for the following hours.

The use of a generator represents a source of NO_x which potentially would destroy O_3, however it was located in a downwind area about 50 m away from the meteorological station and data was taken with the prevailing wind direction from the North-East. The winds are generally quite brisk and relatively steady at this site suggesting exhaust would not reach the meteorological station with appropiate wind direction. The NO_x concentrations measured from DOY 117 to 118 (Fig. 6.7) without a generator running are of about the same magnitude as the two previous days with the generator indicating the generator was not a local source of pollution.

A weak pattern of higher NO and NO_x concentrations was observed during the day compared to the night on DOY 117 (Fig. 6.7) suggesting that light does not affect significantly the production of NO by soil microorganisms. In the morning on DOY 118, the NO_2 and NO_x concentrations increased drastically about four times (from 600 to 1000 h) and decreased back close to zero (from 1020 to 1600 h). Possibly atmospheric mixing diluted NO_x or rainfall cleared it from the air (7 mm of rain fell from 500 to 1000 h). On DOY 87 to 88 nighttime concentrations were highest (Fig. 6.8).

6.1.3.3 Diurnal patterns in fluxes

A diurnal trend of fluxes increasing in the morning, reaching a peak at noon, and decreasing in the afternoon (Fig. 6.9a and b) and night (Fig. 6.9c, d, e, and f) was evident for a few days. Either a limited number of hours of data were available for other days or the NO_x fluxes showed high fluctuations for the entire day. The NO_2 and NO_x fluxes were of about the same magnitude and followed clearly the diurnal pattern for DOY 350 and 33 while the NO flux showed a weak pattern (Fig. 6.9a, b, and c). The NO flux went downward while the NO_2 flux went upward for DOY 115, 116, and 117 (Fig. 6.9d, e, and f) with net NO_x flux fluctuating around zero (Fig. 6.9e and f). Apparently NO was adsorbed in the sugarcane canopy and released back to

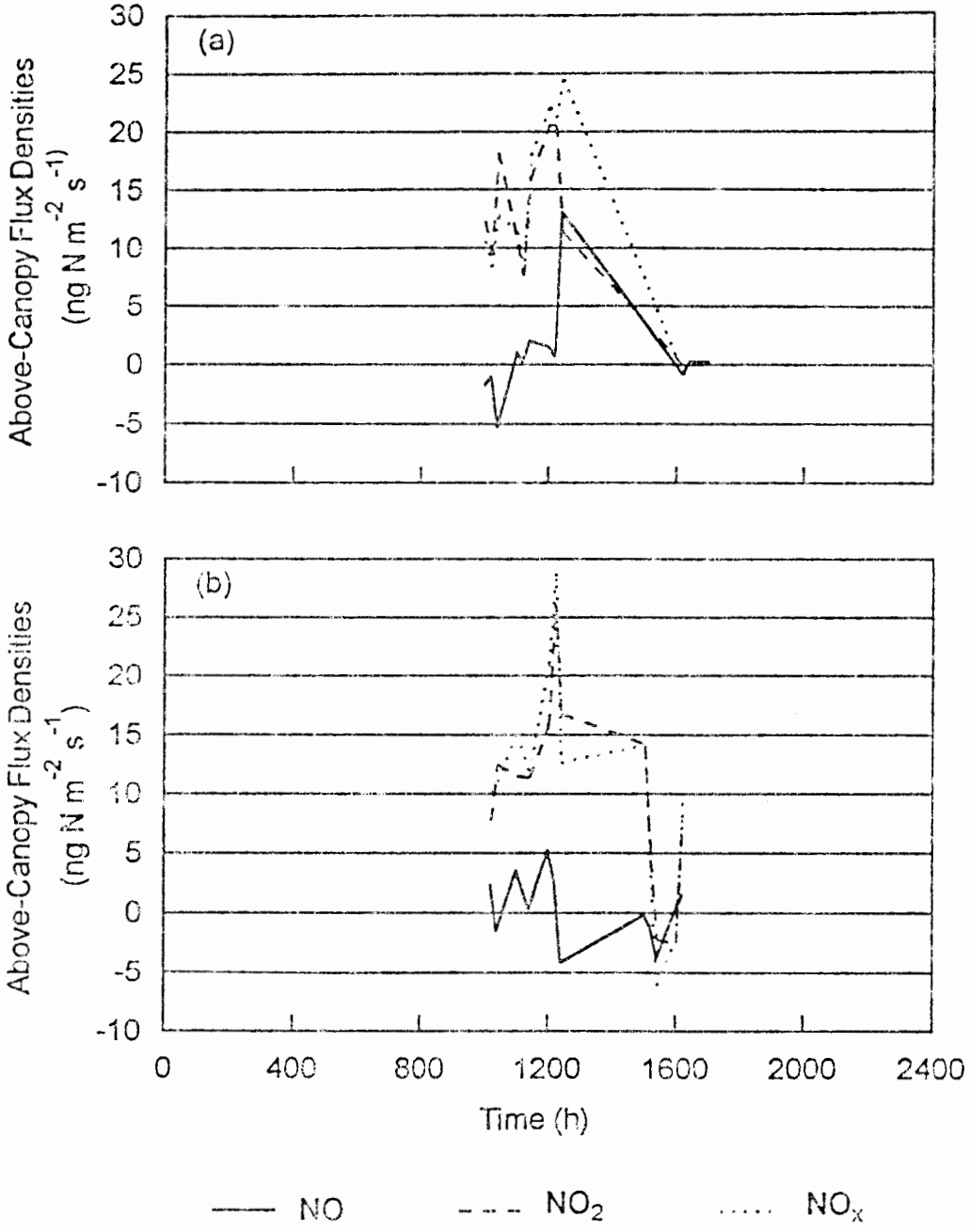

Figure 6.9 Above-canopy flux densities of NO, NO_2, and NO_x as a function of time for (a) DOY 350 in 1993, (b) DOY 33 in 1994. The positive portion of the Y axis indicates upward fluxes and the negative portion indicates downward fluxes.

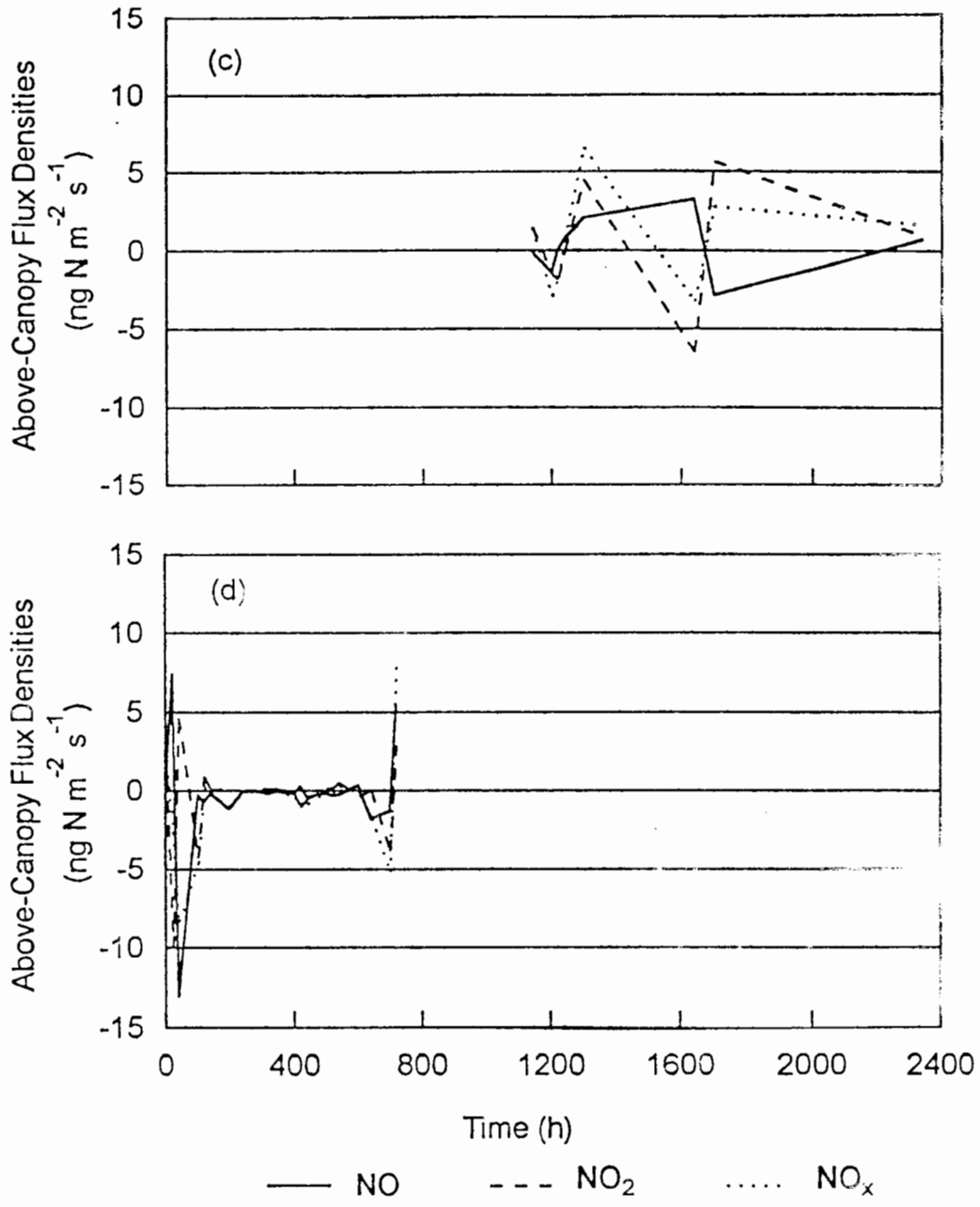

Figure 6.9 (continued) (c) DOY 87 in 1994, (d) DOY 88 in 1994.

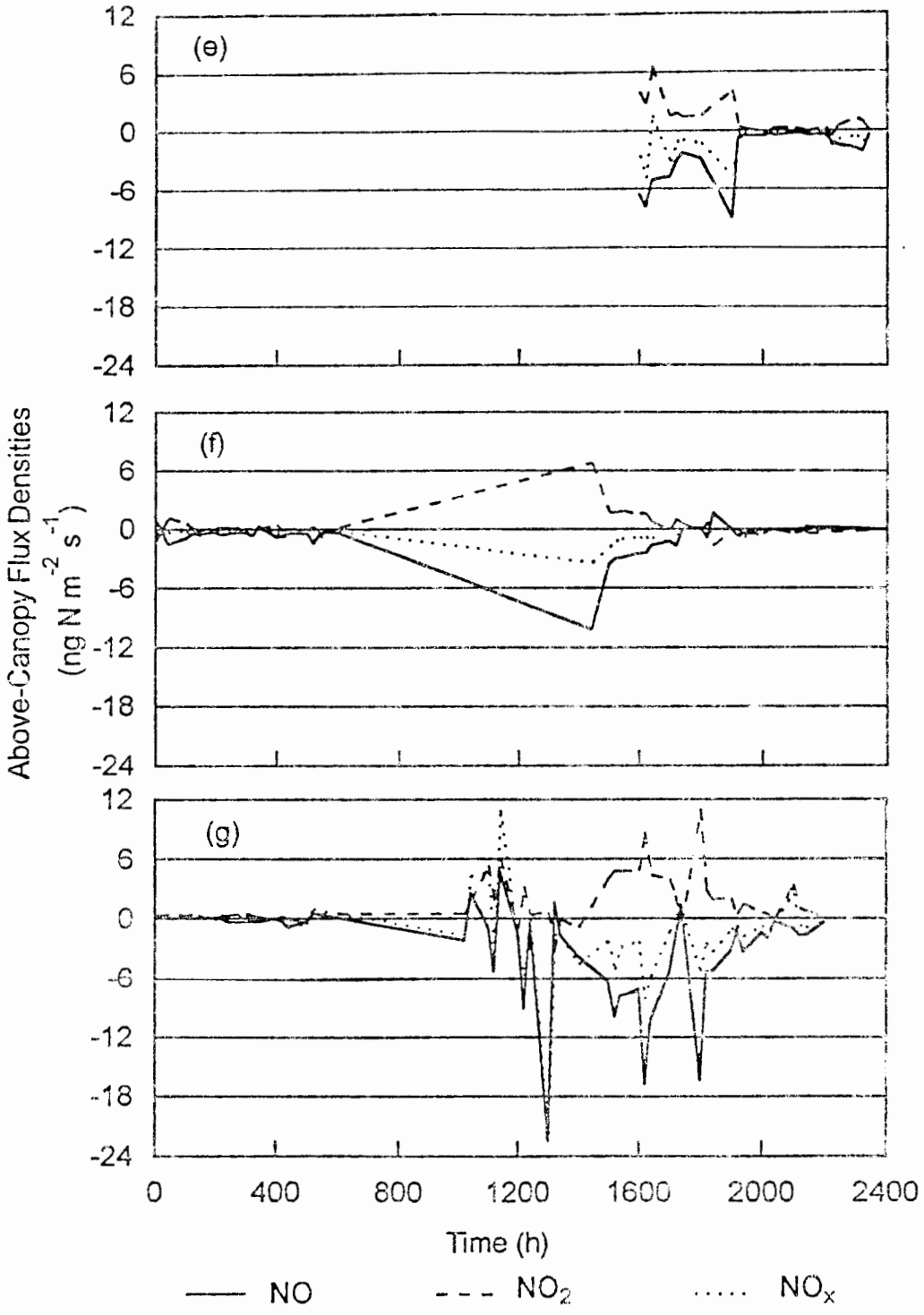

Figure 6.9 (continued) (e) DOY 115, (f) DOY 116, and (g) DOY 117 in 1994.

the atmosphere as NO_2 by the transpiration process. However overall sources and sinks of NO_x are difficult to assess because the NO emissions from the surface were low for these days (1 to 9 ng N m^{-2} s^{-1}) (Fig. 6.2). It is difficult to determine whether the upward and downward flux is affected by the rapid in-air chemical reactions, especially when emissions from the surface, deposition rates, and plant effects must be considered. Due to high fluctuations in NO and NO_2 fluxes, diurnal patterns were not consistent over time. Therefore, daily averages of NO and NO_2 fluxes may not be representative of a true mean flux. NO_2 fluxes were 5 to 20 times larger during the day than at night (Fig. 6.9d, e, and f) indicating that air mixing and plant processes during the day do have an effect on the fluxes.

The diurnal patterns in the above-canopy flux data indicate that characterization of the flux for a day based on a short period of measurement during the daytime will exceed the daily average.

Diurnal changes in volumetric water content were not measured, but it is typical with a wet subsoil as we had that the surface water content increases at night. This phenomenon suggests that NO fluxes might increase at night in response to the surface soil moisture.

6.1.3.4 Comparison of above-canopy NO_x fluxes with surface NO fluxes

A comparison between the NO_x fluxes above the canopy and the field average NO emissions from the surface for the whole study will be made to determine how much NO_x reaches the atmosphere and how the crop influences the NO_x flux. NO emissions from the soil were always away from the surface, whereas the NO_x fluxes above the canopy were generally away from the surface and sometimes towards the surface.

A field average of NO fluxes from the soil (F_{NOfa}) was calculated by multiplying the average NO fluxes from the four sites at each row position (DL and BR) times the surface fraction they represented along the sugarcane rows (Eq. [6.6]). The NO fluxes from DL, SC, and BR measured on 10 days at the beginning of the experiment and their surface fractions were used to obtain this relation.

$$F_{NOfa} = 0.195 * F_{NOdl} + 0.805 * F_{NObr} \qquad [6.6]$$

The daily average above-canopy flux density was determined by averaging the above-canopy fluxes for all available time periods.

The daily NO_x fluxes at 4.5 m were usually away from the surface (that is, surface emissions exceeded deposition) (Fig. 6.10) and 2 times bigger (on average) than the NO emissions from the surface (Fig. 6.11 and 6.12). NO surface fluxes were higher than NO_x above-canopy fluxes on a few days at the beginning of the experiment and were generally

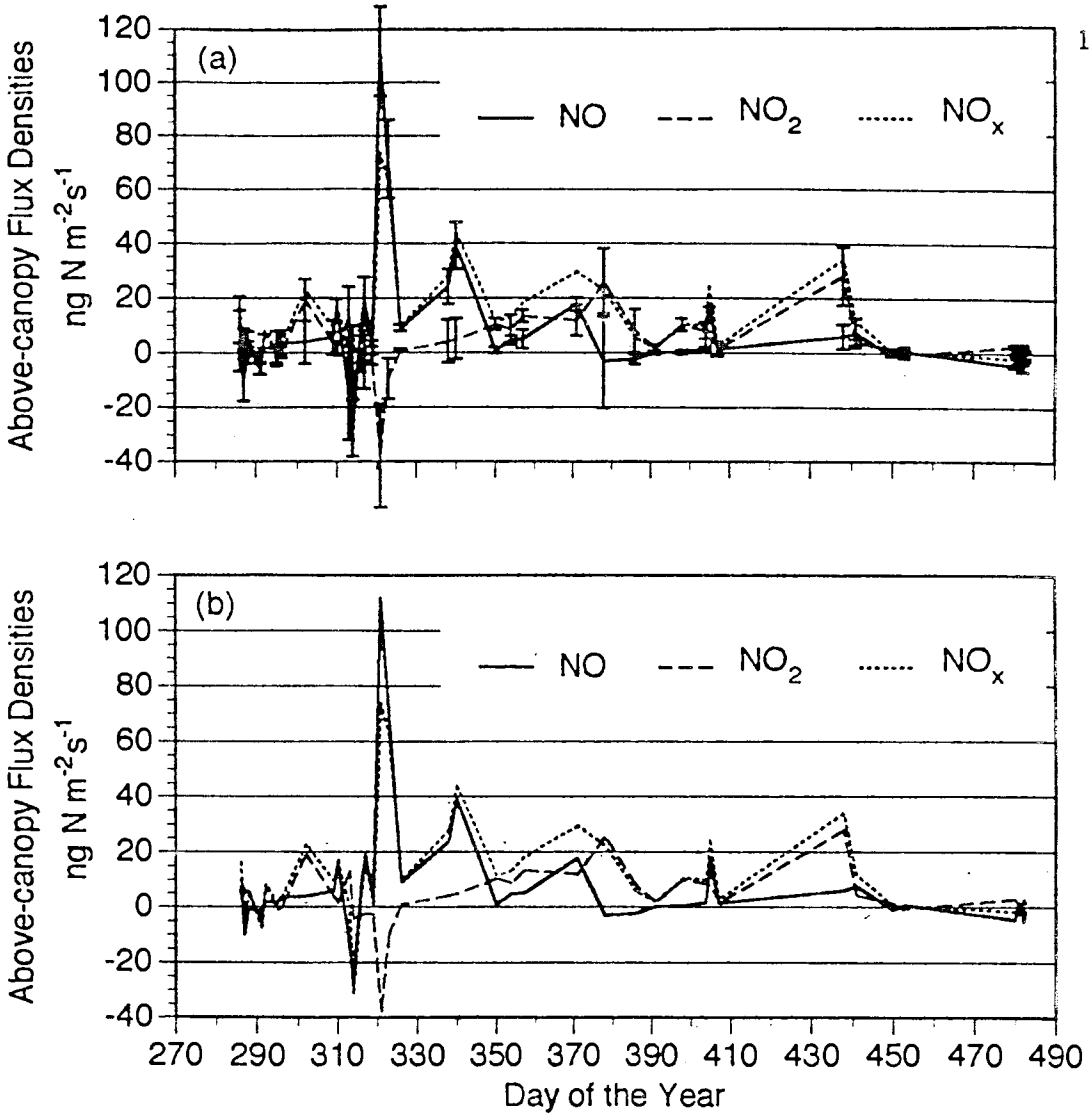

Figure 6.10 The above-canopy NO, NO_2, and NO_x flux densities for the experimental period from DOY 286 in 1993 to DOY 118 in 1994. In the year 1994, 365 d was added to the day of the year. (a) The standard error is shown by a bar; (b) the figure is shown without error bars for visual clarity. The positive portion of the Y axis indicates upward fluxes and the negative portion indicates downward fluxes. For DOY 286 to 340 and 350 to 118 the flux density was calculated using a modelled and measured K, respectively

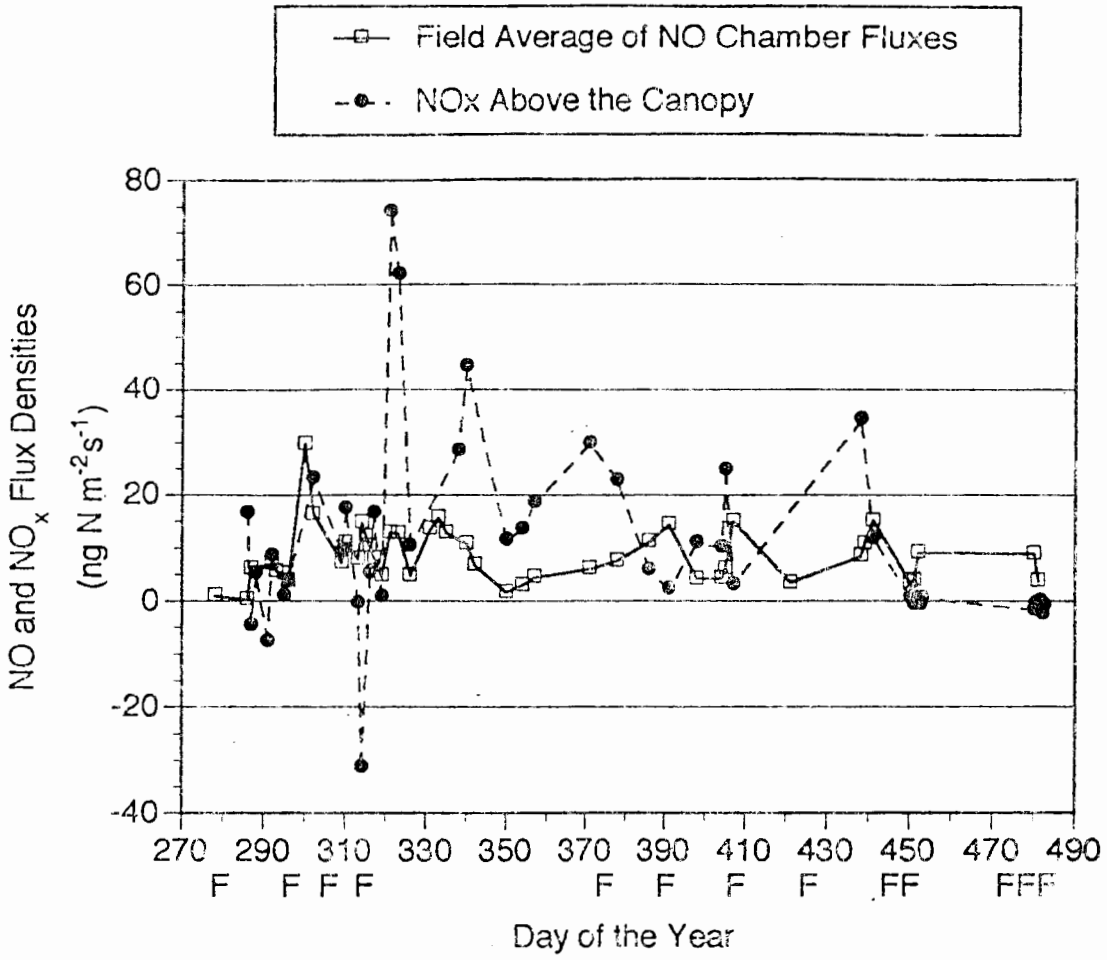

Figure 6.11 A comparison of NO flux density at the soil surface and NO_x flux density above canopy for the experimental period from DOY 286 in 1993 to DOY 118 in 1994. In the year 1994, 365 d was added to the day of the year. The positive portion of the Y axis indicates upward fluxes and the negative portion indicates downward fluxes. Each fertilization is represented by an F along the X axis.

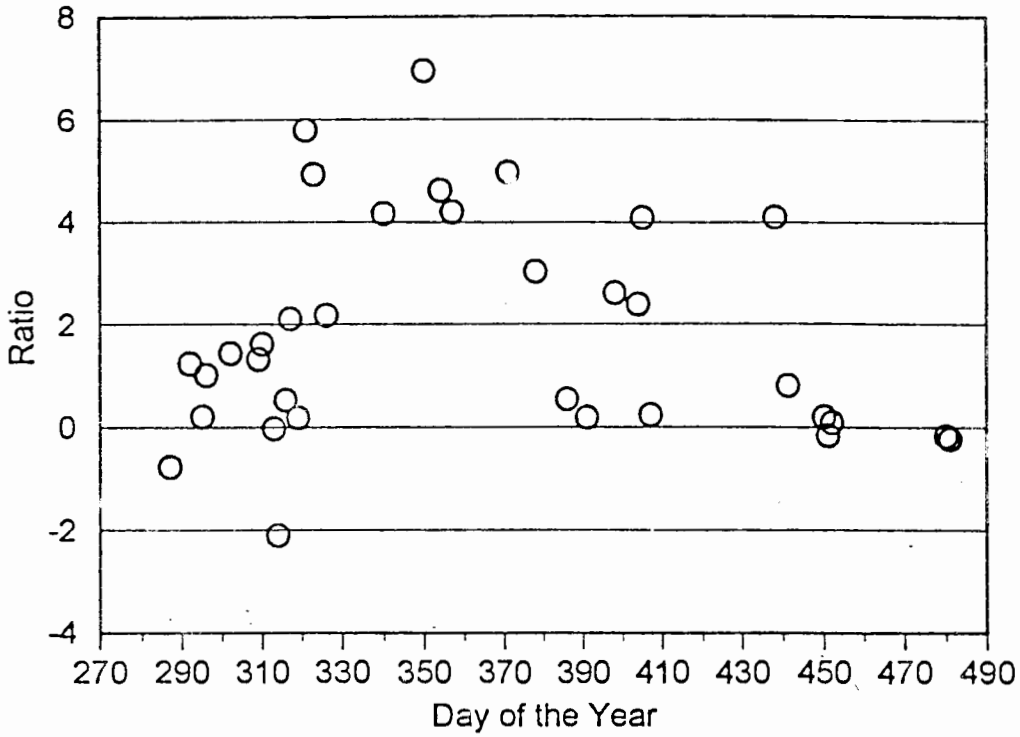

Figure 6.12 Ratios of NO_x fluxes measured above the canopy to those measured at the soil surface for the experimental period from DOY 286 in 1993 to DOY 118 in 1994. In the year 1994, 365 d was added to the day of the year.

higher at the end of the experiment when the leaf area increased from 2 to 6 (Fig. 6.12 and 6.1). At the beginning of the experiment large NO fluxes at BR made the field average large, whereas at the end of the experiment the decrease in fluxes above the canopy could be attributed to the sugarcane canopy. The large ratios (from 2 to 7) observed in the middle of the experiment (Fig. 6.12) could be attributed to experimental errors such as O_3 interference in the analyzer, an error which occurs throughout the experiment.

If the weighing factor to calculate the field average for NO emissions (Eq. [6.6]) from the soil had given a greater weight to the flux at the drip-line row position which was consistently a bigger flux, the chamber field average would have been closer in magnitude to the NO_x fluxes measured above the canopy, but it is not clear that the above-canopy flux magnitude is more valid than the soil-surface flux magnitude. The weighting factor was developed from data early in the season when shading was minimal and other characteristics vary from the end of the study.

Because variability was great between the chamber sites, additional measurement sites could have resulted in the soil surface field average resembling the above-canopy fluxes more closely if the four current measurement sites were not representative.

NO_x fluxes towards the surface were observed on several

days throughout the season suggesting deposition (DOY 287, 291, 313, 314, 86, 115, and 116) (Fig. 6.10) or increases in O_3 fluxes and associated measurement errors. Both of these are probably promoted by similar atmospheric behavior. NO_x fluxes above the surface frequently matched the trends followed by the surface emissions early in the season suggesting that NO emitted from the soil was the important source of the NO_x in the atmosphere (Fig 6.10) and that other processes such as interaction with the canopy were not important yet.

At the beginning of the experiment (DOY 278 to 295) NO fluxes above and below the canopy did not show a clear relationship. Surface NO emissions fluctuated from 0 to 7 ng-N m^{-2} s^{-2} away from the surface whereas fluxes of NO_x above the surface ranged from 7 towards the surface to 16 ng-N m^{-2} s^{-1} away from the surface.

A soil NO emission increase from 4 to 30 and decrease back to 7 ng-N m^{-2} s^{-1} corresponded to a above-canopy NO_x flux increase from 4 to 23 and decrease to 9 ng-N m^{-2} s^{-1} (DOY 296 to 309). At this early stage of canopy development (LAI = 0.17) (Fig. 6.1) the crop had very little effect on the transport of NO_x to the atmosphere. The greatest peak of surface emissions for the whole season was observed during this time period (DOY 300 and 302) (Fig. 6.11) due to significant emissions from SC and BR (Fig. 6.2). Since these row positions comprise most of the surface there was

less horizontal variability throughout the field than during the rest of the measurement period. Here the above-canopy NO_x fluxes were of similar magnitude compared to the surface emissions.

Between DOY 313 to 314 the NO surface emission increased from 8 to 15 ng-N m^{-2} s^{-1} away from the surface whereas the above-canopy NO_x fluxes went from 0 to 31 ng-N m^{-2} s^{-1} towards the surface. The NO_x flux is bidirectional (an emission flux competes with a deposition flux) (e.g. Delany et al., 1986); the emission flux depends on the rate of production from the soil while the deposition flux depends on the atmospheric concentrations. Both a deposition of NO_2 or an increased deposition of O_3 causing increased analyzer interference could explain this non agreement of the chamber and above-canopy fluxes.

A surface NO emission doubling corresponded to an above-canopy NO_x flux increase of nearly 100 times from DOY 319 to 321 (Fig. 6.11). Since NO may be more soluble in the plant liquid than it is in water it may be taken up by plant roots and subsequently emitted through the stomata (A. C. Delany, personal communication to E.A. Graser, 1994). Environmental conditions which would have caused the plant to emit NO particularly at this time are not known. The NO_2 flux toward the surface from DOY 314 to 323 might indicate an O_3 flux increase and an associated increase in analyzer interference which could partly explain the huge NO_x flux.

Possibly the DL soil flux should have been weighted more in determining the field average for these days. By DOY 326 the NO_x fluxes above the surface and NO emissions from the soil were both low (10 and 5 ng-N m^{-2} s^{-1}, respectively).

The effect of a wetting and drying cycle on NO production in soils and its transport to the atmosphere is illustrated from DOY 331 to 340 (Fig 6.5 and 6.11). During this time interval a peak of NO_x flux above the canopy from 24 to 44 ng-N m^{-2} s^{-1} was concurrent with a NO emission from the soil ranging from 10 to 15 ng-N m^{-2} s^{-1}. Another example of NO fluxes above the canopy following a wet and dry cycle is observed from DOY 39 to 42 (404 to 407). The chamber flux increased from 4 to 15 ng N m^{-2} s^{-1} whereas the NO_x flux above the canopy increased from 10 to 24 ng N m^{-2} s^{-1}.

The dependence of the NO_x flux above the surface on the NO emissions from the soil can still be observed from DOY 350 to 6 (371) before it weakens over the following months (Fig. 6.11). The NO_x flux was about 4 times larger than the NO emissions through DOY 13 (378). However the NO emissions from the soil were 2 and 7 times larger than the NO_x fluxes for DOY 21 (386) and 26 (391).

For DOY 33 (398) and 39 (404) the NO emissions from the surface and NO_x fluxes above the canopy were similar and low at about 4 and 10 ng-N m^{-2} s^{-1}, respectively. Upward and downward fluxes can equal or compensate. Delany et al. (1986) called this a compensation level. On DOY 385 and 392

there were emissions from the soil, but only minor fluxes above canopy suggesting deposition equalled emissions.

Two highly windy days (wind speed of 10 m s^{-1}) occurred on DOY 73 and 76. On DOY 73 (438) the NO_x flux above the canopy was about 4 times larger than the emissions from the soil (Fig. 6.11); however, by DOY 76 (441) the NO surface emissions increased by more than half but the NO_x fluxes above the canopy decreased by two thirds. The windiness may have slightly increased the surface NO flux by reducing the NO concentration in the soil, but such an effect is not distinguishable because the soil water content also increased slightly during this time. The NO_x flux reduction on DOY 76 may be due to more mixing deeper into the sugarcane canopy (LAI = 4.9) (Fig. 6.1) and associated deposition on leaves, but it is unclear why this wouldn't have begun on the first windy day. The slight increase in NO surface emissions, while the NO_x fluxes above the canopy decreased drastically, could be explained in terms of an increase in the ozone flux and analyzer interference due to the windiness bringing ozone down from higher in the atmosphere.

Cases of NO emissions from the surface being larger than the NO_x fluxes above the canopy were observed at the end of the experiment corresponding to rapid increases in leaf area index. From DOY 85 (450) to 87 (452) the surface emissions were low and increased 3 fold, but the above-canopy NO_x fluxes stayed nearly constant and near zero (Fig. 6.11). The surface

NO flux decreased from 9 to 4 ng-N m^{-2} s^{-1} from DOY 115 (480) to 116 (481), whereas the above-canopy NO_x flux fluctuated around 1 ng-N m^{-2} s^{-1} toward the surface for DOY 115, 116, and 117 (Fig. 6.11). Deposition or error due to O_3 flux changes can explain low and surface-directed NO_x fluxes, but this is less likely to be the case for both periods DOY 85 to 87 and 115 to 117. Apparently the NO produced in the soil was mostly taken up by plants since the sugarcane canopy was closed (LAI = 6) (Fig. 6.1).

6.1.3.5 Speciation of above-canopy fluxes

This section will discuss the speciation of NO_x fluxes as NO and NO_2 fluxes above the surface. For a short-time period (DOY 296 to 309) at the beginning of the experiment, the NO_x consisted predominantly of NO_2 (Fig. 6.10). This time period corresponds to rapid soil wetting and large NO fluxes at the BR position (Fig. 6.2 and 6.3).

From DOY 313 to 314 the NO_x flux mainly consisted of the NO flux, each towards the surface (14 to 28 ng-N m^{-2} s^{-1}). A NO flux directed towards the surface has not been reported in the literature. Three possible explanations are measurement errors; deposition of NO_2 which is converted to NO above the canopy (Fig. 6.13a); and/or a one-directional conversion of NO to NO_2 below the canopy in the shade, but a two-directional conversion of NO to NO_2 above the canopy due to direct solar radiation (Fig. 6.13b).

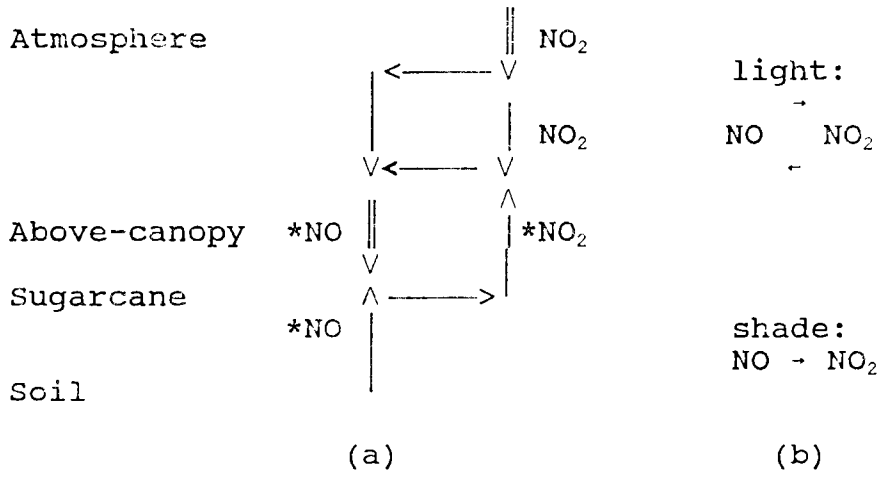

* Measured fluxes.

Figure 6.13. a) Downward flux of NO_2 and its conversion to NO; b) Conversion of NO to NO_2 below and above the canopy. The vertical arrows represent vertical fluxes and the horizontal arrows represent net conversions of species.

From DOY 319 to 321 the NO flux away from the surface and the NO_2 flux toward the surface each peaked, but the NO flux dominated (Fig. 6.10). Since fertilizer was applied on DOY 315 the emission of NO from the sugarcane through the transpiration stream might have been an important source even though the crop was only 2.5 months old (LAI = 0.5) (Fig. 6.1). It is also possible that NO_2 deposition was taken up by the sugarcane and quickly reemitted to the atmosphere as NO through the stomata. The trend in the NO_2 flux toward the surface might indicate an O_3 flux change resulting in analyzer error or reaction effects (Fig. 6.14).

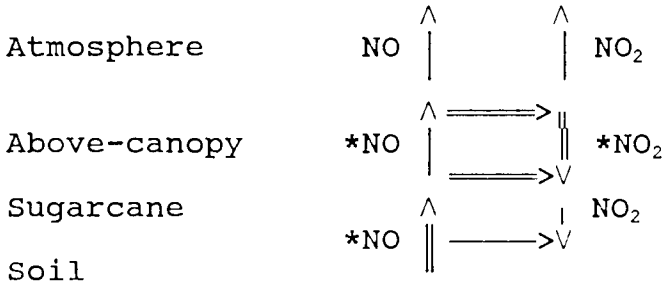

* Measured fluxes

Figure 6.14. Conversion of NO to NO_2 by chemical reaction with O_3.

A dependence of NO fluxes above the canopy on NO emissions from the soil was observed from DOY 331 to 340 (Fig. 6.10 and 6.11). The NO flux above the canopy (9 to 40 ng-N m^{-2} s^{-1}) was concurrent with a NO emission from the soil (10 to 15 ng-N m^{-2} s^{-1}), while the NO_2 flux was relatively low (4 to 5 ng-N m^{-2} s^{-1}). Conversely, from DOY 350 to 6 (371) the NO_2 flux was generally bigger than the NO flux probably due to more time for reaction with air passing through the crop and due to reaction of NO with O_3 to form NO_2 predominating with increased shading. In addition the NO surface emissions continued to increase while the NO flux above the canopy became smaller from DOY 13 (378) to 26 (391) (Fig. 6.10 and 6.11). The NO_2 flux was considerable for these days. From DOY 33 (398) and 39 (404) the NO emissions from the surface and NO_2 fluxes above the surface were similar at about 4 and 10 ng-N m^{-2} s^{-1}, respectively, while the NO flux was about 1 ng-N m^{-2} s^{-1}. This may indicate that the chemical reaction was an efficient and constant source of NO_2.

Strong turbulent mixing appears to affect the chemical reactions as seen on DOY (73) 438 when strong gusty trade winds up to 10 m s^{-1} blew over Oahu. A NO_2 to NO flux ratio of about 5 suggests that a lot of the NO emitted from the soil was converted to NO_2 by reaction with O_3 and that the strong mixing would provide a steady supply of O_3 to react. On the next two windy days (DOY 74 (439) and 76 (441)) the NO_x flux was composed of a higher proportion of NO. The NO_2 flux decrease could be due to increased NO_2 deposition onto the leaves since the strong winds would cause more mixing deeper into the sugarcane canopy (LAI = 4.9) (Fig. 6.1).

A statistical analysis of the effect of environmental factors (such as eddy diffusivity and radiation level) on the ratio of NO_2 flux to NO flux did not identify significant environmental factors.

6.2 Comparison of NO_x fluxes in tropical systems with those from other systems

For the 198 d of this study (of which data was collected on just over 40 d), the average of the measured fluxes yields an estimate of the average seasonal flux for this field which can be compared with other studies. The flux in this study was measured in fall, winter, and spring and may not represent the magnitude that can be reached in summer. The average of the above-canopy NO_x fluxes is 10 ng N m^{-2} s^{-1} or 3.1 kg N ha^{-1} yr^{-1}; however, this number is not completely reliable as discussed. The average of the soil surface NO flux is 9 ng N

m^{-2} s^{-1} or 2.8 kg N ha^{-1} yr^{-1}; this value is thought to be a good approximation of the above-canopy flux for the stage prior to rapid canopy development and for small deposition rates, plant emissions, and soil NO_2 fluxes. This average flux is similar in magnitude to the middle of the range of other chamber fluxes from fertilized and irrigated systems (Table 2.7); for example, Anderson and Levine (1987) measured 7 ng N m^{-2} s^{-1} over one year for temperate crop land; Colbourn et al. (1987 as cited in Johansson et al., 1988) measured 8 ng m^{-2} s^{-1} for July and August for temperate pasture; Johansson et al. (1988) measured 8 ng N m^{-2} s^{-1} for a season for savanna in Venezuela; Anderson et al. (1988 as cited in Williams and Fehsenfeld, 1991) measured 13 ng N m^{-2} s^{-1} for chaparral in California; Kaplan et al. (1988) measured 10 ng N m^{-2} s^{-1} for evergreen forest in Brazil. The flux of 3 kg N ha^{-1} yr^{-1} represents a loss of 0.9% of the 356 kg N ha^{-1} applied to this field (DOY 259 to 469) if this was a total application for a year (fertilization had stopped for this crop cycle). This amount of applied N being lost as NO is similar, that is, slightly higher, compared with other studies (0.8%, Garret, 1991; 0.8%, Anderson and Levine, 1987; 0.5%, Johansson et al., 1988).

This study suggest that on a year-round basis, tropical agriculture contributes similar NO_x fluxes to the atmosphere as those measured seasonally for temperate areas. Possibly summertime fluxes which we did not measure are higher due to warmer temperatures. The fluxes from this sugarcane field

would be much lower in the absence of fertilization and irrigation; so conversions of natural ecosystems to agricultural systems increases NO_x fluxes.

7. SUMMARY AND CONCLUSIONS

The NO soil emissions were highly dependent on fertilizer application and soil volumetric water content. Soil surface NO fluxes followed the volumetric water content by row position. The highest peak occurred when the NO emissions were increased uniformly throughout the whole field and not just at the drip line because of a uniform soil water content provided by rain. The DL NO flux peaks were high due to direct fertilization but the BR NO flux peaks were low even with the same water content suggesting NH_4^+ and NO_3^- were limiting.

In contrast to the surface NO fluxes, which varied by an order of magnitude throughout the study, the NO_x fluxes above the canopy varied by several orders of magnitude. The greater range of above-canopy NO_x fluxes and their non equality to the surface NO fluxes may have been caused by measurement errors: primarily O_3 interference in the NO_2 analyzer, but also any inaccuracy of the modelled K, non-representative chamber sites, inaccurate weighting of row positions in calculating the field average, and any inaccuracy in the chamber data; as well as by non-conservation of NO_x: plant uptake of NO_x, deposition of NO_2 and minor, but potentially variable, NO_2 emissions from the surface.

NO was generally the major component of the NO_x fluxes during the first half of the experiment, whereas by the second half of the experiment the NO_2 flux was the major component of NO_x larger; however, the NO_2 measurement was more prone to

interference by O_3 than the NO measurement. The speciation of NO and NO_2 could be caused by potential seasonal trends in O_3 flux, K, and/or greater light intensity below the above-canopy measurement height at the beginning of the experiment than later with crop shading resulting in NO_2 being cycled more effectively back to NO. A gradual, slight decreasing trend in the NO_x fluxes above the canopy towards the end of the experiment when the sugarcane canopy was nearly closed (LAI = 6), which exceeded the decreasing trend in NO flux at the soil surface, suggests that the vegetation was beginning to reduce NO_x transport from the soil to the atmosphere.

The average of the soil surface NO flux is 9 ng N m^{-2} s^{-1} for the 198-d study. This value is a good approximation of the above-canopy flux (the average was 10 ng N m^{-2} s^{-1}, but problems made this number unreliable) prior to rapid canopy development and for small deposition rates and low NO_2 fluxes. This average is similar to other studies of temperate fertilized and irrigated systems.

APPENDICES

Procedure to determine net mineralization rates in soils (aerobic laboratory incubation method) (Hart et al., 1992)

Clean large organic debris from the soil by hand. Do not grind and sieve the soil. Weigh out two portions of 10-g dry-soil equivalent from each sample and place them in a beaker or plastic cup. Determine initial concentrations of ammonium and nitrate from one portion. Incubate the other portion for 7 days in a dark room (25°C) by covering the cup with a perforated lid to allow gas exchange but minimize water loss. Determine ammonium and nitrate concentrations at the end of incubation period. Net N mineralization rate is calculated by subtracting initial inorganic-N concentrations from final inorganic-N concentrations; net nitrification rates are calculated by subtracting initial nitrate concentrations from final nitrate concentrations. A third subsample is used to determine the gravimetric soil water content.

Extraction procedure :

Add 100 ml of 2M KCl to the soil sample. Shake by hand for about 2 minutes, cover the cup and let it sit for 36 hours. Mix the extract, take a sample, and centrifuge for 10 minutes. Analyze for ammonium and nitrate using a technicon autoanalyzer.

Assessment of nitrification potential by the shaken soil-slurry method (Hart et al., 1992)

Since different nitrification rates from actual field rates may be obtained due to perturbation of the soil while sampling, storing, and incubating; the term "potential" nitrification is used to describe the estimates obtained from a laboratory method. The shaken soil-slurry method involves shaking a sieved soil sample in a dilute ammonium phosphate solution (approximately 1:7 soil:solution ratio), and measuring NO_3^- accumulation over a short time period (24 h). Nitrate immobilization by microorganisms is inhibited by high NH_4^+ concentrations (approximately 1 mM), and denitrification is inhibited because vigorous shaking continuously aerates the slurry. Changes in nitrifier populations are unlikely to occur because the assay is short-term, and substrate and moisture limitations are also eliminated. Thus the nitrification rate measured approximates the maximum nitrification rate (V_{max}) possible at the specific temperature of the incubation.

Reagents :

1) Potassium monobasic phosphate (KH_2PO_4) stock solution, 0.2 M. Dissolve 27.22 g of KH_2PO_4 in 1 liter of water. 2) Potassium dibasic phosphate (K_2HPO_4) stock solution, 0.2 M. Dissolve 34.84 g of K_2HPO_4 in 1 liter of water. 3) Ammonium sulfate {$(NH_4)_2SO_4$} stock solution, 50 mM. Dissolve 6.607 g of $(NH_4)_2SO_4$ in 1 liter of water.

Procedure :

Combine the following in a 1 L volumetric flask, and then bring up to volume: 1.5 mL KH_2PO_4 stock solution, 3.5 mL K_2HPO_4 stock solution, and 15 mL $(NH_4)_2SO_4$ stock solution. Adjust to pH 7.2 by adding dilute H_2SO_4 or NaOH solutions dropwise while the combined solution is stirred. This results in a solution containing 1.5 mM NH_4^+ and 1 mM PO_4^{3-}.

Place 15-g of sieved (2- or 4-mm mesh) field-moist soil in a 250-mL Erlenmeyer flask (weigh 20 g if the soil is wet). Add 100 mL of the combined solution and shake for 24 h on an orbital shaker. Collect solution samples from each flask at 2, 6, and 24 hr intervals. Centrifuge for 8 minutes and analyze for nitrate. Calculate the rate of NO_3^- production (mg-N L^{-1} h^{-1}) by linear regression of solution concentration versus time. Calculate the rate per unit dry soil as follows:

$$\text{Rate}_{(\text{mg-N kg}^{-1}\text{h}^{-1})} = \text{Rate}_{(\text{mg-N L}^{-1}\text{ h}^{-1})} * \frac{0.1\ \text{L} + \Theta_v}{\text{kg oven-dry soil in flask}}$$

where Θ_v is the volume of water in the field-moist soil sample. This equation is valid only if the soil:solution ratio in aliquots removed during sampling are the same as the soil:solution ratio in the original slurry; thus, it is critical that the slurries are shaken before sampling.

REFERENCES

Anderson I.C. and J.S. Levine (1986). Relative rates of nitric oxide and nitrous oxide production by nitrifiers, denitrifiers, and nitrate respirers. Applied and Environmental Microbiology. 51:938-945.

Anderson I.C. and J.S. Levine (1987). Simultaneous field measurements of biogenic emissions of nitric oxide and nitrous oxide. Journal of Geophysical Research. 92:965-976.

Bakwin P.S., S.C. Wofsy, and S. Fan (1990). Measurements of reactive nitrogen oxides (NO_y) within and above a tropical forest canopy in the wet season. Journal of Geophysical Research. 95:16,765-16,772.

Bakwin P.S., S.C. Wofsy, S. Fan, M. Keller, S.E. Trumbore, and J.M. Da Costa (1990). Emission of nitric oxide (NO) from tropical forest soils and exchange of NO between the forest canopy and atmospheric boundary layer. Journal of Geophysical Research. 95:16,755-16,764.

Barrow G.M. (1979). Physical chemistry. McGraw-Hill Book Company, New York. Fourth edition.

Bruce J.P. (1990). The atmosphere of the living planet earth. World meteorological organization, Geneva.

Campbell G.S. (1986). An introduction to environmental biophysics, third edition, Springer-Verlag, New York.

Cellier P. (1985). Tall crop evapotranspiration measurement by an aerodynamic method. Advances in Evapotranspiration. pp. 28-34.

Chalamet A. (1983). Denitrification in the nitrogen cycle. Plenum Press, New York.

Chalk P.M. and C.J. Smith (1983). Chemodenitrification, in Freney J.R. and J.R. Simpson (eds), Gaseous loss of nitrogen from plant-soil systems. Martinus Nijhoff/Dr. W. Junk Publishers, The Hague, Netherlands.

Davidson E.A. (1992). Sources of nitric oxide and nitrous oxide following wetting of dry soil. Soil Science Society of America. J. 56:95-102.

Davidson E.A. (1991). Fluxes of nitrous oxide and nitric oxide from terrestrial ecosystems, in Rogers J.E. and W.B. Whitman (eds), Microbial production and consumption of greenhouse gases: Methane, nitrogen oxides, and halomethanes. American Society for Microbiology, Washington, DC.

Davidson E.A., P.M. Vitousek, P.A. Matson, R. Riley, G. Garcia-Martinez, and J.M. Maass (1991). Soil emissions of nitric oxide in a seasonally dry tropical forest of Mexico. Journal of Geophysical Research. 96:15,439-15,445.

Delany A.C., D.R. Fitzjarrald, D.H. Lenschow, R. Pearson, G.J. Wendel, and B. Woodruff (1986). Direct measurements of nitrogen oxides and ozone fluxes over grassland. Journal of Atmospheric Chemistry 4, 429-444.

Denmead O.T. (1983). Micrometeorological methods for measuring gaseous losses of nitrogen in the field, in Freney J.R. and J.R. Simpson (eds), Gaseous loss of nitrogen from plant-soil systems. Martinus Nijhoff/Dr. W. Junk Publishers, The Hague, Netherlands.

Denmead O.T. and M.R. Raupach (1993). Methods for measuring atmospheric gas transport in agricultural and forest systems, in Agricultural ecosystems effects on trace gases and global climate change, ASA special publication number 55.

Eichner M.J. (1990). Nitrous oxide emissions from fertilized soils: Summary of available data. Journal of Environmental Quality. 19:272-280.

Fenchel T. and T.H. Blackburn (1979). Bacteria and mineral cycling. Academic Press Limited, London.

Fillery I.R.P. (1983). Biological denitrification, in Freney J.R. and J.R. Simpsom (eds), Gaseous loss of nitrogen from plant-soil systems. Martinus Nijhoff/Dr. W. Junk Publishers, The Hague, Netherlands.

Firestone M.K. and E.A. Davidson (1989). Microbiological basis of NO and N_2O production and consumption in soil, in Andreae M.O. and D.S. Schimel (eds), Exchange of trace gases between terrestrial ecosystems and the atmosphere. John Wiley and Sons, Great Britain.

Fitzjarrald D.R. and D. H. Lenschow (1985). Mean concentration and flux profiles for chemically reactive species in the atmospheric surface layer. Atmospheric Environment Vol. 17, No. 12, pp. 2505-2512, 1983.

Fowler D. (1992). Air pollution transport, deposition, and exposure to ecosystems, in Barker J.R. and D.T. Tingey (eds), Air pollution effects on biodiversity, Van Nostrand Reinhold, New York.

Fowler D. and J.H. Duyzer (1989). Micrometeorological techniques for the measurement of trace gas exchange, in Andreae M.O. and D.S. Schimel (eds), Exchange of trace gases between terrestrial ecosystems and the atmosphere. John Wiley and Sons, Great Britain.

Frisel M.J. (ed) (1978). Cycling of mineral nutrients in agricultural ecosystems. Elsevier Scientific Publishing Company, Amsterdam, The Netherlands.

Galbally I.E. (1989). Factors controlling NOx emissions from soils, in Andreae M.O. and Schimel D.S. (eds), Exchange of trace gases between terrestrial ecosystems and the atmosphere. John Wiley and Sons, Great Britain.

Galbally I.E. and C.R. Roy (1983). The fate of nitrogen compounds, in Freney J.R. and J.R. Simpson (eds), Gaseous loss of nitrogen from plant-soil systems. Martinus Nijhoff/Dr. W. Junk Publishers, The Hague, Netherlands.

Gallon J.R. and A.E. Chaplin (1987). An introduction to nitrogen fixation. London Cassell.

Graser E.A., S.B. Verma, and N.J. Rosenberg (1985). The roughness sublayer over a wide-row crop. pp. 125-6. In 17th Conference of Agricultural Forest Meteorology, Scottsdale, AZ. 21-24 May 1885. American Meteorological Society, Boston, MA.

Grantz D.A. and F.C. Meinzer (1991). Regulation of transpiration in field-grown sugarcane: evaluation of the stomatal response to humidity with the Bowen ratio technique. Agricultural and Forest Meteorology. 53:169-183.

Groffman P.M., J.M. Tiedje, G.P. Robertson, and S. Christensen (1987). Denitrification at different temporal and geographical scales: Proximal and distal controls, in Wilson J.R. (ed), Advances in nitrogen cycling in agricultural ecosystems. C.A.B. International, Wallingford, UK.

Halldin S. and A. Lindroth (1992). Errors in net radiometry: Comparison and evaluation of six radiometer designs. Journal of Atmospheric and Oceanic Technology. 9:762-783.

Hart S.C., J.M. Stark, E.A. Davidson, and M.K. Firestone (1992). Nitrogen mineralization, immobilization, and nitrification. Draft chapter for the book: Methods of soil analysis: Biochemical and microbiological properties.

Hayward R.R. (1992). Nitrogen trace gas emissions from soils spanning a 4.5 million year chronosequence in Hawaiian montane rainforest.

Hutchinson G.L. and E.A. Davidson (1993). Processes of production and consumption of gaseous nitrogen oxides in soil, in Agricultural ecosystems effects on trace gases and global climate change, ASA special publication number 55.

Hutchinson G.L. and G.P. Livingston (1993). Use of chamber systems to measure trace gas fluxes, in Agricultural ecosystems effects on trace gases and global climate change, ASA special publication number 55.

Johansson C. (1989). Fluxes of NOx above soil and vegetation, in Andreae M.O. and D.S. Schimel (eds), Exchange of trace gases between terrestrial ecosystems and the atmosphere. John Wiley and Sons, Great Britain.

Johansson C. and E. Sanhueza (1988). Emission of NO from savanna soils during rainy season. Journal of Geophysical Research. 93:14,193-14,198.

Johansson C., H. Rodhe, and E. Sanhueza (1988). Emission of NO in a tropical and cloud forest during the dry season. Journal of Geophysical Research. 93:7180-7192.

Kaplan W.A., S.C. Wofsy, M. Keller, and J.M. Da Costa (1988). Emission of NO and deposition of O_3 in a tropical forest system. Journal of Geophysical Research. 93:1389-1395.

Lenschow D.H. and A.C. Delany (1987). An analytical formulation for NO and NO_2 flux profiles in the atmospheric surface layer. Journal of Atmospheric chemistry. 5:301-309.

Levine J.S., T.R. Augustsson, I.C. Anderson, and J.M. Hoell, Jr. (1984). Tropospheric sources of NOx: Lightning and biology. Atmospheric Environment. 18:1797-1804.

Matson P.A., P.M. Vitousek, J.J. Ewel, M.J. Mazzarino, and G.P. Robertson (1987). Nitrogen transformations following tropical forest felling and burning on a volcanic soil. Ecology. 68:491-502.

Miller A. and J.C. Thompson (1975). Elements of meteorology.Charles E. Merrill Publishing Company, Columbus, Ohio.

Monteith J.L. and M.H. Unsworth (1990). Principles of environmental physics, second edition, published by Edward Arnold, New York.

National Academy of Sciences (1977). Nitrogen oxides. Published by the National Academy of Sciences, Washington, DC.

Oke T.R. (1987). Boundary layer climates. Methuen & Co, New York.

Parrish D.D., E.J. Williams, D.W. Fahey, S.C. Liu, and F.C. Fehsenfeld (1987). Measurement of nitrogen oxide fluxes from soils: Intercomparison of enclosure and gradient measurement techniques. Journal of Geophysical Research. 92:2165-2171.

Paul E.A. and F.E. Clark (1989). Soil microbiology and biochemistry. Academic Press Inc, San Diego, California.

Payne W.J. (1981). Denitrification. John Wiley and Sons, Inc, New York.

Penner J.E., C.S. Atherton, J. Dignon, S.J. Ghan, J.J. Walton, and S. Hameed (1991). Tropospheric nitrogen: A three-dimensional study of sources, distributions, and deposition. Journal of Geophysical Research. 96:959-990.

Rosenberg N.J., B.L. Blad, and S.B. Verma (1983). Microclimate: The biological environment. John Wiley and Sons, Inc, USA.

Robertson G.P. (1993). Fluxes of nitrous oxide and other nitrogen trace gases from intensively managed landscapes: A global perspective, in Agricultural ecosystems effects on trace gases and global climate change, ASA special publication number 55.

Salisbury F.B. and C.W. Ross (1985). Plant physiology. Wadsworth Publishing Company, Belmont, California.

Slemr F. and W. Seiler (1984). Field measurements of NO and NO_2 emissions from fertilized and unfertilized soils. Journal of Atmospheric Chemistry 2, 1-24.

Soil Conservation Service (1976). Soil survey laboratory data and descriptions for some soils of Hawaii. Soil survey investigations report No. 29.

Sprent J.I. (1987). The ecology of the nitrogen cycle. Cambridge University Press, Cambridge, Great Britain.

Stanley C.D., R.E. Green, M.A. Khan, and L.T. Santo (1990). Nitrogen-fertilization rate and soil nitrate distribution for microirrigated sugarcane. Soil Society of America Journal. 54:217-222.

Stull R. B. (1980). An introduction to boundary layer meteorology. Kluwer Academic Publishers, London.

Tisdale S.L., W.L. Nelson, and J.D. Beaton (1986). Soil fertility and fertilizers, Macmillan Publishing Company, New York, p.113-148.